



THE UNIVERSITY  
*of* ADELAIDE

Ontogeny, Systematics and Soft-Part Anatomy  
of Early Cambrian Trilobites from South Australia

**James Dougal Holmes**

**MPhil BSc(EvolBiol) BEc**

Thesis submitted for the degree of

**Doctor of Philosophy**

School of Biological Sciences

Faculty of Sciences

University of Adelaide

**July 2020**



*Everywhere I looked were pivot-points and fulcrums, symmetries and proliferations:  
the thorax points of a winged world.*

– Robert MacFarlane





This work is dedicated to Richard Fortey and David Quammen,  
whose writings prompted me to go back to school and study something important.



# Contents

|  |              |
|--|--------------|
| <b>Figures and Tables .....</b>  | <b>xi</b>    |
| <b>List of Papers .....</b>  | <b>xiv</b>   |
| <b>Summary.....</b>  | <b>xv</b>    |
| <b>Declaration.....</b>  | <b>xvii</b>  |
| <b>Acknowledgements.....</b>   | <b>xviii</b> |
| <br>   |              |
| <b>Chapter 1 – Introduction .....</b>  | <b>1</b>     |
| 1.1    Contextual Statement.....   | 2            |
| 1.1.1    Background and objectives.....  | 2            |
| 1.1.2    Thesis chapters .....   | 2            |
| <br>   |              |
| <b>Chapter 2 – Background .....</b>  | <b>7</b>     |
| 2.1    Trilobites: an introduction.....  | 8            |
| 2.2    The trilobite body plan .....   | 9            |
| 2.3    Trilobite ontogeny .....  | 11           |
| 2.4    Cambrian geology and biostratigraphy of South Australia.....  | 13           |
| 2.5    The Emu Bay Shale <i>Lagerstätte</i> .....  | 16           |
| 2.6    Emu Bay Shale trilobites .....  | 17           |
| 2.7    References.....   | 19           |
| <br>   |              |
| <b>Chapter 3 – The post-embryonic ontogeny of the early Cambrian trilobite <i>Estaingia bilobata</i> from South Australia: trunk development and phylogenetic implications .....</b> | <b>29</b>    |
| Abstract .....   | 31           |
| Introduction.....  | 31           |
| Material and method .....  | 32           |
| Ontogeny of <i>Estaingia bilobata</i> .....  | 33           |
| Terminology.....   | 34           |
| Protaspid period .....   | 34           |
| Meraspid period .....  | 34           |
| Holaspid period .....  | 38           |

|  |    |
|--|----|
| Summary of ontogenetic variation in <i>Estaingia bilobata</i> .....          | 40 |
| Growth rate .....  | 42 |
| Discussion .....   | 43 |
| Trunk Development .....  | 43 |
| Comparison of <i>Estaingia bilobata</i> protaspides with other species ..... | 45 |
| Phylogenetic implications .....  | 46 |
| Conclusion .....   | 47 |
| Acknowledgements .....   | 48 |
| References .....   | 48 |

|   |           |
|---|-----------|
| <b>Chapter 4 – Ontogeny of the trilobite <i>Redlichia</i> from the lower Cambrian (Series 2, Stage 4) Ramsay Limestone of South Australia .....</b> | <b>51</b> |
| 4.1 Abstract.....   | 53        |
| 4.2 Introduction .....  | 54        |
| 4.3 Geological setting .....  | 55        |
| 4.4 Occurrence of <i>Redlichia</i> in the Ramsay and Wirrealpa limestones .....   | 56        |
| 4.5 Material and methods .....  | 58        |
| 4.6 Systematic Palaeontology .....  | 59        |
| 4.7 Post-embryonic development of <i>Redlichia</i> cf. <i>versabunda</i> .....  | 68        |
| 4.7.1 Ontogenetic terminology.....  | 68        |
| 4.7.2 Protaspid period .....  | 69        |
| 4.7.3 Meraspid period.....  | 72        |
| 4.8 Discussion .....  | 74        |
| 4.8.1 Morphological comparisons with other redlichiine protaspides .....  | 74        |
| 4.8.2 Size comparisons with other redlichoid protaspides .....  | 77        |
| 4.8.3 Allometric change and pygidial segmentation throughout ontogeny .....   | 77        |
| 4.8.4 Phylogenetic implications .....   | 78        |
| 4.9 Acknowledgements.....   | 80        |
| 4.10 References .....   | 80        |

|  |            |
|--|------------|
| <b>Chapter 5 – The trilobite <i>Redlichia</i> from the lower Cambrian Emu Bay Shale Konservat-Lagerstätte of South Australia: systematics, ontogeny and soft-part anatomy.....</b> | <b>89</b>  |
| Abstract .....   | 91         |
| Introduction.....  | 91         |
| Location, stratigraphy and taphonomy .....   | 92         |
| Material and methods.....  | 93         |
| Collection bias .....  | 93         |
| Terminology.....   | 94         |
| Traditional morphometric analyses.....   | 94         |
| Geometric morphometrics .....  | 95         |
| Systematic Palaeontology .....   | 96         |
| Ontogeny of <i>Redlichia takooensis</i> .....  | 110        |
| Morphometric analyses results.....   | 110        |
| Summary of growth in <i>Redlichia takooensis</i> .....   | 112        |
| Soft-part anatomy of <i>Redlichia</i> species from the EBS .....   | 113        |
| Antennae.....  | 115        |
| Biramous appendages .....  | 115        |
| Digestive system.....  | 122        |
| Acknowledgements .....   | 125        |
| References.....  | 125        |
| <br>   |            |
| <b>Chapter 6 – Meraspid axial growth gradients in the early Cambrian ellipsocephaloid trilobite <i>Etaingia bilobata</i> from South Australia .....</b>                            | <b>131</b> |
| 6.1 Abstract .....   | 133        |
| 6.2 Introduction.....  | 134        |
| 6.3 Material and methods.....  | 137        |
| 6.3.1 Specimen data .....  | 137        |
| 6.3.2 Measurements.....  | 138        |
| 6.3.3 Initial growth gradient detection.....   | 141        |
| 6.3.4 Model testing.....   | 141        |
| 6.4 Results .....  | 142        |
| 6.5 Discussion .....   | 145        |

|   |   |            |
|---|---|------------|
| 6.5.1   | Trunk growth patterns in <i>Estaingia bilobata</i> .....  | 145        |
| 6.5.2   | Implications of model support .....   | 148        |
| 6.6   | Conclusions .....   | 149        |
| 6.7   | References .....  | 150        |
| <b>Chapter 7 – Ontogeny and phylogeny of Cambrian trilobites.....</b> |   | <b>153</b> |
| 7.1   | Abstract.....   | 155        |
| 7.2   | Introduction .....  | 156        |
| 7.3   | Methodology .....   | 157        |
| 7.4   | Results.....  | 158        |
| 7.5   | Discussion .....  | 159        |
| 7.6   | Conclusions .....   | 165        |
| 7.7   | References .....  | 166        |
| <b>Chapter 8 – Conclusions .....</b>                                  |   | <b>171</b> |
| 8.1   | Summary and future directions .....   | 172        |
| 8.1   | References .....  | 174        |
| <b>Chapter 9 – Supplementary papers .....</b>                         |   | <b>177</b> |
| 9.1   | Supplementary paper 1: Comparisons between Cambrian Lagerstätten assemblages using multivariate, parsimony and Bayesian methods.....  | 178        |
| 9.2   | Supplementary paper 2: An exceptional record of Cambrian trilobite moulting behaviour preserved in the Emu Bay Shale, South Australia.....                                      | 180        |
| 9.3   | Supplementary paper 3: Taxa, turnover and taphofacies: a preliminary analysis of facies-assemblage relationships in the Ediacara Member (Flinders Ranges, South Australia)..... | 182        |
| 9.4   | Supplementary paper 4: The stratigraphic significance of early Cambrian (Series 2, Stage 4) trilobites from the Smith Bay Shale near Freestone Creek, Kangaroo Island..         | 184        |
| <b>Chapter 10 – Supplementary material .....</b>                      |   | <b>187</b> |
| 10.1  | Supplementary material for Chapter 3 .....  | 188        |
| 10.1.1  | Dataset of <i>Estaingia bilobata</i> cranidial measurements..   | 188        |

|        |  |     |
|--------|--|-----|
| 10.2   | Supplementary material for Chapter 5.....                                      | 192 |
| 10.3   | Supplementary material for Chapter 6.....                                      | 193 |
| 10.3.1 | Measurement definitions and abbreviations .....                                | 193 |
| 10.3.2 | Fitting functions and implementation .....                                     | 193 |
| 10.3.3 | References.....  | 197 |
| 10.3.4 | Dataset of <i>LTS<sub>i</sub></i> and <i>PTS<sub>i</sub></i> observations..... | 198 |
| 10.4   | Supplementary material for Chapter 7.....                                      | 202 |
| 10.4.1 | Supplementary Tables and Figures.....  | 202 |
| 10.4.2 | List of characters used in the phylogenetic analysis.....                      | 203 |
| 10.4.3 | References.....  | 210 |
| 10.4.4 | Phylogenetic character matrix.....   | 212 |

## Figures and Tables

### Chapter 2

|                    |   |    |
|--------------------|---|----|
| <b>Figure 2.1:</b> | Major hypothesised positions for trilobites within the arthropod phylogenetic tree .....                        | 8  |
| <b>Figure 2.2:</b> | Dorsal anatomy of the trilobite <i>Estaingia bilobata</i> from the Emu Bay Shale.....                           | 9  |
| <b>Figure 2.3:</b> | Simplified ontogeny of the early Cambrian ellipsocephaloid trilobite <i>Estaingia bilobata</i> .....            | 11 |
| <b>Figure 2.4:</b> | Correlation chart showing Cambrian sections in the Stansbury and Arrowie Basins of South Australia .....        | 14 |
| <b>Figure 2.5:</b> | Map showing fossil localities of the Emu Bay Shale on the north coast of Kangaroo Island, South Australia ..... | 15 |
| <b>Figure 2.6:</b> | The holotype specimen of <i>Redlichia rex</i> from the Emu Bay Shale (Kangaroo Island, South Australia).....    | 19 |

### Chapter 3

|                  |   |    |
|------------------|---|----|
| <b>Figure 1:</b> | Early growth stages of <i>Estaingia bilobata</i> from the Emu Bay Shale.....                                      | 33 |
| <b>Figure 2:</b> | Late stage meraspides of <i>Estaingia bilobata</i> from the Emu Bay Shale .....                                   | 35 |
| <b>Figure 3:</b> | Holaspides of <i>Estaingia bilobata</i> from the Emu Bay Shale.....   | 37 |
| <b>Figure 4:</b> | Specimens of <i>Estaingia bilobata</i> from the Emu Bay Shale showing various morphological characteristics ..... | 39 |
| <b>Figure 5:</b> | Reconstruction of the hypostome in a medium-sized <i>Estaingia bilobata</i> holaspis.                             | 40 |
| <b>Figure 6:</b> | Ontogenetic series of <i>Estaingia bilobata</i> from the Emu Bay Shale .....                                      | 41 |
| <b>Figure 7:</b> | Dorsal reconstruction of a medium-sized <i>Estaingia bilobata</i> holaspis .....                                  | 43 |
| <b>Figure 8:</b> | Cranidial length and width measurements of <i>Estaingia bilobata</i> from the Emu Bay Shale .....                 | 44 |
| <b>Figure 9:</b> | Trunk segmentation schedule of <i>Estaingia bilobata</i> from the Emu Bay Shale .....                             | 45 |

## Chapter 4

|  |    |
|--|----|
| <b>Figure 4.1:</b> Map of south-eastern South Australia and central Yorke Peninsula .....  | 56 |
| <b>Figure 4.2:</b> Correlation chart showing relationships between the Cambrian successions of the Stansbury Basin, Arrowie Basin, and eastern Georgina Basin.....             | 57 |
| <b>Figure 4.3:</b> <i>Redlichia</i> cf. <i>versabunda</i> holaspid cranidia from the Ramsay Limestone.....   | 62 |
| <b>Figure 4.4:</b> <i>Redlichia</i> cf. <i>versabunda</i> specimens from the Ramsay Limestone .....  | 64 |
| <b>Figure 4.5:</b> Plot of axial exoskeletal length against intergenal spine separation for <i>Redlichia</i> cf. <i>versabunda</i> protaspides from the Ramsay Limestone ..... | 69 |
| <b>Figure 4.6:</b> <i>Redlichia</i> cf. <i>versabunda</i> protaspides from the Ramsay Limestone .....  | 71 |
| <b>Figure 4.7:</b> <i>Redlichia</i> cf. <i>versabunda</i> meraspides from the Ramsay Limestone .....   | 73 |
| <b>Figure 4.8:</b> Reconstructions of various ontogenetic stages of <i>Redlichia</i> cf. <i>versabunda</i> from the Ramsay Limestone .....                                     | 79 |

## Chapter 5

|   |     |
|---|-----|
| <b>Figure 1:</b> Measurements taken for the morphometric analyses of <i>Redlichia</i> species from the Emu Bay Shale .....  | 94  |
| <b>Figure 2:</b> Biplots comparing certain morphological characteristics of <i>Redlichia takoensis</i> and <i>Redlichia rex</i> sp. nov. ....   | 95  |
| <b>Figure 3:</b> Large, articulated specimens of <i>Redlichia takoensis</i> from the Emu Bay Shale .....  | 97  |
| <b>Figure 4:</b> Small and medium size specimens of <i>Redlichia takoensis</i> from the Emu Bay Shale .....   | 98  |
| <b>Figure 5:</b> Partial specimens of <i>Redlichia takoensis</i> from the Emu Bay Shale illustrating various aspects of exoskeletal morphology.....   | 99  |
| <b>Figure 6:</b> Detail of ornament on various sections of <i>Redlichia</i> exoskeleton.....  | 100 |
| <b>Figure 7:</b> Small and medium size specimens of <i>Redlichia rex</i> sp. nov. from the Emu Bay Shale .....  | 103 |
| <b>Figure 8:</b> Large, articulated and mostly complete specimens of <i>Redlichia rex</i> sp. nov. from the Emu Bay Shale .....   | 105 |
| <b>Figure 9:</b> Large, articulated and mostly complete specimens of <i>Redlichia rex</i> sp. nov. from the Emu Bay Shale .....   | 106 |
| <b>Figure 10:</b> Specimens of <i>Redlichia rex</i> sp. nov. from the Emu Bay Shale illustrating various aspects of exoskeletal morphology .....  | 107 |
| <b>Figure 11:</b> Dorsal reconstructions of medium-sized specimens of <i>Redlichia takoensis</i> and <i>Redlichia rex</i> sp. nov. ....   | 109 |
| <b>Figure 12:</b> Results of the geometric morphometric landmark analysis on 33 <i>Redlichia takoensis</i> specimens .....  | 111 |
| <b>Figure 13:</b> Slope values and confidence intervals for various bivariate log/log major axis regression models of linear measurements taken from <i>Redlichia takoensis</i> specimens ... | 111 |
| <b>Figure 14:</b> Biplots depicting various aspects of growth in <i>Redlichia takoensis</i> .....   | 112 |
| <b>Figure 15:</b> Size distribution of <i>Redlichia takoensis</i> from the Emu Bay Shale .....  | 113 |
| <b>Figure 16:</b> Specimens of <i>Redlichia</i> with preserved antennae from the Emu Bay Shale .....  | 114 |
| <b>Figure 17:</b> Isolated biramous appendages of <i>Redlichia rex</i> sp. nov. ....  | 116 |
| <b>Figure 18:</b> Isolated biramous appendages of <i>Redlichia rex</i> sp. nov. ....  | 118 |
| <b>Figure 19:</b> Isolated biramous appendages of <i>Redlichia rex</i> sp. nov. ....  | 120 |
| <b>Figure 20:</b> Biramous appendage reconstructions for <i>Redlichia rex</i> sp. nov. ....   | 121 |
| <b>Figure 21:</b> Details of digestive glands in <i>Redlichia takoensis</i> .....   | 123 |



|  |     |
|--|-----|
| <b>Figure 22:</b> Details of digestive structures in <i>Redlichia</i> from the Emu Bay Shale ..... | 124 |
|--|-----|

## Chapter 6

|   |     |
|---|-----|
| <b>Figure 6.1:</b> Various indicators of growth in the meraspid trunk of <i>Estaingia bilobata</i> from the Emu Bay Shale .....                               | 136 |
| <b>Figure 6.2:</b> Axial lengths of different body parts of <i>Estaingia bilobata</i> .....   | 139 |
| <b>Figure 6.3:</b> Lines constructed on <i>Estaingia bilobata</i> specimens to obtain body part length measurements .....                                     | 140 |
| <b>Figure 6.4:</b> Fitting of the best supported models under the Segmental Gradient (SG) and Trunk Gradient (TG) hypotheses to observed <i>RLS</i> data..... | 144 |
| <b>Table 6.1:</b> AIC <sub>c</sub> comparison of the models utilising relative thoracic segment length .....  | 145 |
| <b>Figure 6.5:</b> Growth patterns in the trunk of <i>Estaingia bilobata</i> .....  | 147 |
| <b>Figure 6.6:</b> Predicted relative growth gradients under the TG hypothesis .....  | 149 |

## Chapter 7

|   |     |
|---|-----|
| <b>Figure 7.1:</b> Single most parsimonious tree of 16 Cambrian trilobites.....   | 159 |
| <b>Figure 7.2:</b> Single most parsimonious tree of Cambrian trilobites with various ontogenetic characters mapped..... | 160 |
| <b>Figure 7.3:</b> Protaspides exemplifying features of major early Cambrian trilobite groups ...                       | 162 |

## Chapter 10

|  |     |
|--|-----|
| <b>Figure 10.1:</b> Major axis regression of PC2 against centroid size .....   | 192 |
| <b>Table 10.1:</b> Parameter estimates and pseudo-R <sup>2</sup> values for the SG models.....   | 194 |
| <b>Table 10.2:</b> Parameter estimates and pseudo-R <sup>2</sup> values for the various RG models .....  | 196 |
| <b>Figure 10.2:</b> Fitting of the best supported (RG-C2) model to observed <i>RPS</i> data .....  | 197 |
| <b>Table 10.3:</b> OLS regression coefficients and significance values representing pygidial growth rates across meraspid ontogeny. ....             | 197 |
| <b>Figure 10.3:</b> Strict consensus tree based on two most parsimonious trees obtained after removing ontogenetic characters from the analysis..... | 202 |
| <b>Table 10.4:</b> Taxa included in the phylogenetic analysis and references used to obtain character information .....                              | 202 |

## List of Papers

### Thesis chapters:

**Holmes, J.D., Paterson, J.R. & García-Bellido, D.C.** 2020a . The post-embryonic ontogeny of the early Cambrian trilobite *Estaingia bilobata* from South Australia: trunk development and phylogenetic implications. *Papers in Palaeontology*: doi:10.1002/spp2.1323.

**Holmes, J.D., Paterson, J.R., Jago, J.B. & García-Bellido, D.C.** *in review*. Ontogeny of the trilobite *Redlichia* from the lower Cambrian (Series 2, Stage 4) Ramsay Limestone of South Australia. *Geological Magazine*.

**Holmes, J.D., Paterson, J.R. & García-Bellido, D.C.** 2020b. The trilobite *Redlichia* from the lower Cambrian Emu Bay Shale *Konservat-Lagerstätte* of South Australia: systematics, ontogeny and soft-part anatomy. *Journal of Systematic Palaeontology*, **18**: 295–334.

**Holmes, J.D., Paterson, J.R. & García-Bellido, D.C.** Meraspid axial growth gradients in the early Cambrian ellipsocephaloid trilobites *Estaingia bilobata* from South Australia. *Unpublished manuscript, intended for submission to Paleobiology*.

**Holmes, J.D., Paterson, J.R. & García-Bellido, D.C.** Ontogeny and phylogeny of Cambrian trilobites. *Unpublished manuscript, intended for submission to Journal of Paleontology (or similar)*.

### Supplementary papers:

**Holmes, J.D., García-Bellido, D.C. & Lee, M.S.Y.** 2018. Comparisons between Cambrian Lagerstätten assemblages using multivariate, parsimony and Bayesian methods. *Gondwana Research*, **55**: 30–41.

**Drage, H.B., Holmes, J.D., Daley, A.C. & García-Bellido, D.C.** 2018. An exceptional record of Cambrian trilobite moulting behaviour preserved in the Emu Bay Shale, South Australia. *Lethaia*, **51**: 473–492.

**Reid, L.M., Holmes, J.D., Payne, J.L., García-Bellido, D.C. & Jago, J.B.** 2018. Taxa, turnover and taphofacies: a preliminary analysis of facies-assemblage relationships in the Ediacara Member (Flinders Ranges, South Australia). *Australian Journal of Earth Sciences*: doi:10.1080/08120099.2018.1488767.

**Jago, J.B., Bentley, C.J., Paterson, J.R., Holmes, J.D., Lin, T.R. & Sun, X.W.** 2020. The stratigraphic significance of early Cambrian (Series 2, Stage 4) trilobites from the Smith Bay Shale near Freestone Creek, Kangaroo Island. *Australian Journal of Earth Sciences*: doi:10.1080/08120099.2020.1749882.

## Summary

The Cambrian ‘explosion’ is one of the most important events in the history of life on Earth. Much of the higher level taxonomic diversity recognised in metazoan animals appeared during this period, and it is at this time that we see the rapid development of modern-style marine ecosystems and associated ecological interactions such as predation. Rare fossil deposits known as *Konservat-Lagerstätte* that preserve the soft parts of organisms offer us ‘windows’ into life in the immediate aftermath of the Cambrian explosion. The Emu Bay Shale from Kangaroo Island (South Australia) contains the only known Cambrian *Konservat-Lagerstätte* in the Southern Hemisphere, and offers important insights into life in the epicontinental seas of East Gondwana approximately 512 million years ago. Unlike the majority of other similar deposits, the Emu Bay Shale *Lagerstätte* is dominated by trilobites, an extinct class of biomineralising arthropods. Trilobites are one of the first important, diverse animal groups to appear in the fossil record, and as such are useful for answering important questions about early animal evolution. The conditions that allowed the preservation of soft parts in the Emu Bay Shale were also conducive to preserving complete, articulated trilobite specimens that are required to conduct detailed morphological investigations (including those related to growth) in these early arthropods.

This thesis reviews the systematics and taxonomic descriptions of three species of trilobite from the Emu Bay Shale (*Estaingia bilobata*, *Redlichia takooensis* and *Redlichia rex* sp. nov.), as well as *Redlichia* cf. *versabunda* from the Ramsay Limestone (Yorke Peninsula, South Australia), with particular emphasis on ontogenetic development. Instances of extremely rare soft-part preservation of appendages and digestive structures in the two *Redlichia* species from the Emu Bay Shale are described. A complete post-embryonic ontogenetic series of articulated specimens is described for *E. bilobata*, and the segmental growth dynamics of this trilobite’s trunk region are investigated using morphometrics. An ontogenetic series is also described for *R. cf. versabunda* based largely on cranidia, and includes exceptionally well-preserved protaspides (the earliest trilobite larval stage). Finally, results from these studies are incorporated into a phylogenetic analysis aimed at exploring the importance of ontogenetic characters in trilobite evolutionary relationships. Results

reaffirm the importance of studying developmental processes in extinct organisms such as trilobites, particularly in 'primitive' examples such as those from the early Cambrian Period, to understanding the evolution of complex life on Earth.

## Declaration

I certify that this work contains no material which has been accepted for the award of any other degree or diploma in my name in any university or other tertiary institution and, to the best of my knowledge and belief, contains no material previously published or written by another person, except where due reference has been made in the text. In addition, I certify that no part of this work will, in the future, be used in a submission in my name for any other degree or diploma in any university or other tertiary institution without the prior approval of the University of Adelaide and where applicable, any partner institution responsible for the joint award of this degree. The author acknowledges that copyright of published works contained within this thesis resides with the copyright holder(s) of those works. I give permission for the digital version of my thesis to be made available on the web, via the University's digital research repository, the Library Search and also through web search engines, unless permission has been granted by the University to restrict access for a period of time. I acknowledge the support I have received for my research through the provision of an Australian Government Research Training Program Scholarship and the Constance Fraser Supplementary Scholarship from the University of Adelaide.

**James Dougal Holmes**

14<sup>th</sup> July 2020

## Acknowledgements

Firstly, I would like to thank my supervisors Diego García-Bellido and John Paterson for their support, advice and friendship during my candidature. Their doors were always open when I needed to discuss a problem, and I thank them for their guidance and willingness to drop whatever they were doing to help me.

I have been based at the South Australian Museum for over five years, during which I have met many wonderful people that have influenced my life and work for the better. Thanks to my museum family including Tory Botha, Christian Ceccon, Andrea Crowther, Felicity Coutts, Mike Gemmell, Ben McHenry, Mark Hutchinson, Catherine Nielsen, Alessandro Palci, Mark Pharaoh and Neville Pledge, and everyone else at the museum who made me feel welcome. Special thanks to Mary-Anne Binnie for her endless patience and assistance in accessing and collecting Emu Bay Shale material.

Thanks to our collaborators on the Emu Bay Shale project Greg Edgecombe, Allison Daley, Harriet Drage, Bob Gaines, Jim Gehling, Lee Ann Hally, Jim Jago, Mike Lee and Natalie Schroeder for their discussions and insight, and our regular volunteers Ronda Atkinson and Carol and Trevor Ireland. Special thanks to Katrina Kenny for her assistance in organising the Emu Bay Shale field seasons, and her reconstructions (and our endless discussions) of the Emu Bay Shale trilobites and other animals. Thanks also to Kirra Bailey, Russell Bicknell, Glenn Brock, Aaron Camens, Ellie Ellis, Lars Holmer, Marjorie Jones, Pierre Kruse, John Laurie, Javier Ortega-Hernández, Dennis Rice, Emma-Lee Thomson and Emily Tilby, and others already mentioned above, for assistance with the Emu Bay Shale collection efforts in the field. Special thanks to landowners Paul and Carmen Buck for generously allowing access to the field sites at Big Gully.

Many others have given freely of their time in the form of discussions, hosting me on trips, and helping to organise financial assistance to attend conferences during my candidature. Those not already mentioned above include Chao Chang, Mary Droser, Frankie Dunn, Nigel

Hughes, Lukáš Laibl, Alex Liu and Claire Mellish. Special thanks to Giuseppe Fusco for discussions and assistance relating to the morphometric methods used in Chapter 6.

Finally, thanks to Marissa Betts and Lily Reid for putting up with my incessant talk about trilobites, and to my parents Allan and Gail Holmes for their unwavering support in (almost) everything I do.

This work was supported by a Research Training Program (RTP) scholarship from the Australian Government and the Constance Fraser Scholarship from the University of Adelaide.

I acknowledge that the material in Chapter 4 was collected on Narungga Traditional Lands, and work conducted during my PhD also occurred on the Traditional Lands of the Adnyamathanha, Anēwan, Peramangk and Kurna peoples.





# **Chapter 1**

## Introduction

## 1.1 Contextual Statement

### 1.1.1 Background and objectives

This thesis examines the palaeobiology of four species (representing two genera) of trilobite from early Cambrian sediments of South Australia, in particular focusing on ontogeny. In doing so, it aims to fill a knowledge gap concerning patterns of growth in some of Earth's oldest animals. The exceptional preservation of fossil material found at a number of early Cambrian sites across South Australia, particularly within the Emu Bay Shale on Kangaroo Island, provide some of the most detailed records of articulated trilobites known from sediments of this age, including soft-part anatomy and complete growth series. The work presented in this study is the first instance these South Australian examples have been described in detail, in general based on large numbers of specimens allowing in-depth quantitative analysis. The major aim of this work is to provide an increased understanding of the palaeobiology of these trilobites by providing updated systematic palaeontological descriptions (where necessary), description of non-biomineralised structures (soft-part anatomy), descriptions of ontogenetic series, and morphometric analyses designed to characterise and model growth dynamics. The results of these are then compared with what is known for other trilobites, with the aim of better understanding both the evolution of development and the phylogenetic relationships within this extinct group.

### 1.1.2 Thesis chapters

The main body of this thesis is organised into six chapters: an initial introduction and general literature review (Chapter 2), followed by five papers published in, or intended to be submitted to, international scientific journals (Chapters 3–7 = Papers 1–5). Paper 1 has been published in *Papers in Palaeontology*, Paper 2 is currently under review with *Geological Magazine*, Paper 3 has been published in the *Journal of Systematic Palaeontology*, Paper 4 is intended for submission to *Paleobiology*, and Paper 5 is intended for submission to the *Journal of Paleontology* (or similar). Chapter 8 provides a brief discussion and presents potential future directions of research. In addition to the papers in the main body of the

thesis, the title pages of a further four supplementary papers published during the candidature (but not considered for examination purposes) are listed in Chapter 9 (Appendix 1). Paper 6 has been published in *Gondwana Research*, Paper 7 has been published in *Lethaia*, and Papers 8 and 9 published in the *Australian Journal of Earth Sciences*. Chapter 10 (Appendix 2) contains supplementary material for the papers in the main body of the thesis.

Chapter 2 provides a general introduction to trilobites and the Cambrian geology of South Australia. The aim of this is to provide context for the following papers and is not intended as an exhaustive literature review.

Chapter 3 (Paper 1) describes the ontogeny of the trilobite *Estaingia bilobata* from the Cambrian Series 2 (Stage 4) Emu Bay Shale on the north coast of Kangaroo Island. Prior to this, *E. bilobata* had only been described based on limited material from the shoreline localities of the Emu Bay Shale at Emu Bay and Big Gully. This paper utilises data from several thousand articulated specimens collected from two recently opened quarries approximately 400 m inland from the coastal exposures at Big Gully. Based on these, the entire post-embryonic ontogeny of *Estaingia bilobata* is described and reconstructed. Several morphological features not previously noted are also described, and the phylogenetic implications discussed. This represents one of the most complete growth series known for any trilobite, and forms the basis for the more in-depth study of trunk growth dynamics in Chapter 6. Fieldwork for the Emu Bay Shale part of the project (represented by Papers 1, 3 and 4) was conducted across five field seasons during the candidature: April 2017, September 2017, April 2018, September 2018 and April 2019. Extensive use was also made of material collected prior to this (mostly since 2007) and housed in the South Australian Museum.

Chapter 4 (Paper 2) describes the ontogeny of the trilobite *Redlichia cf. versabunda* from the Cambrian Series 2 (Stage 4) Ramsay Limestone of Yorke Peninsula in South Australia. It provides a counterpoint to Paper 1, as the material consists of a very different type of preservation, being comprised of three-dimensionally preserved disarticulated sclerites preserved in limestone (compared with the complete, articulated specimens compressed in mudstone presented in Paper 1). This preservation has resulted in some of the most well-preserved protaspides (the earliest trilobite growth stage) known. A relatively complete ontogenetic series of meraspid (juvenile) and holaspid (adult) cranidia is

described, as are various other sclerites. The tentative recognition of this species from South Australia provides a link with the Cambrian successions of northern Australia, and the potentially significant biostratigraphic implications are discussed. The majority of the material considered in this paper was collected by Mr Brent Bowman and has until recently been held in the unregistered collections of the South Australian Museum. A short field trip was made in December 2019 in an attempt to find the original fossil collection locality south of Curramulka, resulting in the collection of several additional specimens.

Chapter 5 (Paper 3) provides an in-depth study of the trilobite *Redlichia* from the Emu Bay Shale. *Redlichia* has been known from the Emu Bay Shale since the early 1950s, and it has long been thought that only one species (*Redlichia takoensis*) occurred in the formation. This paper demonstrates that certain specimens originally attributed to this species belong to a second, new species that was named *Redlichia rex*. The paper provides detailed descriptions of both species, a geometric morphometric analysis of ontogenetic shape change in holaspid (adult) specimens of *Redlichia takoensis*, as well as descriptions of soft-part anatomy; in particular the biramous appendages of *R. rex*, representing some of the most well-preserved examples for any trilobite. These display a distinctive tripartite exopod structure similar to certain other early Cambrian arthropods, the phylogenetic implications of which are discussed.

Chapter 6 (Paper 4) is an in-depth, quantitative analysis of trunk development during the meraspid (juvenile) period of *E. bilobata* from the Emu Bay Shale. This involved taking landmark measurements and analysing the relative axial lengths of different parts of the exoskeleton at different growth stages to determine how growth was controlled in this early arthropod. Such detailed analysis has only been published for one other trilobite species (the much younger *Aulacopleura koninckii* from the Silurian Period). This paper shows that similar trunk growth gradients to that discovered for *A. koninckii* also operated in the much older *E. bilobata*, although based on data from a wider portion of the meraspid period it appears that the latter species grew in a slightly different manner to that originally hypothesised for the former, and did not conform to the standard assumption of growth in arthropods (Dyar's Rule of a constant per-moult growth rate). The broader implications for understanding growth in trilobites are discussed.

Chapter 7 (Paper 5) places many of the findings and discussion points from the previous papers in a phylogenetic context. A previously published database of Cambrian

trilobites was used to create a smaller data matrix of species for which detailed ontogenetic information is known, including two of the species described in the preceding papers: *E. bilobata* (Papers 1 and 4) and *R. cf. versabunda* (Paper 2). Several new ontogenetic characters were added and existing characters modified. A phylogenetic tree was produced using a simple parsimony algorithm and the signal of the ontogenetic characters interpreted by how these mapped on the tree topology. The importance and limitations of ontogenetic characters in relation to trilobite phylogeny are discussed.

Chapter 8 concludes the thesis with a short discussion of the major findings of the study, and discusses future directions of research resulting from these.



## **Chapter 2**

### Background

## 2.1 Trilobites: an introduction

The trilobites are a class of marine arthropods that appeared in the early Cambrian Period (c. 521 Ma) and flourished during the early-mid Palaeozoic, after which they gradually declined, eventually disappearing in the great Permian-Triassic extinction event (c. 252 Ma)—a period of some 270 million years. Their biomineralised (calcitic) exoskeletons fossilised readily, and as such these animals have one of the best known fossil records, with over 22,000 known species (Adrain 2013; Paterson 2020). As arthropods, trilobites are members of the Ecdysozoa—animals that grow by periodically moulting their exoskeleton (Aguinaldo *et al.* 1997)—meaning that a single animal could produce many potential fossils.

The precise phylogenetic position of the group is somewhat debated (see Fig. 2.1). Trilobites are crown-group euarthropods and were formerly thought to be most closely related to chelicerates (Cotton & Braddy 2004). They are now placed within the Artiopoda (a group containing trilobites and their close relatives) and most likely represent stem-mandibulates based on patterns of head tagmosis (Scholtz & Edgecombe 2005; 2006).

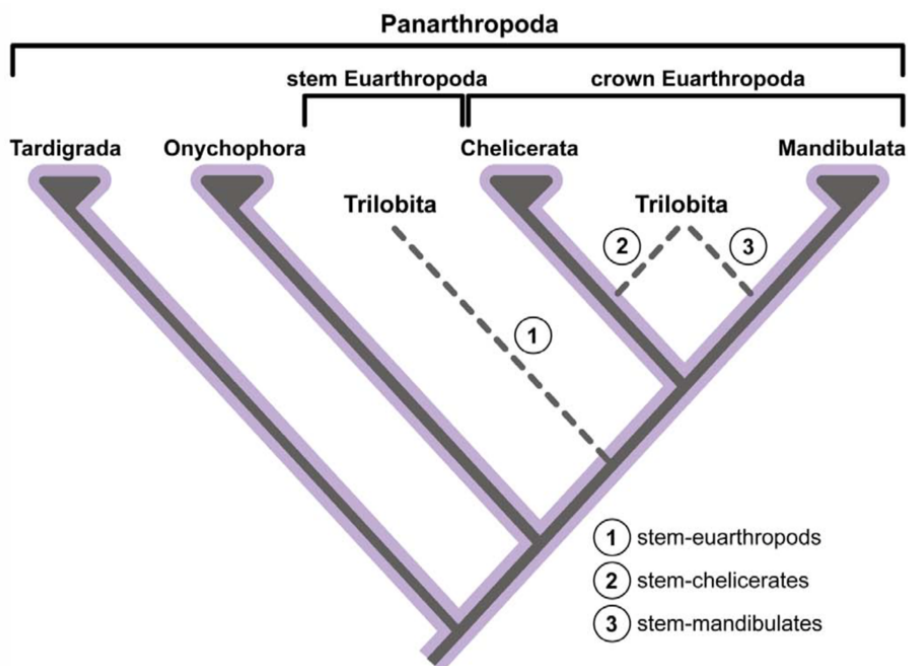


**Figure 2.1:** Major hypothesised positions for trilobites within the arthropod phylogenetic tree (modified from fig. 1 of Ortega-Hernández & Brena 2012).



## 2.2 The trilobite body plan

Mature trilobites are divided into three major sections along the anterior-posterior axis (Fig. 2.2): the cephalon (or head region), a thorax comprised of articulating segments, and a pygidium (or tail region). The name of the group, however, comes from the longitudinal trilobed division of the body. Trilobites have a distinctive central axial lobe defined by the glabella within the cephalon and the axial rings of the trunk (= thorax + pygidium), and two pleural lobes to either side (Fig. 2.2).

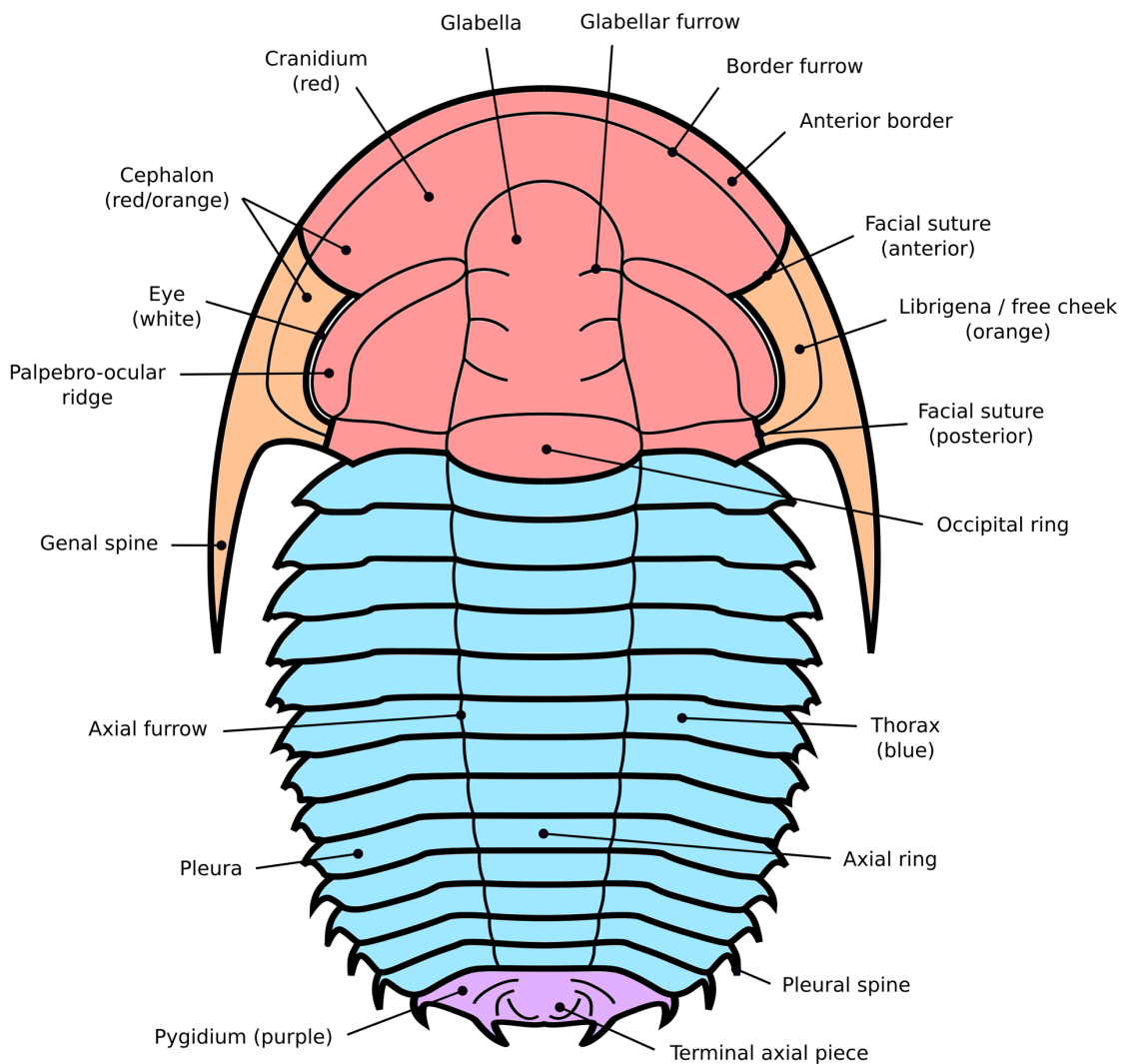


**Figure 2.2:** Dorsal anatomy of the trilobite *Estaimgia bilobata* from the Emu Bay Shale (Kangaroo Island, South Australia). This species exhibits the general features of the trilobites considered in this study, most of which are from the Order Redlichiida.

Knowledge of this group is based mainly on the morphology of the dorsal exoskeleton, which due to its original composition of (predominantly) calcium carbonate fossilised readily. Rare instances of appendages and other non-biomineralised structures such as muscle and gut tissue being preserved are known from certain *Konservat-Lagerstätten*, or fossil deposits that preserve 'soft parts' of organisms as well as skeletal material (e.g. Gutiérrez-Marco *et al.* 2017; Holmes *et al.* 2020b; Hou *et al.* 2009; Shu *et al.* 1995; Whittington 1975; 1980; Whittington & Almond 1987; Zeng *et al.* 2017). From these, it is known that trilobites generally had a single pair of pre-oral uniramous antennae, posterior to which were homonomous (i.e. of the same form), biramous (two-branched) appendages, each bearing an inner walking 'leg' or endopodite composed of multiple segment-like podomeres, and an outer exopodite that may have functioned to aerate the gills (Hughes 2003b, Suzuki & Bergström 2008). There were usually three pairs of biramous appendages in the cephalon, one pair for each thoracic segment, and likely one pair for all but the most posterior pygidial segments (Whittington 1997).

The homonomous nature of trilobite appendages has been called 'archaic' in contrast with the highly differentiated appendages between and within different tagmata (particularly cephalic appendages associated with feeding) in extant mandibulate arthropods (Budd 2000). The more limited level of tagmosis within trilobites, likely a more basal condition, makes it difficult to infer homologies with modern groups that show more derived traits. Nevertheless, certain trilobite body plan characteristics have been inferred to represent developmental homologies with extant arthropods, e.g. the anterior antennae, the cephalic/trunk boundary, and the caudal region (Hughes 2003a; b). Euarthropods share a basal condition of ten Hox genes, and the undifferentiated appendages of the cephalic tagma in trilobites suggest overlapping domains of Hox gene expression that produce more specialised structures in mandibulate arthropods, with the trunk also representing an area of overlapping expression domains similar to that seen in modern arthropods (Hughes 2003a; b). The antennae likely represent an area of Hox gene non-expression, e.g. it has been shown in the beetle *Tribolium* that the default appendages produced when Hox gene expression is inhibited are antennae (Beeman *et al.* 1993).

## 2.3 Trilobite ontogeny

Trilobite growth was direct, with no major metamorphoses, and followed a stepwise progression due to the moult cycle. Post-embryonic trilobite ontogeny has generally been divided into three major phases (Fig. 2.3). During the first, or protaspid period, the dorsal shield was composed of a single, fused plate (Chatterton & Speyer 1997). The meraspid period commenced when an articulation formed between the cephalon and the trunk. During the meraspid period, segments were generally added at a subterminal generative zone near the posterior of the pygidium, and released from the anterior to become fully articulating segments of the thorax—rates and timing of segment production and release varied between different taxa (Hughes *et al.* 2006). The holaspid period commenced when the full number of adult thoracic segments was achieved. The great majority of trilobites did not continuously add segments throughout life. Rather, they displayed what is termed hemianamorphic development, with an increasing number of segments during an initial anamorphic phase, followed by an epimorphic phase with continued moulting and growth after a stable segment number had been reached (Minelli *et al.* 2003).

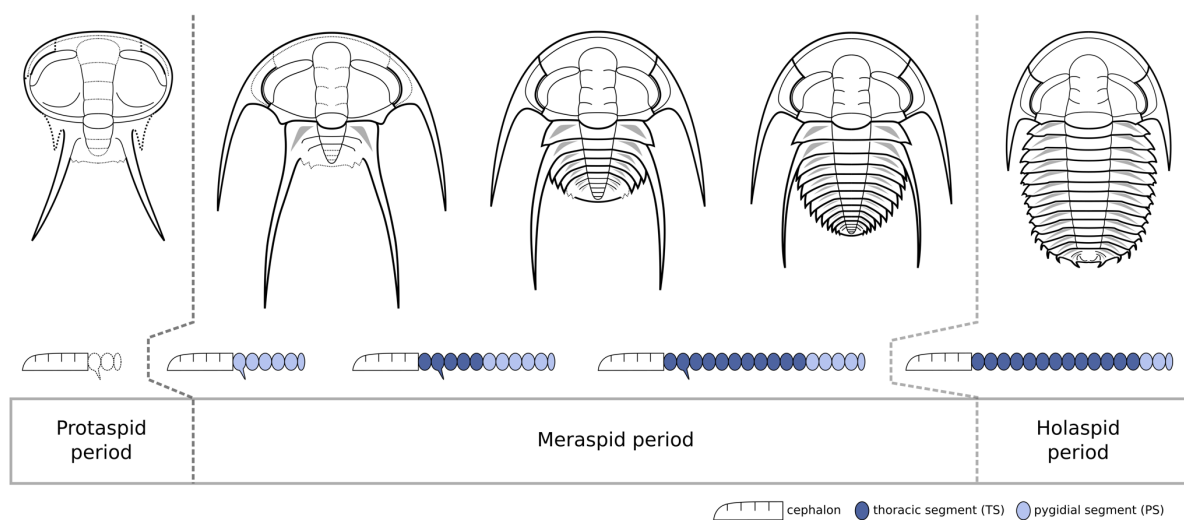


**Figure 2.3:** Simplified ontogeny of the early Cambrian ellipsocephaloid trilobite *Estaingia bilobata* progressing from protaspid through meraspid to the holaspid period. Only certain growth stages are shown here; the complete ontogenetic series of this trilobites is described in Chapter 3.

Ontogenetic series of articulated trilobites for which the majority of developmental stages are known are rare, although quite a number have been published in recent years

(e.g. Dai & Zhang 2013; Dai *et al.* 2014; 2017; Du *et al.* 2019; 2020; Holmes *et al.* 2020a; Hou *et al.* 2015; 2017; Hughes *et al.* 2017). In general, these have been largely limited to description/reconstruction, and traditional morphometrics, e.g. length/width ratios and Principle Component Analysis (PCA) of linear measurements. In contrast to other species, the growth dynamics of the Silurian trilobite *Aulacopleura koninckii* from the Czech Republic have been extensively studied over the past 25 years. Hughes and Chapman (1995) used PCA of linear measurements and landmark analysis to explore patterns of shape variation and segment number in *A. koninckii* during the meraspid and holaspid periods. An examination of growth control in the trunk region by Fusco *et al.* (2004) showed that growth during the meraspid period followed Dyar's rule, a geometric progression common in arthropod growth where the pre- to post-moult size ratio remains the same across ontogeny. A constancy in size variation across meraspid stages suggested that growth was targeted during this period, and that variation observed in the number of holaspid thoracic segments was determined early in development (Fusco *et al.* 2004). Geometric morphometric analysis of landmarks was conducted by Hammer and Harper (2006, p. 148) on a subset of the dataset of Hughes and Chapman (1995). They found several instances of ontogenetic shape change including allometries in cephalic structures, as well as evidence for tectonic shearing. Hong *et al.* (2014) re-examined patterns of growth in *A. koninckii* using geometric morphometrics on a new dataset, and found subtle size-related shape changes in both the cephalon and trunk during the meraspid period, while allometry was restricted to the trunk (mainly the pygidium) in holaspides. They also reiterated the gradual nature of shape change in this trilobite, in part due to the precise control of shape relative to size, despite a variable number of thoracic segments in adult forms. Fusco *et al.* (2014) examined relative thoracic segment size and position through meraspid ontogeny and identified an axial growth gradient in the trunk, with higher rates of growth towards the posterior. Modelling of this gradient suggested that growth of trunk segments was likely controlled by their changing position within a continuous growth field, which may have been under the control of signalling molecules such as morphogens. Similar axial growth gradients in the cephalon during the meraspid period, and both the cephalon and trunk during the holaspid period, were identified by Fusco *et al.* (2016). Hughes *et al.* (2017) modelled the ontogeny of *A. koninckii* using parameter estimates based on results of the previously mentioned studies, and in doing so moved away from the largely descriptive approach previously used

in ontogenetic reconstructions of fossil animals. Furthermore, Hughes *et al.* (2017) suggested that similar investigations focusing on early Cambrian trilobites, that prior to this study had not been undertaken, were likely to be of particular importance given their phylogenetically basal position, potentially allowing original character states to be identified. The comprehensive nature of investigations into development and growth control in *A. koninckii* provides something of a case study for similar studies focusing on other trilobites, such as *Estaingia bilobata* from the Emu Bay Shale (see below).

## 2.4 Cambrian geology and biostratigraphy of South Australia

Cambrian sediments crop out in South Australia within the Stansbury and Arrowie Basins and represent one of the most complete early Cambrian (Terreneuvian/Series 2) successions known anywhere in the world. These form part of a thick succession of Neoproterozoic-Cambrian sediments deposited within the Adelaide Geosyncline (also called the Adelaide Rift Complex or Adelaide Fold Belt) during a series of rift cycles beginning c. 827 Ma and associated with the breakup of Rodinia (Preiss 2000). Cambrian sedimentation is associated with the last of these cycles, commencing due to rifting associated with the Petermann Orogeny (550 Ma) and ending with the Delamerian Orogeny (~500 Ma) (Zang *et al.* 2004).

The Cambrian succession contains a diverse biota that includes trilobites, molluscs, archaeocyaths, brachiopods, acritarchs, coralomorphs and various other shelly fossils (Jago *et al.* 2006; 2018). Four trilobite zones are recognised in South Australia (in ascending order): the *Parabadiella huoi*, *Pararaia tatei*, *Pararaia bunyeroensis* and *Pararaia janeae* Zones (Jell in Bengtson *et al.* 1990) (Fig. 2.4). There is currently no zonation above these, with only three species recognised from younger horizons. In the Arrowie Basin, *Redlichia* cf. *versabunda* (previously identified as *Redlichia guizhouensis* and redescribed in Chapter 4) is known from the Wirrealpa Limestone and the Aroona Creek Limestone (Daily 1976; Jago & Zang 2006; Jell in Bengtson *et al.* 1990; Paterson & Brock 2007), and *Onarapsis rubra* from the Moodlatana Formation (Jell in Bengtson *et al.* 1990). In the Stansbury Basin *Redlichia* cf. *versabunda* is known from the Ramsay Limestone (see Chapter 4), and *Pagetia* cf. *edura* from

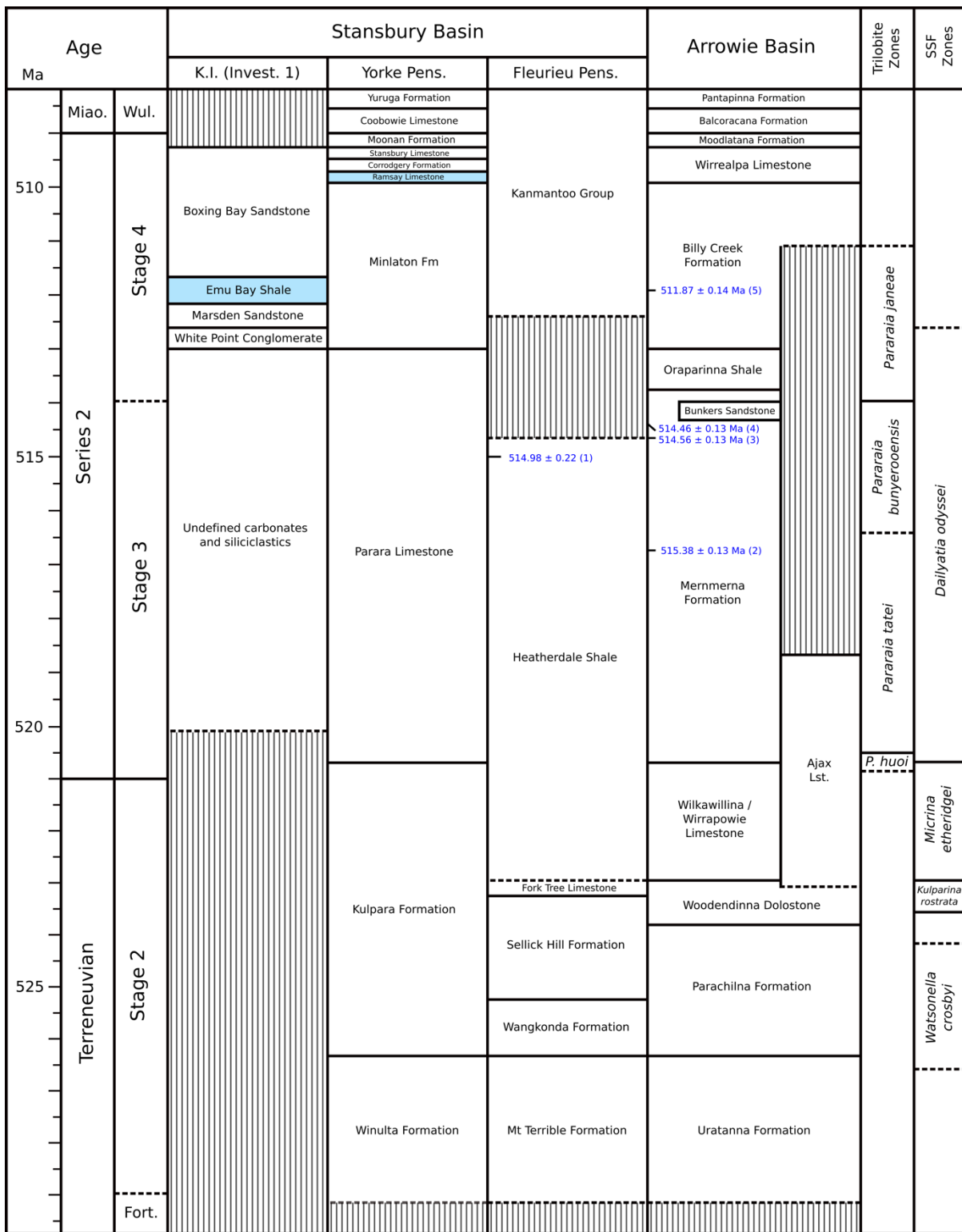


**Figure 2.4:** Correlation chart showing Cambrian sections in the Stansbury and Arrowie Basins of South Australia. From left to right: Investigator 1 drillhole in the vicinity of Big Gully (Kangaroo Island), Yorke Peninsula, Fleurieu Peninsula and Arrowie Basin. Correlations based mainly on those of Betts *et al.* (2018; *in review*) and Jago *et al.* (2012).

the Coobowie Limestone (the youngest trilobite known from South Australia and indicative of a Wuliuan age) (Jago & Kruse 2019). Recently, a new biostratigraphic scheme for the lower Cambrian of South Australia was established by Betts *et al.* (2016; 2017) based on three shelly fossil zones: the *Kulparina rostrata* Zone (oldest), *Micrina ehtheridgei* Zone, and the *Dailyatia odyssei* Zone (youngest). This was integrated with  $\delta^{13}\text{C}/\delta^{18}\text{O}$  isotope chemostratigraphic data and CA-TIMS radiometric dates by Betts *et al.* (2018), helping to robustly place these successions within a global context.

The fossil material considered directly in this study comes from the Kangaroo Island and Yorke Peninsula successions of the Stansbury Basin. The succession on Kangaroo Island contains the internationally recognised Emu Bay Shale *Konservat-Lagerstätte* (Cambrian Series 2, Stage 4). The vast majority of material dealt with here is sourced from the *Lagerstätte* (Chapters 3, 5 and 6), with the remainder coming from the younger (late Stage 4) Ramsay Limestone (Chapter 4) of the Yorke Peninsula succession (Fig. 2.4).

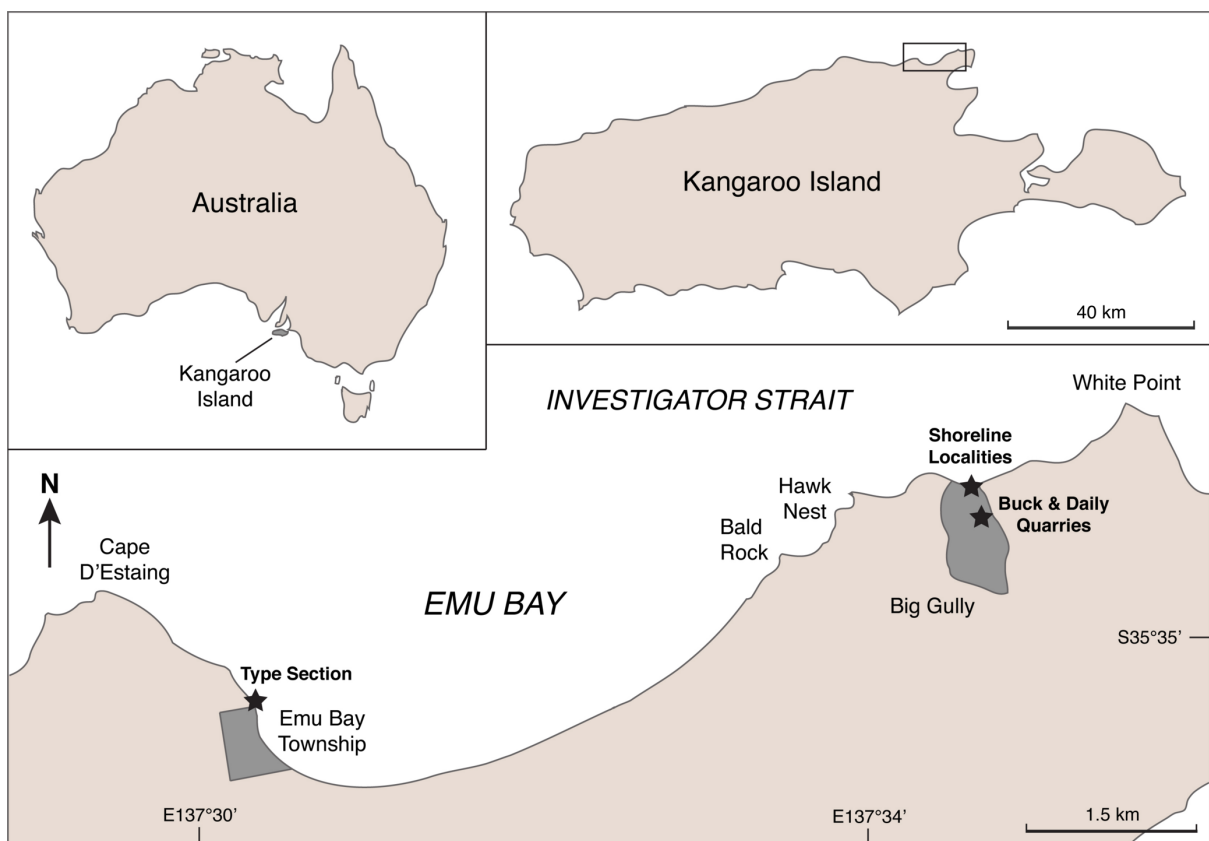


**Figure 2.5:** Map showing fossil localities of the Emu Bay Shale on the north coast of Kangaroo Island, South Australia. The locality adjacent to the Emu Bay township has long been considered the ‘type section’ of the formation; but see discussion in Jago *et al.* (2020).

## 2.5 The Emu Bay Shale *Lagerstätte*

The Emu Bay Shale from Kangaroo Island, South Australia, contains one of the most important Cambrian fossil deposits in the world, housing the only known Cambrian *Konservat-Lagerstätte* in the Southern Hemisphere. South Australian geologist R. C. Sprigg discovered the first fossils from the Emu Bay Shale in 1952, when he found trilobites in what has long been considered the type-section of the formation (but see discussion in Jago *et al.* 2020), approximately 200 m northwest of the Emu Bay jetty on the north coast of Kangaroo Island (Sprigg 1955) (Fig. 2.5). In late 1954, University of Adelaide PhD student B. Daily discovered the Emu Bay Shale *Lagerstätte* when he found soft-bodied fossils and trilobites near the mouth of 'Big Gully', approximately 7 km east of the Emu Bay township (Daily 1956). Pocock (1964) described the trilobite *Estaingia bilobata* (with material from both localities), but interestingly no formal description of soft-bodied material collected from the Big Gully locality was published until Glaessner (1979) described the 'bivalved' arthropods *Isoxys communis* and *Tuzoia australis*, as well as the palaeoscolecoid *Palaeoscolex antiquus* (now assigned to *Wronascolex*; see García-Bellido *et al.* 2013b) and the problematic 'worms' *Myoscolex ateles* and *Vetustovermis planus*. Jell in Bengtson *et al.* (1990) described a large redlichiid trilobite from the *Lagerstätte* as *Redlichia takooensis*, originally known from South China (Lu 1950). The first specimens of the giant Cambrian predatory stem-arthropod *Anomalocaris* were described by McHenry and Yates (1993), and a PhD project undertaken by Chris Nedin shortly afterwards resulted in a series of papers (Nedin 1995b; 1997; 1999; Nedin & Jenkins 1999). More recently, Paterson and Jago (2006) described two new species of trilobite, *Holyoakia simpsoni* and *Megapharanaspis nedini*, from Big Gully.

In 2007, excavation of a new site ('Buck Quarry' after landowners P. and C. Buck) was commenced approximately 400 m inland from the coastal outcrops that has yielded a range of taxa previously unknown from the Emu Bay Shale (Daley *et al.* 2013; Edgecombe *et al.* 2011; García-Bellido *et al.* 2009; 2013a; 2013b; 2014; Paterson *et al.* 2010; 2011; 2012; 2015). The biota now comprises some 50 species including sponges, cancellorids, brachiopods, hyoliths, polychaetes, lobopodians, soft-bodied arthropods, trilobites and vetulicolians (Paterson *et al.* 2016). For a comprehensive summary of the history of investigations into the Emu Bay Shale, see Jago and Cooper (2011).

The *Lagerstätte* occurs mainly within the lower 10–12 m of the formation and is



preserved in dark grey mudstones interspersed with centimetre-scale silt and fine sand horizons, the depositional environment of which is interpreted to represent a pro-delta expression of a fan delta complex, adjacent to a zone of active tectonic uplift to the north of present day coastline (Gehling *et al.* 2011; Paterson *et al.* 2018). The Emu Bay Shale forms part of the Kangaroo Island Group, and is 78 m thick at the coast (Daily *et al.* 1979) and approximately 60 m thick at Buck Quarry, with the *Lagerstätte*-bearing mudstones eventually pinching out 150–200 m further south (García-Bellido *et al.* 2009). The formation unconformably overlies the Marsden Sandstone (formerly the top of the White Point Conglomerate, see Gehling *et al.* 2011) and is conformably overlain by the Boxing Bay Formation at the coast; although the latter channels into the Emu Bay Shale further inland (Daily *et al.* 1979; Gehling *et al.* 2011). The geology of the Emu Bay Shale is described in detail by Gehling *et al.* (2011)—also see Hall *et al.* (2011), Gaines (2014) and McKirdy *et al.* (2011).

The Emu Bay Shale has been correlated with the lower Cambrian (Series 2, Stage 4) *Pararaia janeae* trilobite zone of mainland South Australia (Bengtson *et al.* 1990; Betts *et al.* 2018; Paterson & Brock 2007), and is dated at approximately 512 Ma.

## 2.6 Emu Bay Shale trilobites

The Emu Bay Shale *Lagerstätte* contains abundant specimens of the trilobites *Redlichia takooensis* and *Estaingia bilobata*, the latter being present on surfaces in densities of up to 630 individuals per square metre (J. R. Paterson, unpub. data). Rarer species include *Redlichia rex* (see below), *Balcoracania dailyi*, *Megapharanaspis nedini* and *Holyoakia simpsoni* (Paterson & Jago 2006; Pocock 1970).

*Estaingia bilobata* is a small ellipsocephaloid trilobite (holaspid specimens range from c. 5–30 mm in length) with 13 thoracic segments, narrow librigenae with long genal spines, and a short, wide pygidium with two pairs of marginal spines. Meraspides of *E. bilobata* are common within the Emu Bay Shale, representing an essentially complete ontogenetic series. Chapter 3 provides a comprehensive description of this, and Chapter 6 investigates patterns of growth in relation to trunk segmentation across the series. *Estaingia bilobata* was first described by Pocock (1964), as part of which he used regression

analysis of basic linear cranial measurements as support for a single population (or species)—although he did not figure or discuss any juvenile specimens. Nedin (1995a) briefly discussed the ontogeny of this species, describing meraspides of degree (number of thoracic segments) 1, 7, 10 and 12, from the small number of specimens (possibly six) he had available. He also used biplots of several linear measurements to discuss changes in cranial proportions across ontogeny (mainly in holaspides). Nedin and Jenkins (1999) used linear measurements to compare ontogenies of *E. bilobata* with the closely related middle Cambrian *Xystridura* and suggested that the latter evolved from the former via heterochrony (a change in the timing/rate of development resulting in a change in size/shape).

Prior to this study it was thought that only one species of *Redlichia* occurred within the Emu Bay Shale. This species (originally identified as '*R. takoensis*') was thought to have a very large size range, across which occurred obvious changes in relative proportions (particularly within the cephalon), with larger specimens exhibiting narrower posterior margins of the librigenae, smaller intergenal angles, and longer genal spines (Paterson & Jago 2006). Chapter 5 recognises that these specimens actually represent two species: the smaller, more common *R. takoensis*, and a new species that was named *Redlichia rex* due to its very large size (Fig. 2.6). Various instances of soft-part preservation in *Redlichia* are known from the Emu Bay Shale, including biramous appendages, antennae and digestive structures; these are also described in Chapter 5. In contrast to *E. bilobata*, there are very few confirmed meraspides of *R. takoensis* from the Emu Bay Shale (only one specimen is reliably identified as a late-stage meraspis), although ontogenetic change in the proportions of certain structures is recognised in holaspides and investigated in Chapter 5 using geometric morphometrics.

Fossil deposits that preserve trilobites are often dominated by disarticulated exoskeletons due to scavenging of remains, winnowing and aggregation by water movement, or containing moulted exuviae. However, the conditions responsible for exceptional soft-part preservation within the Emu Bay Shale are also conducive to preserving complete trilobite specimens. It is suggested that fluctuations of the oxycline (i.e. the boundary between oxic and anoxic conditions) was responsible for 'mass kill' events within the deposit (Paterson *et al.* 2016). Anoxic or dysoxic conditions would have both suppressed scavenging activity and slowed the decay of soft tissue (including integument

holding the dorsal shield together), allowing specimens to become buried before disarticulation occurred. There is also little evidence for water movement at stratigraphic levels where soft-bodied preservation occurs (Gehling *et al.* 2011). The combination of abundant and complete trilobite specimens within the Emu Bay Shale provides the perfect opportunity to examine post-embryonic development in some of the oldest known arthropods.



**Figure 2.6:** The holotype specimen of *Redlichia rex* from the Emu Bay Shale (Kangaroo Island, South Australia). This species is described in Chapter 5. Specimen is 11.9 cm long.

## 2.7 References

- Adrain, J.M.** 2013. A synopsis of Ordovician trilobite distribution and diversity. Pp. 297–336 in D.A.T. Harper and T. Servais (eds) *Early Palaeozoic Biogeography and Palaeogeography. Geological Society of London, Memoir, 38.*
- Aguinaldo, A.M.A., Turbeville, J.M., Linford, L.S., Rivera, M.C., Garey, J.R., Raff, R.A. & Lake, J.A.** 1997. Evidence for a clade of nematodes, arthropods and other moulting animals. *Nature*, **387**: 489–493.

- Beeman, R.W., Stuart, J.J., Brown, S.J. & Denell, R.E.** 1993. Structure and function of the homeotic gene complex, (HOM-C) in the beetle, *Tribolium castaneum*. *Bioessays*, **15**: 439–444.
- Bengtson, S., Conway Morris, S., Cooper, B.J., Jell, P.A. & Runnegar, B.N.** 1990. Early Cambrian fossils from South Australia. *Memoirs of the Association of Australasian Palaeontologists*, **9**: 1–364.
- Betts, M.J., Claybourn, T.M., Holmer, L.E., Skovsted, C.B., Myrow, P.M., Stemmerik, L., Topper, T.P., Park, T-Y. S., Hughes, N.C. and Brock, G.A.** *In review*. Integrated chronostratigraphy of the lower Cambrian Byrd Group, Transantarctic Mountains. *Geology*.
- Betts, M.J., Paterson, J.R., Jacquet, S.M., Andrew, A.S., Hall, P.A., Jago, J.B., Jagodzinski, E.A., Preiss, W.V., Crowley, J.L., Brougham, T., Mathewson, C.P., García-Bellido, D.C., Topper, T.P., Skovsted, C.B. & Brock, G.A.** 2018. Early Cambrian chronostratigraphy and geochronology of South Australia. *Earth-Science Reviews*, **185**: 498–543.
- Betts, M.J., Paterson, J.R., Jago, J.B., Jacquet, S.M., Skovsted, C.B., Topper, T.P. & Brock, G.A.** 2016. A new lower Cambrian shelly fossil biostratigraphy for South Australia. *Gondwana Research*, **36**: 176–208.
- Betts, M.J., Paterson, J.R., Jago, J.B., Jacquet, S.M., Skovsted, C.B., Topper, T.P. & Brock, G.A.** 2017. Global correlation of the early Cambrian of South Australia: Shelly fauna of the *Dalmanites* Zone. *Gondwana Research*, **46**: 240–279.
- Budd, G.E.** 2000. Ecology of nontrilobite arthropods and lobopods in the Cambrian. Pp. 404–427 in A.Y. Zhuravlev and R. Riding (eds) *The Ecology of the Cambrian Radiation*. Columbia University Press, New York.
- Chatterton, B.D.E. & Speyer, S.E.** 1997. Ontogeny. Pp. 173–247 in R.L. Kaesler (ed) *Treatise on Invertebrate Paleontology, Part O, Revised. Arthropoda 1, Trilobita 1, (Introduction, Order Agnostida, Order Redlichiida)*. Geological Society of America and University of Kansas Paleontological Institute, Boulder, Colorado and Lawrence, Kansas.
- Cotton, T.J. & Braddy, S.J.** 2004. The phylogeny of arachnomorph arthropods and the origin of the Chelicerata. *Transactions of the Royal Society of Edinburgh: Earth Sciences*, **94**: 169–193.
- Dai, T. & Zhang, X.** 2012. Ontogeny of the redlichiid trilobite *Metaredlichia cylindrica* from the lower Cambrian (Stage 3) of South China. *Journal of Paleontology*, **86**: 646–651.

- Dai, T. & Zhang, X.** 2013. Ontogeny of the redlichiid trilobite *Eoredlichia intermediata* from the Chengjiang Lagerstätte, lower Cambrian, southwest China. *Lethaia*, **46**: 262–273.
- Dai, T., Zhang, X. & Peng, S.** 2014. Morphology and ontogeny of *Hunanocephalus ovalis* (trilobite) from the Cambrian of South China. *Gondwana Research*, **25**: 991–998.
- Dai, T., Zhang, X.-L., Peng, S.-C. & Yao, X.-Y.** 2017. Intraspecific variation of trunk segmentation in the oryctocephalid trilobite *Duyunaspis duyunensis* from the Cambrian (Stage 4, Series 2) of South China. *Lethaia*, **50**: 527–539.
- Daily, B.** 1956. The Cambrian in South Australia. Pp. 91-147 in J. Rodgers (ed) *El sistema Cámbrico, su palaeogeografía y el problema de su base*. 20th International Geological Congress, Mexico, 1956.
- Daily, B.** 1976. The Cambrian of the Flinders Ranges: 25th International Geological Congress, Excursion Guide 33A, pp. 15–19.
- Daily, B., Milnes, A.R., Twidale, C.R. & Bourne, J.A.** 1979. Geology and geomorphology. Pp. 1–38 in M.J. Tyler, J.K. Ling and C.R. Twidale (eds) *Natural History of Kangaroo Island*. Royal Society of South Australia, Adelaide.
- Daley, A.C., Paterson, J.R., Edgecombe, G.D., García-Bellido, D.C., Jago, J.B.** 2013. New anatomical information on *Anomalocaris* from the Cambrian Emu Bay Shale of South Australia and a reassessment of its inferred predatory habits. *Palaeontology*, **56**: 971-990.
- Du, G.-Y., Peng, J., Wang, D.-Z., Wang, Q.-J., Wang, Y.-F. & Zhang, H.** 2019. Morphology and developmental traits of the trilobite *Changaspis elongata* from the Cambrian Series 2 of Guizhou, South China. *Acta Palaeontologica Polonica*, **64**: 797–813.
- Du, G.-Y., Peng, J., Wang, D.-Z., Wen, R.-Q. & Liu, S.** 2020. Morphology and trunk development of the trilobite *Arthricocephalus chauveaui* from the Cambrian Series 2 of Guizhou, South China. *Historical Biology*, **32**: 174–186.
- Edgecombe, G.D., García-Bellido, D.C. & Paterson, J.R.** 2011. A new leanchoiliid megacheiran arthropod from the lower Cambrian Emu Bay Shale, South Australia. *Acta Palaeontologica Polonica*, **56**: 385–400.
- Fusco, G., Hong, P.S. & Hughes, N.C.** 2014. Positional specification in the segmental growth pattern of an early arthropod. *Proceedings of the Royal Society of London B*, **281**: 20133037.

- Fusco, G., Hong, P.S. & Hughes, N.C.** 2016. Axial growth gradients across the postprotaspid ontogeny of the Silurian trilobite *Aulacopleura koninckii*. *Paleobiology*, **42**: 426–438.
- Fusco, G., Hughes, N.C., Webster, M. & Minelli, A.** 2004. Exploring developmental modes in a fossil arthropod: growth and trunk segmentation of the trilobite *Aulacopleura koninckii*. *The American Naturalist*, **163**: 167–183.
- Gaines, R.R.** 2014. Burgess Shale-type preservation and its distribution in space and time. Pp. 123–146 in M. Laflamme, J.D. Schiffbauer and S.A.F. Darroch (eds) *Reading and Writing of the Fossil Record: Preservational Pathways to Exceptional Fossilization. The Paleontological Society Papers*, **20**.
- García-Bellido, D.C., Edgecombe, G.D., Paterson, J.R. & Ma, X.** 2013a. A ‘Collins’ monster’-type lobopodian from the Emu Bay Shale Konservat-Lagerstätte (Cambrian), South Australia. *Alcheringa*, **37**: 474–478.
- García-Bellido, D.C., Lee, M.S.Y., Edgecombe, G.D., Jago, J.B., Gehling, J.G. & Paterson, J.R.** 2014. A new vetulicolian from Australia and its bearing on the chordate affinities of an enigmatic Cambrian group. *BMC Evolutionary Biology*, **14**: 214.
- García-Bellido, D.C., Paterson, J.R. & Edgecombe, G.D.** 2013b. Cambrian palaeoscolecids (Cycloneuralia) from Gondwana and reappraisal of species assigned to *Palaeoscolex*. *Gondwana Research*, **24**: 780–795.
- García-Bellido, D.C., Paterson, J.R., Edgecombe, G.D., Jago, J.B., Gehling, J.G. & Lee, M.S.Y.** 2009. The bivalved arthropods *Isoxys* and *Tuzoia* with soft-part preservation from the Lower Cambrian Emu Bay Shale Lagerstätte (Kangaroo Island, Australia). *Palaeontology*, **52**: 1221–1241.
- Gehling, J.G., Jago, J.B., Paterson, J.R., García-Bellido, D.C. & Edgecombe, G.D.** 2011. The geological context of the Lower Cambrian (Series 2) Emu Bay Shale Lagerstätte and adjacent stratigraphic units, Kangaroo Island, South Australia. *Australian Journal of Earth Sciences*, **58**: 243–257.
- Glaessner, M.F.** 1979. Lower Cambrian Crustacea and annelid worms from Kangaroo Island, South Australia. *Alcheringa*, **3**: 21–31.
- Gutiérrez-Marco, J.C., García-Bellido, D.C., Rábano, I. & Sá, A.A.** 2017. Digestive and appendicular soft-parts, with behavioural implications, in a large Ordovician trilobite from the Fezouata Lagerstätte, Morocco. *Scientific Reports*, **7**: 39728.

- Hall, P.A., McKirdy, D.M., Halverson, G.P., Jago, J.B. & Gehling, J.G.** 2011. Biomarker and isotopic signatures of an early Cambrian Lagerstätte in the Stansbury Basin, South Australia. *Organic Geochemistry*, **42**: 1324–1330.
- Hammer, Ø. & Harper, D.A.T.** 2006. *Paleontological Data Analysis*. Blackwell Publishing, Oxford.
- Holmes, J.D., Paterson, J.R. & García-Bellido, D.C.** 2020a. The post-embryonic ontogeny of the early Cambrian trilobite *Estaingia bilobata* from South Australia: trunk development and phylogenetic implications. *Papers in Palaeontology*: doi:10.1002/spp2.1323.
- Holmes, J.D., Paterson, J.R. & García-Bellido, D.C.** 2020b. The trilobite *Redlichia* from the lower Cambrian Emu Bay Shale Konservat-Lagerstätte of South Australia: systematics, ontogeny and soft-part anatomy. *Journal of Systematic Palaeontology*, **18**: 295–334.
- Hong, P.S., Hughes, N.C. & Sheets, H.D.** 2014. Size, shape, and systematics of the Silurian trilobite *Aulacopleura koninckii*. *Journal of Paleontology*, **88**: 1120–1138.
- Hou, J.-B., Hughes, N.C., Lan, T., Yang, J. & Zhang, X.-G.** 2015. Early postembryonic to mature ontogeny of the oryctocephalid trilobite *Duodingia duodingensis* from the lower Cambrian (Series 2) of southern China. *Papers in Palaeontology*, **1**: 497–513.
- Hou, J.-B., Hughes, N.C., Yang, J., Lan, T., Zhang, X.-G. & Dominguez, C.** 2017. Ontogeny of the articulated yiliangellinine trilobite *Zhangshania typica* from the lower Cambrian (Series 2, Stage 3) of southern China. *Journal of Paleontology*, **91**: 86–99.
- Hou, X., Clarkson, E.N.K., Yang, J., Zhang, X., Wu, G. & Yuan, Z.** 2009. Appendages of early Cambrian *Eoredlichia* (Trilobita) from the Chengjiang biota, Yunnan, China. *Earth and Environmental Science Transactions of the Royal Society of Edinburgh*, **99**: 213–223.
- Hughes, N.C.** 2003a. Trilobite body patterning and the evolution of arthropod tagmosis. *Bioessays*, **25**: 386–395.
- Hughes, N.C.** 2003b. Trilobite tagmosis and body patterning from morphological and developmental perspectives. *Integrative and Comparative Biology*, **43**: 185–206.
- Hughes, N.C. & Chapman, R.E.** 1995. Growth and variation in the Silurian proetide trilobite *Aulacopleura koninckii* and its implications for trilobite palaeobiology. *Lethaia*, **28**: 333–353.
- Hughes, N.C., Hong, P.S., Hou, J. & Fusco, G.** 2017. The development of the Silurian trilobite *Aulacopleura koninckii* reconstructed by applying inferred growth and segmentation dynamics: a case study in Paleo-Evo-Devo. *Frontiers in Ecology and Evolution*, **5**: 37.

- Hughes, N.C., Minelli, A. & Fusco, G.** 2006. The ontogeny of trilobite segmentation: a comparative approach. *Paleobiology*, **32**: 602–627.
- Jago, J.B., Bentley, C.J., Paterson, J.R., Holmes, J.D., Lin, T.R. & Sun, X.W.** 2020. The stratigraphic significance of early Cambrian (Series 2, Stage 4) trilobites from the Smith Bay Shale near Freestone Creek, Kangaroo Island. *Australian Journal of Earth Sciences*: doi:10.1080/08120099.2020.1749882.
- Jago, J.B. & Cooper, B.J.** 2011. The Emu Bay Shale Lagerstätte: a history of investigations. *Australian Journal of Earth Sciences*, **58**: 235–241.
- Jago, J.B., Gehling, J.G., Betts, M.J., Brock, G.A., Dalgarno, C.R., García-Bellido, D.C., Haslett, P.G., Jacquet, S.M., Kruse, P.D., Langsford, N.R., Mount, T.J. & Paterson, J.R.** 2018. The Cambrian System in the Arrowie Basin, Flinders Ranges, South Australia. *Australian Journal of Earth Sciences*: doi:10.1080/08120099.08122018.01525431.
- Jago, J.B., Gehling, J.G., Paterson, J.R., Brock, G.A. & Zang, W.** 2012. Cambrian stratigraphy and biostratigraphy of the Flinders Ranges and the north coast of Kangaroo Island, South Australia. *Episodes*, **35**: 247–255.
- Jago, J.B. & Kruse, P.D.** 2019. Significance of the middle Cambrian (Wuliuan) trilobite *Pagetia* from Yorke Peninsula, South Australia. *Australian Journal of Earth Sciences*: doi:10.1080/08120099.2019.1643405.
- Jago, J.B., Zang, W.-L., Sun, X., Brock, G.A., Paterson, J.R. & Skovsted, C.B.** 2006. A review of the Cambrian biostratigraphy of South Australia. *Palaeoworld*, **15**: 406–423.
- Jago, J.B. & Zang, W.L. (eds)** 2006. *XI International Conference of the Cambrian Stage Subdivision Working Group: Field Guide*. Geological Society of Australia, South Australian Division, Adelaide, 59 pp.
- Lu, Y.-H.** 1950. On the genus *Redlichia* with description of its new species. *Geological Review*, **15**: 157–170.
- McHenry, B. & Yates, A.** 1993. First report of the enigmatic metazoan *Anomalocaris* from the Southern Hemisphere and a trilobite with preserved appendages from the Early Cambrian of Kangaroo Island, South Australia. *Records of the South Australian Museum*, **26**: 77–86.
- McKirdy, D.M., Hall, P.A., Nedin, C., Halverson, G.P., Michaelsen, B.H., Jago, J.B., Gehling, J.G. & Jenkins, R.J.F.** 2011. Paleoredox status and thermal alteration of the lower



Cambrian (Series 2) Emu Bay Shale Lagerstätte, South Australia. *Australian Journal of Earth Sciences*, **58**: 259–272.

- Minelli, A., Fusco, G. & Hughes, N.C.** 2003. Tagmata and segment specification in trilobites. *Special Papers in Palaeontology*, **70**: 31–43.
- Nedin, C.** 1995a. The Emu Bay Shale, a Lower Cambrian fossil Lagerstätten, Kangaroo Island, South Australia. *Memoirs of the Association of Australasian Palaeontologists*, **18**: 31–40.
- Nedin, C.** 1995b. The palaeontology and palaeoenvironment of the Early Cambrian Emu Bay Shale, Kangaroo Island, South Australia. Unpublished PhD thesis, University of Adelaide.
- Nedin, C.** 1997. Taphonomy of the Early Cambrian Emu Bay Shale Lagerstätte, Kangaroo Island, South Australia. *Bulletin of National Museum of Natural Science*, **10**: 133–141.
- Nedin, C.** 1999. *Anomalocaris* predation of nonmineralized and mineralized trilobites. *Geology*, **27**: 987–990.
- Nedin, C. & Jenkins, R.J.F.** 1999. Heterochrony in the Cambrian trilobite *Hsuaspis*. *Alcheringa*, **23**: 1–7.
- Ortega-Hernández, J. & Brena, C.** 2012. Ancestral patterning of tergite formation in a centipede suggests derived mode of trunk segmentation in trilobites. *PLoS ONE*, **7**: e52623.
- Paterson, J.R.** 2020. The trouble with trilobites: classification, phylogeny and the cryptogenesis problem. *Geological Magazine*, **157**: 35–46.
- Paterson, J.R. & Brock, G.A.** 2007. Early Cambrian trilobites from Angorichina, Flinders Ranges, South Australia, with a new assemblage from the *Pararaia bunyeroensis* Zone. *Journal of Paleontology*, **81**: 116–142.
- Paterson, J.R., Edgecombe, G.D., García-Bellido, D.C., Jago, J.B. & Gehling, J.G.** 2010. Nektaspid arthropods from the Lower Cambrian Emu Bay Shale Lagerstätte, South Australia, with a reassessment of lamellipedian relationships. *Palaeontology*, **53**: 377–402.
- Paterson, J.R., Edgecombe, G.D. & Jago, J.B.** 2015. The ‘great appendage’ arthropod *Tanglangia*: biogeographic connections between early Cambrian biotas of Australia and South China. *Gondwana Research*, **27**: 1667–1672.
- Paterson, J.R., Gaines, R.R., García-Bellido, D.C. & Jago, J.B.** 2018. The Emu Bay Shale fan delta complex: palaeoenvironmental conditions affecting the community structure of a

- unique Cambrian Lagerstätte. P. 59 in *International Conference on Ediacaran and Cambrian Sciences, Programme and Abstracts*, 196 pp. 12–16 August, Xi'an, China.
- Paterson, J.R., García-Bellido, D.C. & Edgecombe, G.D.** 2012. New artiopodan arthropods from the early Cambrian Emu Bay Shale Konservat-Lagerstätte of South Australia. *Journal of Palaeontology*, **86**: 340–357.
- Paterson, J.R., García-Bellido, D.C., Jago, J.B., Gehling, J.G., Lee, M.S.Y. & Edgecombe, G.D.** 2016. The Emu Bay Shale Konservat-Lagerstätte: a view of Cambrian life from East Gondwana. *Journal of the Geological Society, London*, **173**: 1–11.
- Paterson, J.R., García-Bellido, D.C., Lee, M.S.Y., Brock, G.A., Jago, J.B. & Edgecombe, G.D.** 2011. Acute vision in the giant Cambrian predator *Anomalocaris* and the origin of compound eyes. *Nature*, **480**: 237–240.
- Paterson, J.R. & Jago, J.B.** 2006. New trilobites from the lower Cambrian Emu Bay Shale Lagerstätte at Big Gully, Kangaroo Island, South Australia. *Memoirs of the Association of Australasian Palaeontologists*, **32**: 43–57.
- Pocock, K.J.** 1964. *Estaingia*, a new trilobite genus from the lower Cambrian of South Australia. *Palaeontology*, **7**: 458–471.
- Pocock, K.J.** 1970. The Emuellidae, a new family of trilobites from the lower Cambrian of South Australia. *Palaeontology*, **13**: 522–562.
- Preiss, W.V.** 2000. The Adelaide Geosyncline of South Australia and its significance in Neoproterozoic continental reconstruction. *Precambrian Research*, **100**: 21–63.
- Scholtz, G. & Edgecombe, G.D.** 2005. Heads, Hox and the phylogenetic position of trilobites. Pp. 139–165 in S. Koenemann and R.A. Jenner (eds) *Crustacea and Arthropod Relationships*. CRC Press, Boca Raton.
- Scholtz, G. & Edgecombe, G.D.** 2006. The evolution of arthropod heads: reconciling morphological, developmental and palaeontological evidence. *Development genes and evolution*, **216**: 395–415.
- Shu, D., Geyer, G., Chen, L. & Zhang, X.** 1995. Redlichiacean trilobites with preserved soft-parts from the Lower Cambrian Chengjiang fauna (South China). *Berigeria, Special Issue*, **2**: 203–241.
- Sprigg, R.C.** 1955. The Point Marsden Cambrian beds, Kangaroo Island, South Australia. *Transactions of the Royal Society of South Australia*, **78**: 165–168.

- Suzuki, Y. & Bergström, J.** 2008. Respiration in trilobites: a reevaluation. *Gff*, **130**: 211–229.
- Whittington, H.B.** 1975. Trilobites with appendages from the Middle Cambrian, Burgess Shale, British Columbia. *Fossils and Strata*, **4**: 97–136.
- Whittington, H.B.** 1980. Exoskeleton, moult stage, appendage morphology, and habits of the Middle Cambrian trilobite *Olenoides serratus*. *Palaeontology*, **23**: 171–204.
- Whittington, H.B. & Almond, J.E.** 1987. Appendages and Habits of the Upper Ordovician Trilobite *Triarthrus eatoni*. *Philosophical Transactions of the Royal Society B: Biological Sciences*, **317**: 1–46.
- Whittington, H.B.** 1997. The Trilobite Body. Pp. 87–135 in R.L. Kaesler (ed) *Treatise on Invertebrate Paleontology, Part O, Revised. Arthropoda 1, Trilobita 1, (Introduction, Order Agnostida, Order Redlichiida)*. Geological Society of America and University of Kansas Paleontological Institute, Boulder, Colorado and Lawrence, Kansas.
- Zang, W.-L., Jago, J.B., Alexander, E.M. & Paraschivoiu, E.** 2004. A review of basin evolution, sequence analysis and petroleum potential of the frontier Arrowie Basin, South Australia. Pp. 243–256 in P.J. Boulton, D.R. Johns and S.C. Lang (eds) *PESA Eastern Australasian Basins Symposium II, Adelaide, 19–22 September, 2004*. Petroleum Exploration Society of Australia, Special Publication.
- Zeng, H., Zhao, F., Yin, Z. & Zhu, M.** 2017. Appendages of an early Cambrian metadoxidid trilobite from Yunnan, SW China support mandibulate affinities of trilobites and arthropods. *Geological Magazine*, **154**: 1306–1328.



## Chapter 3

The post-embryonic ontogeny of the early Cambrian trilobite *Estaingia bilobata* from South Australia: trunk development and phylogenetic implications

**Holmes, J.D., Paterson, J.R. & García-Bellido, D.C.** 2020. The post-embryonic ontogeny of the early Cambrian trilobite *Estaingia bilobata* from South Australia: trunk development and phylogenetic implications. *Papers in Palaeontology*, doi.org/10.1002/spp2.1323.

## Statement of Authorship

|                      |  |
|----------------------|--|
| Title of paper:      | The post-embryonic ontogeny of the early Cambrian trilobite <i>Estaingia bilobata</i> from South Australia: trunk development and phylogenetic implications  |
| Publications status  | Published  |
| Publication details: | Holmes, J.D., Paterson, J.R. & García-Bellido, D.C. 2020a . The post-embryonic ontogeny of the early Cambrian trilobite <i>Estaingia bilobata</i> from South Australia: trunk development and phylogenetic implications. <i>Papers in Palaeontology</i> , doi.org/10.1002/spp2.1323. |

### Principal author

|                                      |  |
|--------------------------------------|--|
| Name of principal author (candidate) | James D. Holmes  |
| Contribution to the paper            | Collected specimens, measured and photographed all specimens considered, conducted all analyses, wrote the manuscript, drew up all figures and acted as corresponding author.  |
| Overall percentage (%)               | 90   |
| Certification                        | This paper reports on original research I conducted during the period of my Higher Degree by Research candidature and is not subject to any obligations or contractual agreements with a third party that would constrain its inclusion in this thesis. I am the primary author of this paper. |
| Signature/date                       | 07/07/2020   |

### Co-author contributions

By signing the Statement of Authorship, each author certifies that:

- i. the candidate's stated contribution to the publication is accurate (as detailed above);
- ii. permission is granted for the candidate to include the publication in the thesis; and
- iii. the sum of all co-author contributions is equal to 100% less the candidate's stated contribution.

|                           |   |
|---------------------------|---|
| Name of co-author         | John R. Paterson  |
| Contribution to the paper | Collected specimens, supervised development of work and helped to evaluate and edit the manuscript. |
| Signature/date            | 13/7/2020   |

|                           |   |
|---------------------------|---|
| Name of co-author         | Diego C. García-Bellido   |
| Contribution to the paper | Collected specimens, supervised development of work and helped to evaluate and edit the manuscript. |
| Signature/date            | 8/7/2020  |

**LIBRARY NOTE:**

The following article on pages 31–50 has been removed  
due to copyright.

It is also available online to authorised users at:  
<https://doi.org/10.1002/spp2.1323>

## Chapter 4

### Ontogeny of the trilobite *Redlichia* from the lower Cambrian (Series 2, Stage 4) Ramsay Limestone of South Australia

(this paper is formatted for *Geological Magazine*)

**Holmes, J.D., Paterson, J.R., Jago, J.B. & García-Bellido, D.** *in review*. Ontogeny of the trilobite *Redlichia* from the lower Cambrian (Series 2, Stage 4) Ramsay Limestone of South Australia. *Geological Magazine*.



## Statement of Authorship

Title of paper: Ontogeny of the trilobite *Redlichia* from the lower Cambrian (Series 2, Stage 4) Ramsay Limestone of South Australia

Publications status: Submitted for publication (in review)

Publication details: Holmes, J.D., Paterson, J.R., Jago, J.B. & García-Bellido, D.C. *in review*. Ontogeny of the trilobite *Redlichia* from the lower Cambrian (Series 2, Stage 4) Ramsay Limestone of South Australia. *Geological Magazine*.

### Principal author

Name of principal author (candidate): James D. Holmes

Contribution to the paper: Conducted fieldwork, measured and photographed all specimens considered, conducted all analyses, wrote the manuscript, drew up all figures and acting as corresponding author.

Overall percentage (%): 90

Certification: This paper reports on original research I conducted during the period of my Higher Degree by Research candidature and is not subject to any obligations or contractual agreements with a third party that would constrain its inclusion in this thesis. I am the primary author of this paper.

Signature/date: 07/07/2020

### Co-author contributions

By signing the Statement of Authorship, each author certifies that:

- i. the candidate's stated contribution to the publication is accurate (as detailed above);
- ii. permission is granted for the candidate to include the publication in the thesis; and
- iii. the sum of all co-author contributions is equal to 100% less the candidate's stated contribution.

Name of co-author: John R. Paterson

Contribution to the paper: Evaluated and edited the manuscript.

Signature/date: 13/7/2020

Name of co-author: Diego C. García-Bellido

Contribution to the paper: Evaluated and edited the manuscript.

Signature/date: 8/7/2020

Name of co-author: James B. Jago

Contribution to the paper: Provided access to specimens, evaluated and edited the manuscript. Located the original collection site.

Signature/date: 9/7/2020

#### 4.1 Abstract

Studies that reveal detailed information about trilobite growth, particularly early developmental stages, are crucial for improving our understanding of the phylogenetic relationships within this iconic group of fossil arthropods. Here we document an essentially complete ontogeny of the trilobite *Redlichia* cf. *versabunda* from the Cambrian Series 2 (late Stage 4) Ramsay Limestone of Yorke Peninsula in South Australia, including some of the best-preserved protaspides (the earliest biomineralized trilobite larval stage) known for any Cambrian trilobite. These protaspid stages exhibit similar morphological characteristics to many other taxa within the Suborder Redlichiina, especially to closely related species such as *Metaredlichia cylindrica* from the early Cambrian of China. Morphological patterns observed across early developmental stages of different groups within the Order Redlichiida are discussed. Although redlichiine protaspides exhibit similar overall morphologies, certain ontogenetic characters within this suborder have potential phylogenetic signal, with different superfamilies characterised by unique trait combinations in these early growth stages.

#### **Keywords:**

Redlichiida; Redlichiidae; protaspid; meraspid; arthropod; early Cambrian

## 4.2 Introduction

Trilobites are one of the most recognised and well-studied Palaeozoic groups. However, despite over 150 years of research and >22,000 described species, the relationships between higher-level groups within this iconic class of fossil arthropods remain unclear (Adrain, 2011; Paterson, 2020). Advances in our understanding of the ontogeny of different trilobite groups will help to resolve these problems by providing crucial information for phylogenetic analyses (e.g. Edgecombe *et al.* 1988; Fortey & Chatterton, 1988; Chatterton *et al.* 1990; Chatterton & Speyer, 1997; Hughes *et al.* 2017). Determining the relationships between Cambrian trilobites in particular will help to illuminate not only the origins of the class (e.g., by providing information on character polarities; Paterson *et al.* 2019), but also assist in resolving how some post-Cambrian clades are related to Cambrian taxa (the so-called ‘cryptogenesis problem’: see Paterson, 2020 and references therein). Developmental information from early Cambrian trilobites considered to be ‘primitive’, such as those belonging to the Order Redlichiida, is therefore of high importance.

Within the Redlichiida (specifically the suborder Redlichiina *sensu* Adrain, 2011), instances where multiple, well-preserved protaspides (the earliest biomineralised larval stage) are known is limited to less than ten species. The most informative of these are silicified specimens of the estangioid *Ichangia ichangensis* Zhang, 1957 and several indeterminate species described by Zhang & Pratt (1999) and Zhang & Clarkson (2012). Protaspides from several other ellipsocephaloid species preserved in shale or mudstone are also well known, including the ellipsocephalid *Ellipsostrenua granulosa* (Ahlberg, 1983) (Laibl *et al.* 2018) and the estangioid *Estangia sinensis* (Zhang, 1953) (Dai & Zhang, 2012a). Early ontogenetic information for the other major redlichiine superfamilies Redlichioidea and Paradoxidoidea is more limited, although Laibl *et al.* (2017) described ‘giant’ protaspides of two paradoxidid species from the Miaolingian of the Czech Republic, and Dai & Zhang (2012b) presented well-preserved examples of the redlichiid *Metaredlichia cylindrica* (Zhang, 1953) from Cambrian Stage 3 of Hubei Province, China. Protaspides are either unknown from other examples of redlichiine ontogenies (e.g. Dai & Zhang, 2013), or represent relatively poorly preserved or isolated examples that do not provide detailed morphological information of protaspid stages (e.g. Westergård, 1936; Lu, 1940; Kautsky,

1945; Whittington, 1957; Šnajdr, 1958; Pocock, 1970; Öpik, 1975; Zhang *et al.* 1980; Pillola, 1991; Palmer & Rowell, 1995; Hou *et al.* 2017).

Here we describe a relatively complete post-embryonic ontogenetic series of the trilobite *Redlichia* cf. *versabunda* Öpik, 1970 from the Cambrian Series 2 (late Stage 4) Ramsay Limestone of Yorke Peninsula (South Australia), including some of the best preserved redlichoid protaspides known to date.

### 4.3 Geological setting

The Ramsay Limestone on Yorke Peninsula, and its temporal equivalents the Wirrealpa and Aroona Creek limestones (Flinders Ranges), form part of the second major depositional sequence of the Cambrian succession in the Stansbury and Arrowie basins (as defined by Gravestock, 1995; Gravestock & Shergold, 2001), representing relatively warm, shallow marine environments during the last major transgression of the Cambrian in South Australia. These units are considered contemporaneous based on the co-occurrence of Daily's (1956) 'Faunal Assemblage 10' (e.g. Horwitz & Daily, 1958; Daily, 1990; Brock & Cooper, 1993).

The Ramsay Limestone is known from central Yorke Peninsula in the Stansbury Basin (Fig. 4.1a), where it crops out in a small area about seven kilometres south of Curramulka as 'dark, blue-grey, mottled, argillaceous limestone' (Daily, 1990, p. 223), as well as in the subsurface from a number of drill holes in the general vicinity (Fig. 4.1b). It has a maximum thickness of 85 m in the Stansbury West-1 well, within which Daily (1990) reported shelly fossils (including *Redlichia*) from oolitic, sandy and dolomitic limestones about 15 m below the top of the formation. The Ramsay Limestone is 68.6 m thick in the Stansbury Town-1 well, although only a 3 m section in the upper part of the formation was cored, consisting of interbedded grey, nodular, argillaceous limestone and black, pyritic, micaceous siltstone/mudstone containing *Redlichia* and other shelly fossils (Daily, 1968, 1990; Gravestock *et al.* 2001). Lower portions of the Ramsay Limestone were also intersected by the Minlaton-1, Minlaton-2 and Cur-D1B drill holes, with the formation represented in these by dark-to-light grey, mottled, nodular limestones interbedded variously with shales, siltstones, planar stromatolites and evaporites (Ludbrook, 1965; Daily, 1990; Gravestock *et*

al. 2001). *Redlichia* was reported by Daily (1957) from the basal c. 25 m of the formation in Minlaton-1. The Ramsay Limestone conformably overlies conglomerates, arkoses and evaporites of the Minlaton Formation and conformably underlies the shales, siltstones and calcareous sandstones of the Corrodery Formation (Fig. 4.2) (Daily, 1990; Gravestock *et al.* 2001).

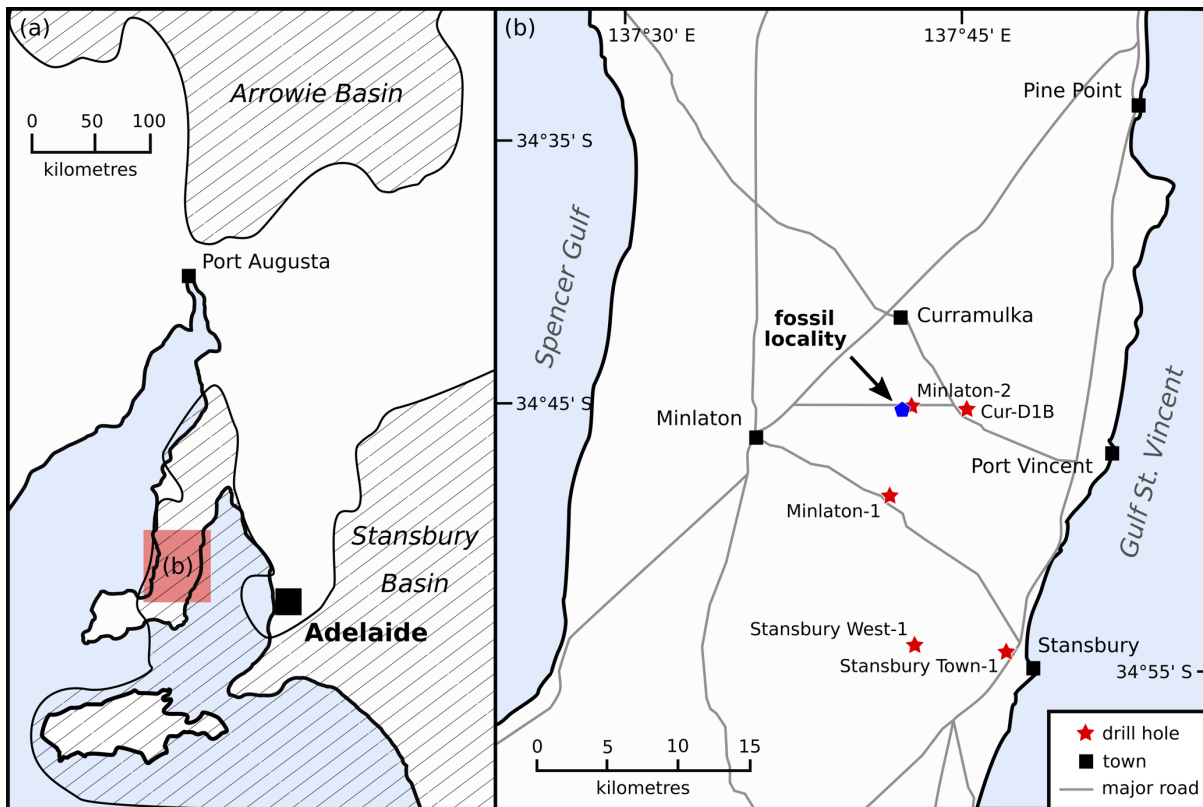


**Figure 4.1:** (a) Map of south-eastern South Australia showing the location of the area shown in (b) and the locations of the Stansbury and Arrowie basins. (b) Map of central Yorke Peninsula showing the locality within the Ramsay Limestone where material considered in this study was collected (pentagon), as well as the locations of several drill holes that intersect the formation in the vicinity (stars).

#### 4.4 Occurrence of *Redlichia* in the Ramsay and Wirrealpa limestones

Trilobites within the upper part of the Cambrian succession in South Australia (i.e. above the first major depositional sequence of Gravestock, 1995 and Gravestock & Shergold, 2001) are rare. Only three instances in three successive formations are currently recognised from the



*Redlichia* was first reported (as *Olenellus* sp.) in South Australia from the Wirrealpa Limestone by Etheridge (1905). Daily (1956) noted *Redlichia* aff. *nobilis* as part of his 'Faunal Assemblage 10' from the Wirrealpa and Aroona Creek limestones. Öpik (1970, p. 7) reported 'undescribed forms [...] with delicate ornaments of lines and granules, reminiscent in this aspect of *Redlichia versabunda*' from both the Wirrealpa and Ramsay limestones (he referred to the latter as the Wirrealpa Limestone), and Daily (1982, p. 60) reported a species 'allied to *R. versabunda*' from the Wirrealpa Limestone at the western end of Brachina Gorge in the Flinders Ranges. Jell in Bengtson *et al.* (1990) subsequently described *Redlichia guizhouensis* Zhao in Lu *et al.* 1974 from the Wirrealpa Limestone about 7 km northwest of the Wirrealpa homestead, and Paterson & Brock (2007) described fragmentary silicified specimens of the same species from the Wirrealpa Limestone at Balcoracana Creek on the eastern side of the Bunkers Range. There have been various reports of *Redlichia* from core samples of the Ramsay Limestone (see above), and in his brief description of the formation, Daily (1990) mentioned the presence of *Redlichia* aff. *nobilis* in outcrop of the Ramsay Limestone south of Curramulka on Yorke Peninsula. Given the morphological similarities between *R. versabunda*, *R. nobilis* and *R. guizhouensis*, it is almost certain that all of these reports refer to the same taxon (the latter two species are considered as possible synonyms: Jell in Zhang, 1985; Bengtson *et al.* 1990; Zhang, 2003).

Previously, the presence of '*R. guizhouensis*' in the Wirrealpa Limestone has allowed correlation with the *R. nobilis* (= *R. guizhouensis*) Zone of the Lungwangmiaoan Stage (= upper Duyunian) of China (Bengtson *et al.* 1990; Brock & Cooper, 1993; Paterson & Brock, 2007). The reassignment of this species to *R. cf. versabunda* suggests correlation with the slightly older *Redlichia chinensis* Zone, a species it apparently co-occurs with in northern Australia (see discussion below).

#### 4.5 Material and methods

All specimens documented herein are housed in the South Australian Museum, Adelaide (specimen number prefix SAM P). Most specimens from the Ramsay Limestone considered here (SAM P57716–57794) were collected and prepared by Mr. Brent Bowman from a locality approximately 7 km SSW of Curramulka (34°45'25" S, 137°42'50" E), from float at

the edge of a farm track adjacent to poorly outcropping Ramsay Limestone. Specimen SAM P57795 was collected by J. D. Holmes from float in a quarry approximately 200 m WSW of the original locality (34°45'27" S, 137°42'40" E).

Specimens were prepared using a pneumatic percussive needle and then whitened with ammonium chloride sublimate using the method set out by Teichert (1948). External moulds were cast in latex before whitening and photography. Large specimens were photographed using a Canon EOS 5DS digital SLR camera with a Canon MP-E 65 mm 1:2.8 macro lens, a Cognisys Stackshot 3X stacking system, and the Canon EOS Utility software. Small specimens were photographed using an Olympus SZX7 binocular microscope with an Olympus SC50 camera attachment and the Olympus cellSens Standard v.1.17 software, and stacked using the HeliconFocus v.7.5.4 Pro software. Measurements of specimens were taken using ImageJ v.2.0.0 (Schneider *et al.* 2012).

Morphological terminology generally follows Whittington & Kelly (1997); for a discussion of ontogenetic terminology, see Section 6 below. For clarity, informal use of higher-level taxonomic names are as follows: 'redlichiine' for Suborder Redlichiina; 'redlichoid' for Superfamily Redlichioidea; and 'redlichiid' for Family Redlichiidae.

#### 4.6 Systematic Palaeontology

Class Trilobita Walch, 1771

Order Redlichiida Richter, 1932

Suborder Redlichiina Richter, 1932

Superfamily Redlichioidea Poulsen, 1927

Family Redlichiidae Poulsen, 1927

Genus *Redlichia* Cossmann, 1902

**Type species.** *Hoeferia noetlingi* (Redlich, 1899) from the early Cambrian of the Salt Range, in what is now Pakistan.

**Discussion.** In two monographs, Öpik (1958, 1970) reviewed the concept of this genus based largely on *Redlichia forresti* (Etheridge in Foord, 1890) from the Ord Basin of Western



Australia and the Northern Territory (Öpik, 1958), and addressed the taxonomy of *Redlichia* species in northern Australia (Öpik, 1970). In doing so, he recognised four previously described species: *R. forresti*, *R. idonea* Whitehouse, 1939, *R. venulosa* (Whitehouse, 1939) and *R. chinensis* Walcott, 1905, and erected nine new species. Many of these new species were based on small numbers of incomplete specimens, and in some cases questionable interpretations; for example, *R. amadeana* was based partly on the presence of bacculae, but re-examination of material assigned to this taxon showed no evidence of these cranidial structures (Kruse, 1998; Laurie in Kruse *et al.* 2004). As such, there is suspicion that Öpik (1970) ‘oversplit’ Australian occurrences of this genus, and his specimens are in need of review (Laurie in Kruse *et al.* 2004).

Öpik (1970) recognised ten species of *Redlichia* from the Thornton Limestone in western Queensland (including seven new species), with seven species being reported from a c. 2 m section of shale and siltstone at a single locality (M426); it is likely that a number of these are conspecific. Many of Öpik’s new species were diagnosed on minor differences between isolated cranidia, and it is now recognised that there can be considerable intraspecific variation within trilobite species, including those of *Redlichia*. For example, Laurie in Kruse *et al.* (2004) noted significant variation in the expression of the axial furrow and the continuity of the glabella with the fixigenae in specimens of *R. forresti* from the Ord Basin; see Laurie (2016) for further discussion. This was originally considered a diagnostic character of *Mesodema*, which has since been synonymised with *Redlichia* (Öpik, 1958, 1970). Such variation also occurs amongst specimens preserved in limestone with minimal taphonomic distortion, e.g. the cranidial width/length ratio of *R. cf. versabunda* from the Ramsay Limestone described herein varies from 105–127% and is seemingly unrelated to ontogeny. Likewise, the recognition of two distinct types of ornament in the one species documented herein (pustulose in smaller, and Bertillon in larger specimens) has not been previously described in other *Redlichia* occurrences from the one locality.

*Redlichia cf. versabunda* Öpik, 1970

Figs 4.3, 4.4, 4.6, 4.7

1905 *Olenellus* sp. Etheridge, p. 247, pl. 25, fig. 1.

1919 *Olenellus?* sp. Etheridge, p. 382, pl. 39, fig. 1.

1956 *Redlichia* aff. *nobilis* Daily, p. 115, 121, 132, not figured.

cf. 1970 *Redlichia versabunda* Öpik, p. 27, pl. 9, figs 1–5.

cf. 1970 *Redlichia leptota* Öpik, p. 32, fig. 4, pl. 11, figs 3–5, pl. 12, figs 1–5.

1990 *Redlichia guizhouensis* Zhou; Jell in Bengtson *et al.*, p. 267, fig. 179.

2007 *Redlichia guizhouensis* Zhou; Paterson & Brock, p. 124, fig. 6.

**Material.** 80 specimens, including 31 protaspides, 30 cranidia (mostly meraspides and small holaspides), two librigenae, eight hypostomes and nine pygidia.

**Occurrence.** Ramsay Limestone (Yorke Peninsula) and Wirrealpa Limestone (Flinders Ranges) in South Australia, and probably the Stansbury Limestone (Yorke Peninsula), Aroona Creek Limestone (Flinders Ranges), and Thornton Limestone (western Queensland).

**Description.** The following description applies to larger holaspide specimens unless otherwise stated; for comparison with smaller specimens, see Section 6 below.

Cranidium highly convex; anterior cranial width (tr.) averaging 113% of total length (sag.). Anterior margin moderately curved. Anterior branches of facial sutures ( $\gamma$ - $\beta$ ) sub-horizontal (tr.) and slightly bowed towards posterior; distal section ( $\beta$ - $\alpha$ ) initially angling posterolaterally away from axis, curving sharply forwards to angle slightly adaxially at margin. Glabella tapering moderately towards anterior, highly convex (sag., tr.), approximately 70–75% as wide (tr.) across anterior of eye ridges as across occipital lobe. Frontal lobe well rounded, almost truncate in some specimens (e.g. Fig. 4.3e). Axial furrows generally straight, moderately well developed, extending to shallow preglabellar furrow. Glabellar furrows generally continuous, although often hard to see axially. S1 continuous, moderately curved towards posterior, less well developed axially than laterally, with deeper pits close to axial furrow. S2 gently curved posteriorly, poorly developed but usually discernible for about two-thirds distance from axial furrow to axis; continuous in well preserved specimens but very poorly developed axially. S3 generally straight (tr.), very poorly developed, more obvious in certain specimens (e.g. Fig. 4.3d, e). Occipital furrow (SO) continuous, shallow and straight axially, well developed and angling slightly forwards laterally. Occipital ring large, sub-triangular, angling slightly upwards posteriorly and terminating in axial node. Frontal area length (sag.) approximately 20% that of cranidium. Very short (sag.) preglabellar field in the largest specimen (2% cranial length: Fig. 4.3i),

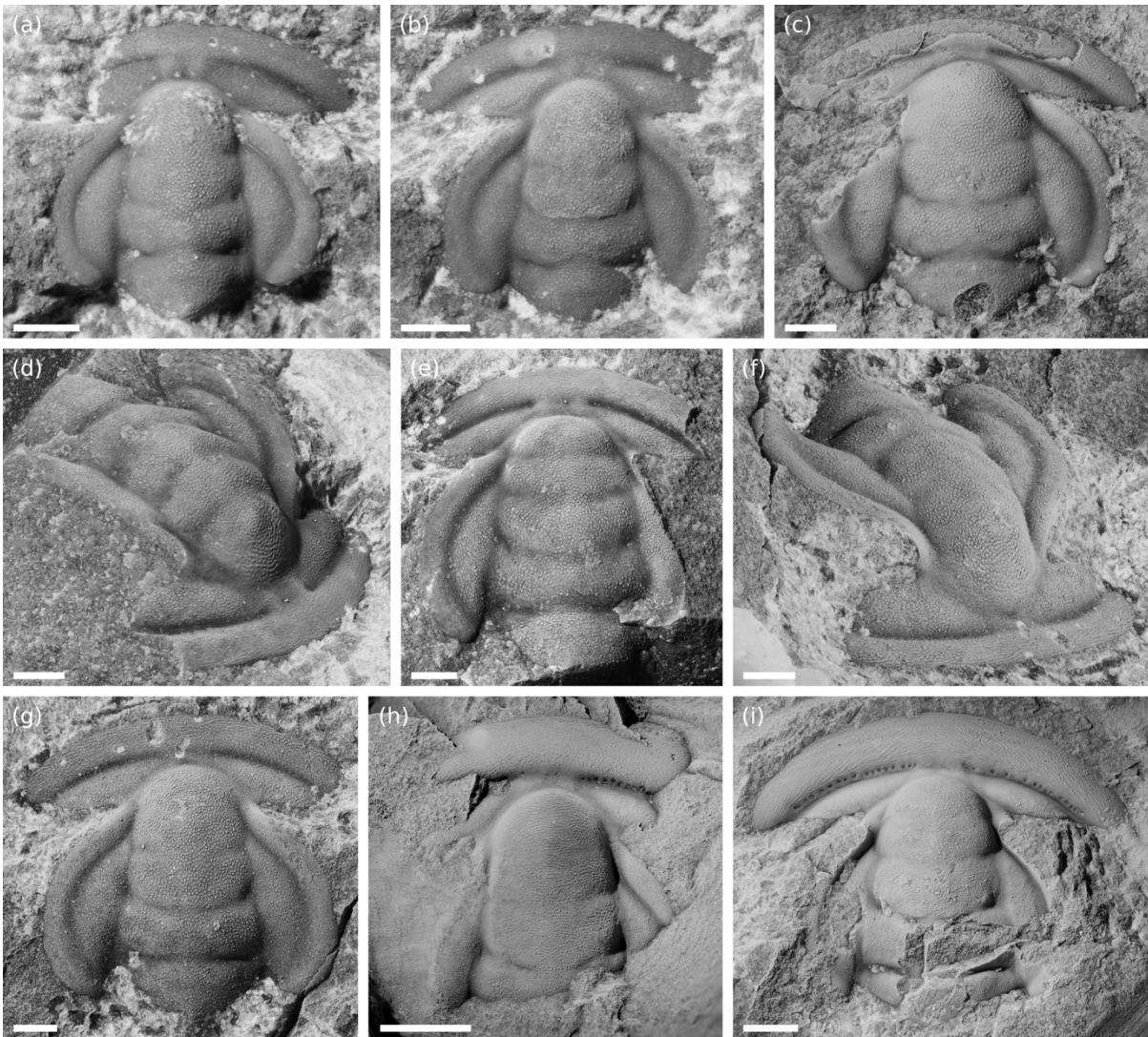


**Figure 4.3:** *Redlichia cf. versabunda* holaspid cranidia from the Ramsay Limestone (Yorke Peninsula, South Australia). (a) SAM P57723. (b) SAM P57720. (c) SAM P57724. (d) Anterolateral oblique view of SAM P57722. (e) SAM P57722. (f) Anterolateral oblique view of SAM P57717. (g) SAM P57712. (h) SAM P57717. (i) SAM P57795. (i) SAM P57716. Specimens are arranged in order of size, from smallest (top left) to largest (bottom right). Note the transition from pustulose ornament in smaller specimens to Bertillon ornament in the largest two specimens. Scale bars: (a–g) = 1 mm; (h, i) = 3 mm.

longer in smaller holaspides (c. 3–7% cranidial length: e.g. Fig. 4.3a, b). Distinct plectrum with medial depression; plectrum width (tr.) approximately half that of frontal glabellar lobe.

Pre-ocular field moderately convex, steeply downsloping to narrow, well-developed anterior border furrow. Anterior border wide (sag., exsag.), usually moderately convex (sag., exsag.); width (sag.) 10–18% cranidial length in holaspides, slightly wider axially; border of

the largest specimen is very wide (c. 18%) and highly convex (Fig. 4.3i). A line of pits along the posterior extremity of the border is clearly visible in this specimen (Fig. 4.3i); these pits are also present in smaller holaspides, but not as well developed (e.g. Fig. 4.3g). Palpebro-ocular ridge wide, crescentic, anterior margin meeting axial furrow adjacent to S3, posterior margin adjacent to rear half of occipital ring and very close to axial furrow. Palpebral area moderately convex, widest (tr.) at about level of L1 or S1, separated from palpebro-ocular ridge by wide, shallow palpebral furrow posteriorly, becoming narrower and deeper anteriorly. Maximum width (tr.) across palpebral lobes approximately equal to cranial length (sag.). Posterolateral projections not known, but presumably small and narrow (exsag.) based on the librigenae.

Hypostome subquadrate, anterior margin not fully known, but appears to be gently curved; anterior wings not preserved in available material. The posterolateral margin bears a pair of large, laterally projecting posterior wings, and a more posterior pair of short spines. In the smallest specimen (Fig. 4.4g), the posterior wings are wider (tr.), and the posterior spines much longer (sag.). The lateral margin between anterior and posterior wings is gently concave (where known), as is that between posterior wings and spines. Posterior margin gently posteriorly-curved axially. Middle body ovate, divided into anterior and posterior lobes by shallow middle furrow; anterior lobe ovate, highly convex (sag., tr.), approximately 65% total length (sag.) of hypostome; posterior lobe sub-semicircular, smaller, approximately 20% hypostomal length (sag.). Lateral and posterior borders wide near posterior wings/spines, narrower elsewhere. Maculae present as effaced areas in lateral sections of middle furrow (e.g. Fig. 4.4i). Large specimens covered in Bertillon ornament (except in the vicinity of middle furrow), transitioning to terrace lines on border (Fig. 4.4i); smaller specimens have a less obvious, pustulose ornament (Fig. 4.4h). Rostral plate not known.

The two known librigenae are quite small (Fig. 4.4a, b: 7–8 mm in length). Moderately curved lateral margin extending to long, curved, gently tapering, strongly advanced genal spine, approximately 65% total librigenal length (exsag., including spine). High eye socle, separated from genal field by shallow eye socle furrow. Genal field crescentic, highly convex, widest at mid-point (exsag.), downsloping to broad, shallow lateral border furrow. Border relatively flat, widest (tr.) at midpoint of genal field (exsag.) near base of genal spine (c. 80–90% maximum genal field width). Genal field with close-



packed, pustulose ornament extending on to border and morphing to terrace lines marginally.

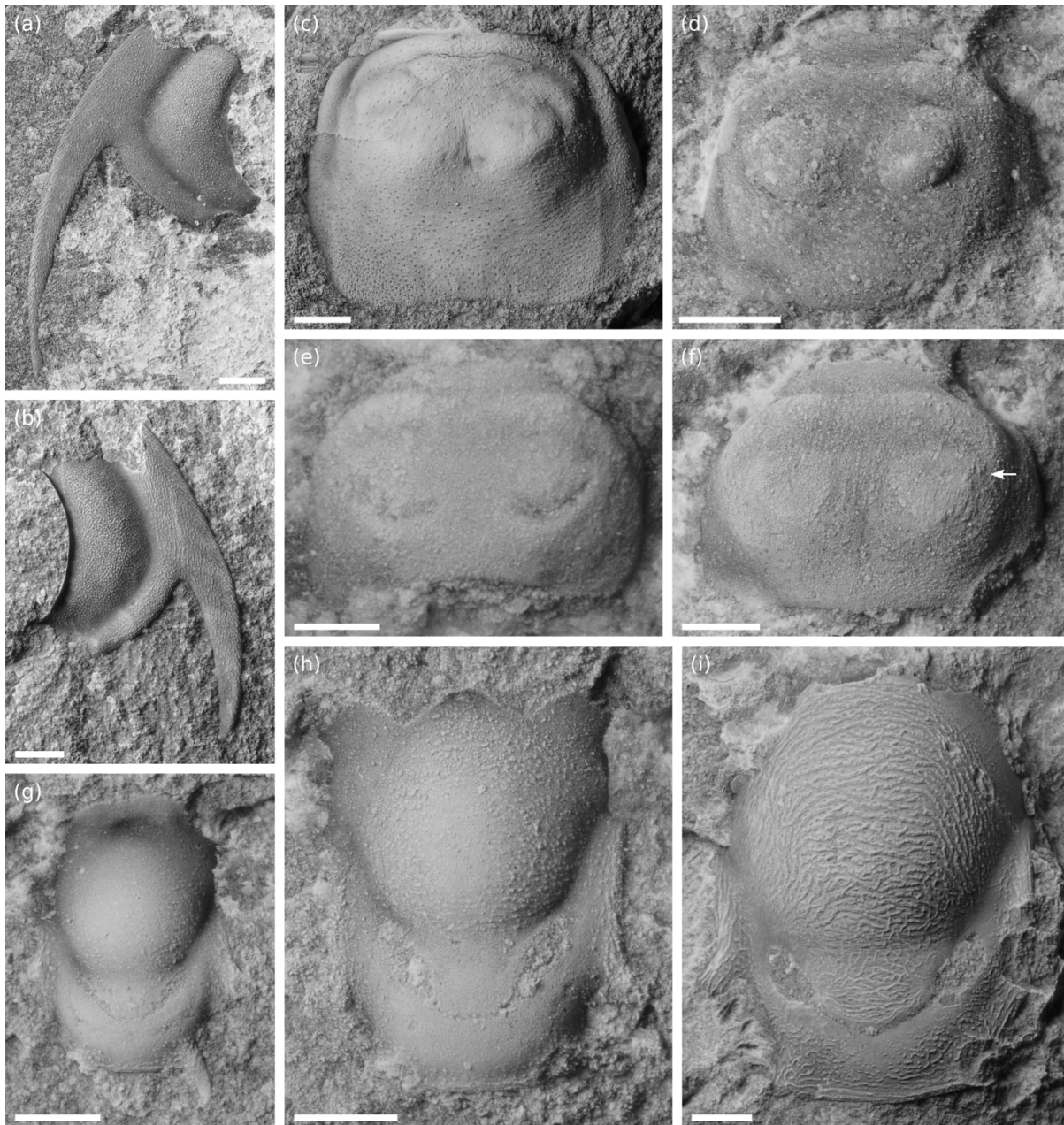


**Figure 4.4:** *Redlichia* cf. *versabunda* specimens from the Ramsay Limestone (Yorke Peninsula, South Australia). (a) Left librigena (SAM P57792). (b) Right librigena (SAM P57793). (c) Large pygidium (SAM P57794). (d) Small holaspid pygidium (SAM P57783). (e) Very small holaspid(?) pygidium (SAM P57780). (f) Small holaspid pygidium; arrow denotes the level where a faint furrow is present, delineating the second axial ring (SAM P57784). (g) Mid-stage(?) meraspid hypostome with extended posterolateral spine (SAM P57772). (h) Medium-sized hypostome (SAM P57774). (i) Large hypostome; note distinct Bertillon ornament in this large specimen compared with pustulose ornament in (h) (SAM P57775). Scale bars: (a–d, i) = 1 mm; (e) = 200  $\mu$ m; (f–h) = 400  $\mu$ m.

Pygidium subquadrate, about 75% as long (sag.) as wide (tr.) in large specimens (exc. articulating half-ring), about 65% as long as wide in smaller specimens (Fig. 4.4c–f). Anterior margin straight to gently curved axially, becoming more curved at anterolateral corners. Lateral margins gently bowed outwards; posterior margin with slight medial embayment in large specimens (Fig. 4.4c). Axial region ovoid in shape, with two short (sag.) axial rings and a terminal axial piece. Antermost axial ring clearly defined, the second clearly visible laterally, less so axially; second ring poorly defined in smaller specimens. Terminal axial piece subtriangular and bilobate, as delineated by posteromedial crease. Axial rings and terminal axial piece separated by poorly developed axial ring furrows. Pleural area comprised of one moderately well-defined anterior pleura with clear pleural furrow that wraps around axis to point posteriorly. Terminal area wide, about 75% pygidial width (tr.), and very long, about one third pygidial length (sag.).

**Remarks.** South Australian specimens assignable to this species have most recently been described as *Redlichia guizhouensis* from the Wirrealpa Limestone of the Flinders Ranges (see Jell in Bengtson *et al.* 1990; Paterson & Brock, 2007), although their similarity to *R. nobilis* or *R. versabunda* has been noted by a number of authors (e.g. Daily, 1956; 1982; Öpik, 1968). *Redlichia guizhouensis* is a species originally described from China, based on a single cranidium, and no other material has since been referred to this taxon, other than the above-mentioned specimens from the Wirrealpa Limestone. It has been suggested previously that *R. guizhouensis* may be synonymous with *R. nobilis* (Jell in Zhang, 1985; Bengtson *et al.* 1990; Zhang, 2003). Cranidia from the Ramsay and Wirrealpa limestones are similar to the type specimen of *R. guizhouensis* from China in some respects: they have an anterior cranial width equal to about 110% of the cranial length, relatively wide palpebral lobes, and a wide, convex anterior border. However, the single specimen of *R. guizhouensis* from China (see Lu *et al.* 1974, pl. 31, fig. 10) has a narrower, less conical glabella, and is much narrower across the palpebral area (tr. width approximately 87% that of cranial length, compared to subequal in cranidia from the Ramsay and Wirrealpa limestones). Given the probable synonymy of *R. guizhouensis* and *R. nobilis*, and the general lack of distinguishing features of the former, assigning Australian material to *R. guizhouensis* is not supported by the available evidence.

Specimens from the Ramsay and Wirrealpa limestones resemble *R. nobilis* in having similar cranial proportions (anterior cranial width c. 110% of length), as well posteriorly curved and strongly divergent anterior branches of the facial sutures. However, *R. nobilis* has a less conical glabella (similar to *R. guizhouensis*) and narrower palpebral lobes (see Zhang & Jell, 1987, pl. 5, figs 5, 6), and also differs with regard to pygidial morphology (as pointed out by Jell in Bengtson *et al.* 1990); the pygidium of *R. nobilis* is more ovoid and shorter (sag.), with a much shorter terminal area ending in an arched posterior margin (see Zhang & Jell, 1987, pl. 7, fig. 4). Jell (in Bengtson *et al.* 1990) cautioned that this may be a result of dimorphism, as noted by Öpik (1958) for *R. forresti*; this is the only published example of such variation in *Redlichia*. Öpik (1958) interpreted this variation as sexual dimorphism and rejected an ontogenetic explanation (for no apparent reason), despite the fact that the unusual ‘male’ pygidium occurred only in very small specimens. Moreover, neither of the two specimens he figured appear to have the full complement of 18 thoracic segments (Öpik, 1958: pl. 2, figs 1–3). In fact, the pygidia of these specimens appear similar to the transitional meraspid pygidia of certain other redlichiines, for example, those of *Estaingia bilobata* Pocock, 1964 from the Emu Bay Shale, South Australia (Holmes *et al.* in press).

*Redlichia versabunda* was first described by Öpik (1970) from two localities in western Queensland that he considered to be the Beetle Creek Formation—the ‘Yelvertoft Bed’ near Yelvertoft Homestead (M426) and a locality west of Mt Isa on May Downs Station (M262)—as well as from the Thorntonia Limestone at a locality further to the south (D41). All three localities are now considered to be within or equivalent to the ‘lower’ Thorntonia Limestone (sometimes referred to as the Hay River Formation: Smith *et al.* 2013) (Fig. 4.2). Our comparison of the Ramsay Limestone specimens with *R. versabunda* from western Queensland is based on close similarities with the material originally assigned to that taxon by Öpik (1970), as well as certain other co-occurring species he erected, in particular, *Redlichia leptota*. The specimens from the Ramsay Limestone conform to Öpik’s (1970) diagnosis for *R. versabunda* in having: (1) an anterior cranial width (tr.) of about 110% of the cranial length (sag.); (2) ‘slightly curved and strongly divergent’ anterior branches of the facial sutures (seemingly more divergent in the Ramsay specimens, although this is possibly due to differences in preservation); (3) an anterior border furrow with small pits in the lateral portions that is interrupted by a plectrum (or ‘swelling reminiscent of a

plectrum') in the axial region; (4) relatively wide palpebral lobes extending close to the axial furrow at the rear of the occipital ring; (5) Bertillon ornament on the glabella, with more pustulose ornament on the interocular cheeks and palpebral lobes (as seen in the largest two specimens from the Ramsay Limestone; Fig. 4.3h, i); and (6) a 'trapezoidal' or subtriangular occipital ring with a medial node (Öpik, 1970, p. 28). Small (but probable holaspid) specimens from the Ramsay Limestone (Fig. 4.3a–g) also display the above characteristics, except that they have dense pustulose ornament (weakly aligned in slightly larger specimens, e.g. Fig. 4.3d–g) in place of the Bertillon ornament of large specimens, and they have a longer (sag.) preglabellar field (and therefore plectrum) that relates to ontogeny (see Section 6 below). The Ramsay Limestone specimens are also very similar to figured specimens assigned to *R. lepta* by Öpik (1970), a species he described from the Thornton Limestone (and co-occurring with *R. versabunda* and *R. chinensis*). Specimens assigned by Öpik (1970) to *R. versabunda* have cranial lengths of 12.8–14.0 mm, while those of *R. lepta* range from 3.6–8.0 mm. The morphological differences between these 'species' therefore correspond to the ontogenetic variation seen in specimens from the Ramsay Limestone. As such, we suggest that *R. versabunda* and *R. lepta* are conspecific, with *R. versabunda* being the senior synonym described first in Öpik's (1970) monograph. It is possible that other species co-occurring with *R. versabunda* in the Thornton Limestone are also conspecific. For example, Öpik (1970) erected *Redlichia mayalis* from locality M262 (where it co-occurs with *R. versabunda*), based on two cranidia with bluntly rounded frontal glabellar lobes, similar to certain specimens from the Ramsay Limestone (e.g. Fig. 4.3e). *Redlichia vertumnia* (based on two cranidia from M262) is also similar. Given the uncertain validity of many *Redlichia* species from the Thornton Limestone (and Öpik's Australian species in general), plus the absence of illustrated pygidia of *R. versabunda* or *R. lepta* from the Georgina Basin, we feel it is best to place the South Australian specimens under open nomenclature until a review of Öpik's (1958, 1970) material is completed and/or new specimens from the type localities are documented.

Previously, the Wirrealpa Limestone (Arrowie Basin) has been correlated with the *Redlichia nobilis* Zone of the (upper) Lungwangmiaoan Stage (= upper Duyunian) of China, based largely on the presence of '*R. guizhouensis*' (Jell in Bengtson *et al.* 1990; Paterson & Brock, 2007). Other Australian formations such as the Ramsay Limestone (Stansbury Basin), Tindall Limestone (Daly Basin), and Montejinni Limestone (Wisio Basin), as well as the Gum



Ridge Formation, Thornton Limestone and Top Springs Limestone in the Georgina Basin are also considered contemporaneous with the Wirrealpa Limestone, based on co-occurring shelly taxa such as the linguliformean brachiopods *Kostjubella djagoran* (Kruse, 1990) and *Schizopholis napuru* (Kruse, 1990) (Brock & Cooper, 1993; Gravestock *et al.* 2001; Paterson & Brock, 2007; Percival & Kruse, 2014; Popov *et al.* 2015). The close comparison of *Redlichia* specimens from the Ramsay and Wirrealpa limestones with those of *R. versabunda* (and *R. lepta*) from the Georgina Basin would suggest correlation with the slightly older *Redlichia chinensis* Zone of China, equivalent to the mid-Lungwangmiaoan (upper Duyunian), based on the co-occurrence of *R. versabunda* and *R. lepta* with *R. chinensis* in the Thornton Limestone (Öpik, 1970). However, Öpik's (1970) identification of *R. chinensis* from Australian localities has been questioned by Kruse *et al.* (2004, p. 19), given the small number of illustrated specimens. As such, and given the uncertainty surrounding the specimens from the Ramsay and Wirrealpa limestones being conspecific with *R. versabunda* (and *R. lepta*) from northern Australia, this correlation remains tentative.

#### **4.7 Post-embryonic development of *Redlichia cf. versabunda***

##### **4.7.1 Ontogenetic terminology**

As with holaspid morphology, ontogenetic terms generally follow Whittington and Kelly (1997), except we use 'trunk' instead of 'protopygidium' for protaspides (after Hughes *et al.* 2006). We use 'intergenal spine separation' in the sense of Laibl *et al.* (2018, after Webster, 2007) to refer to the distance between the posterior fixigenal (or 'intergenal') spines of protaspides.

The protaspid period has previously been subdivided into substages (e.g. anaprotaspis, metaprotaspis) based on the appearance of a distinct trunk and a furrow separating this from the cephalon. We follow the recommendation of Chatterton & Speyer (1997) and Edgecombe *et al.* (1988) in avoiding these terms, as they likely do not represent homologous stages across all trilobites. It should be noted that this argument may also apply to the broader protaspid, meraspid and holaspid periods defined above; however, these are widely used and useful for discussion and descriptive purposes.

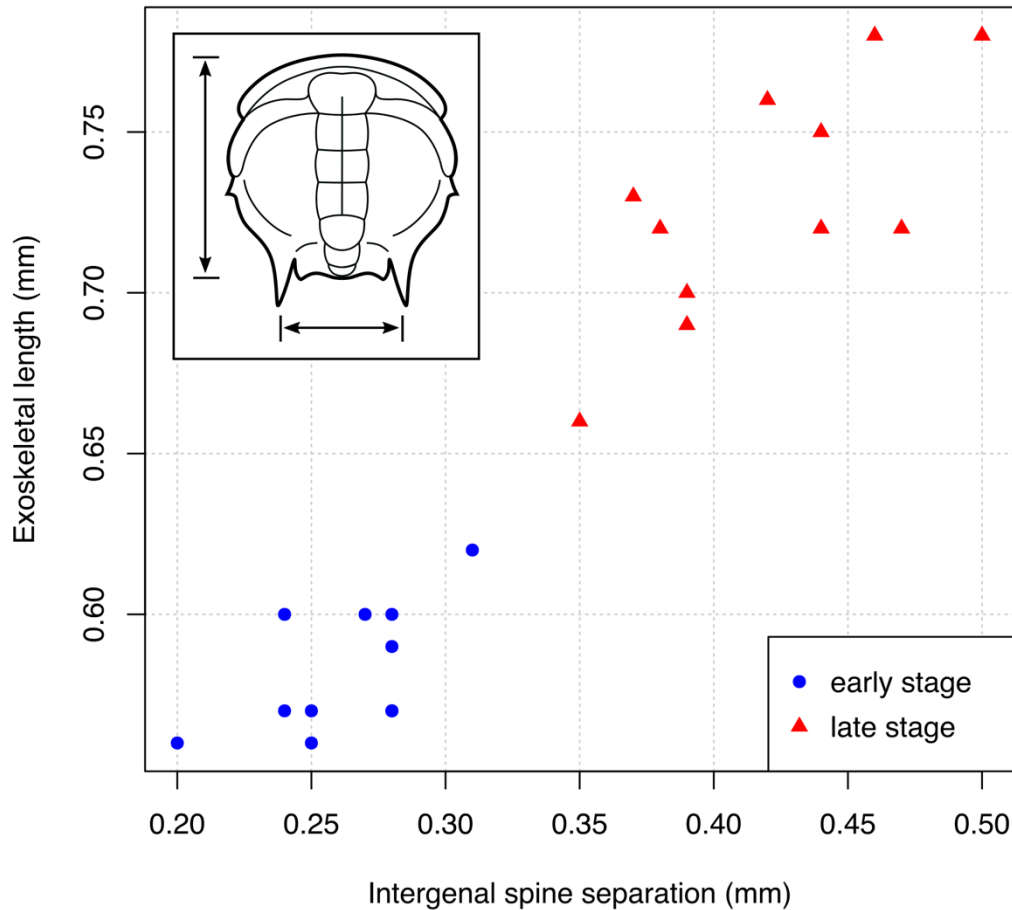


**Figure 4.5:** Plot of axial exoskeletal length against intergenal spine separation for *Redlichia cf. versabunda* protaspides from the Ramsay Limestone. Intergenal spine separation represents the distance between posterior fixigenal spine bases that will become the intergenal spines/angles. Blue circles represent early stage protaspides with no visible trunk, and red triangles represent late stage protaspides with a distinct trunk; these groups are clearly separated based on these size measures. See inset for visual of measurement definitions.

#### 4.7.2 Protaspid period

Two stages can be recognised in protaspides of *Redlichia cf. versabunda* from the Ramsay Limestone: an early stage with no visible trunk, and a later stage with a distinct trunk; these stages form two distinct size clusters (Fig. 4.5). In early protaspides (Fig. 4.6a–g), the exoskeleton is ovoid and moderately convex, ranging from 0.56–0.62 mm in length and 0.63–0.72 mm in width (averaging 117% as wide as long). The axis is composed of five segments; the occipital ring, three glabellar lobes (L1–L3) and the frontal lobe (LA). The

glabella is raised slightly above the surrounding exoskeleton in profile view, gently expanding anteriorly from SO–S3 with an inflated, truncate, slightly bilobed frontal lobe almost reaching the anterior margin, approximately twice the width of the occipital lobe. A shallow, narrow medial furrow divides glabellar lobes L1–LA. The axial furrows are wide, shallow and slightly bowed outwards, separated from a very shallow preglabellar/border furrow (= change in slope) by a wide (sag., tr.), relatively deep fossula. The glabellar furrows are wide (sag.) and continuous (tr.), as is the occipital furrow. The anterior border is narrow and not well defined. The palpebro-ocular ridge is crescentic and gently convex, extending laterally from the posterior of the frontal lobe, then curving towards the posterior, reaching a level just anterior of S1. The fixigenal area is large, approximately the same width as the glabella at its widest point (about level with L2); it is semicircular, highly convex, downsloping, and bounded laterally by a broad palpebral furrow (= change of slope), which extends rearwards to a less obvious posterior border furrow. There appears to be slight expression of the segmental boundaries defined by the glabellar furrows in the fixigenal area (Fig. 4.6a–d). Baculae are present as small protrusions laterally adjacent to the anterior of the occipital ring, separated from the glabella by the axial furrows. A small, laterally-directed anterior fixigenal spine is present just behind the posterior branch of the facial suture (Fig. 4.6a, e, f). The posterior margin bears two large, broad (tr.) fixigenal ('intergenal') spines or protrusions; length (sag.) approximately equal to that of the occipital lobe in the longest specimens (Fig. 4.6f, g). The posterolateral margin between the anterior and posterior fixigenal spines is gently rounded and appears to bear at least one additional fixigenal spine (Fig. 4.6f); the border in this region widens towards the posterior. The posterior border behind the occipital ring is very short (sag.), with the margin slightly protruding posteromedially. Librigenae not known, but appear to have been small, crescentic and laterally orientated.

Later stage protaspides (Fig. 4.6h–n) range from 0.66–0.78 mm in length and 0.68–0.83 mm in width (averaging 115% as wide as long), and are similar to early stage examples, with the following exceptions: the exoskeleton is less convex and the glabella narrower (tr.) along its length, with the axial furrows close to parallel and more developed, and the medial furrow less obvious; the fixigenal area is wider (tr.), baculae are less obvious, and the palpebral lobes are longer (exsag.), reaching to about the level of S1 or L1; a very short (sag.) preglabellar field is present and the anterior border is more clearly defined; the

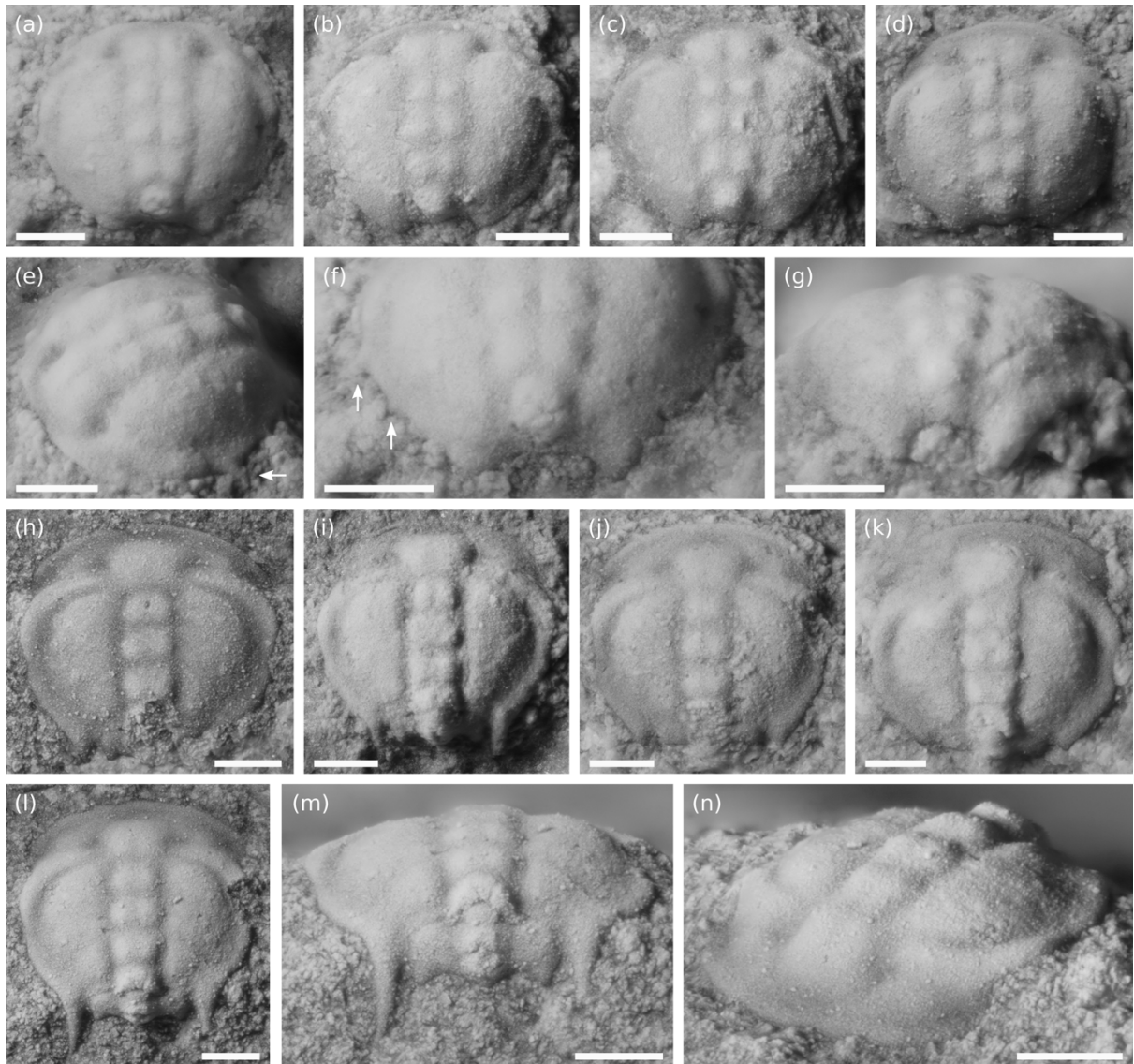


**Figure 4.6:** *Redlichia cf. versabunda* protaspides from the Ramsay Limestone (Yorke Peninsula, South Australia). (a–g) Early stage protaspides with no discernible trunk. (h–n) Late stage protaspides with distinct trunk. (a) SAM P57752. (b) SAM P57753. (c) SAM P57754. (d) SAM P57756. (e) Anterolateral oblique view of SAM P57752 showing anterior fixigenal spine (arrow). (f) Posterior detail of SAM P57752—note anterior and posterolateral fixigenal spines (arrows). (g) Posterior view of SAM P57751 showing details of posterior fixigenal spines. (h) SAM P57765. (i) SAM P57741. (j) SAM P57768. (k) SAM P57746. (l) SAM P57750. (m) Posterior view of SAM P57750 showing details of trunk and posterior fixigenal spines. (n) Lateral view of SAM P57750. All scale bars 200  $\mu\text{m}$ .

posterior fixigenal (intergenal) spines are much longer and more pointed, and the intergenal spine separation wider (Figs 4.5, 4.6l, m), resulting in the posterior part of the exoskeleton becoming less rounded; and a distinct trunk is present, the clearest examples of which appear to display two axial segments and a pair of pleural spines, separated from the

cephalon by a narrow, well-defined furrow, but without a distinct articulation (i.e. the anterolateral margins of the trunk appear 'fused' to the cephalon) (Fig. 4.6m).

#### 4.7.3 Meraspid period

Meraspid cranidia range from 0.86 mm to about 4 mm in length (Fig. 4.7). Due to the disarticulated nature of the specimens, it is difficult to determine the exact point of the meraspid/holaspid transition. Nevertheless, cranidia larger than about 4 mm in length (sag.) show very minimal allometric change, suggesting that these probably belong to holaspides or very late-stage meraspides. The morphology of *Redlichia cf. versabunda* meraspides from the Ramsay Limestone spans a continuum of variation between that of the protaspides and holaspides described above; the major changes across this period are summarised below.

Early meraspid cranidia are sub-quadrate with later stages becoming more ovoid. In the smallest meraspides, the glabella tapers slightly from LO–L3, with an inflated frontal lobe that is slightly wider than the occipital lobe (Figs 4.7a, 4.8c); the frontal lobe has a subtle medial depression that in slightly later stages develops into a distinctly bilobed frontal lobe (Figs 4.7c, d, 4.8d), which gradually disappears about midway through the meraspid period as the glabella shortens and a distinct preglabellar field with plectrum develops (Figs 4.7e–h, 4.8e). In later stage meraspides, the glabella widens considerably and gradually lengthens again, becoming more tapered and conical in shape (Figs 4.7i–l, 4.8f, g). The preglabellar field decreases in length, becoming very short in holaspides (Figs 4.3, 4.8h). In early meraspides, the glabellar furrows are continuous but weakly impressed medially (Fig. 4.7a–f); the occipital furrow is continuous and well-developed; these gradually become less well-developed during ontogeny (e.g. Fig. 4.7g–l). A distinct medial node is present on the occipital ring in well-preserved specimens from the early meraspid period onwards.

In early meraspides, the palpebro-ocular ridge extends laterally from the posterior of LA (with which it is partly continuous, separated by a weakly impressed axial furrow), curving towards the posterior, extending to about the level of S1 or L1 (exsag.); across the meraspid period, this becomes more isolated from the glabella at the anterior, and extends further towards the posterior of the cranidium and curves adaxially, with the posterior extremity being close to the axial furrow near the occipital ring in holaspides. Across the



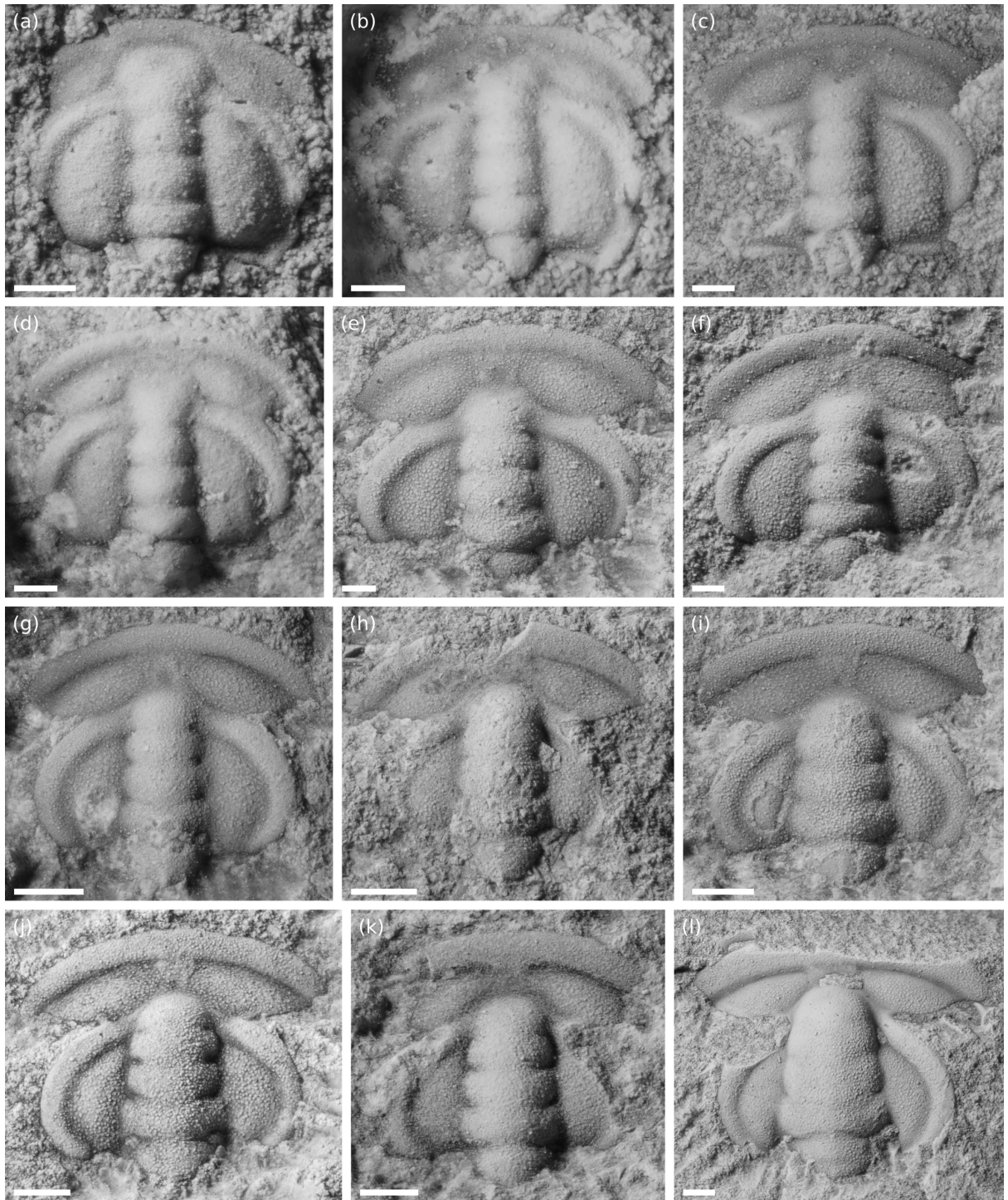


**Figure 4.7:** *Redlichia* cf. *versabunda* meraspides from the Ramsay Limestone (Yorke Peninsula, South Australia). Specimens are arranged in order of size, from smallest (top left) to largest (bottom right). (a) SAM P57730. (b) SAM P57739. (c) SAM P57734. (d) SAM P57727. (e) SAM P57733. (f) SAM P57738. (g) SAM P57735. (h) SAM P57736. (i) SAM P57740. (j) SAM P57726. (k) SAM P57728. (l) SAM P57731. Note the initial retraction of the glabella and development of a distinct preglabellar field with plectrum in smaller meraspides, followed by the extension of the glabella and reduction of the preglabellar field in later stages. Across the meraspid period the glabella also changes shape from clavate to conical. Scale bars: (a–f) = 200  $\mu$ m; (g–l) = 500  $\mu$ m.

same period, the fixigenal area gradually narrows (tr.), the anterior border widens (sag., exsag.), and the anterior branches of the facial sutures gradually lengthen (tr.). The posterior fixigenal ('intergenal') spines present in protaspides shorten dramatically in the earliest meraspides and presumably disappear, and the intergenal spine separation widens considerably.

The smallest known hypostome from the Ramsay Limestone is 1.36 mm long, and therefore likely belongs to a mid-late stage meraspis of *R. cf. versabunda* based on size comparisons with the cranidia. It is similar in morphology to adult hypostomes, except the posterior wings are wider and the single posterior spine preserved is much longer (Fig. 4.4g). The smallest pygidium is 0.38 mm long, and exhibits a single obvious axial ring and a bilobed terminal piece (Fig. 4.4e); morphology and size suggest this is possibly from a very early holaspis. The terminal area is much shorter (sag.) than in late holaspides, with a shallow but obvious medial embayment. Pygidia likely belonging to slightly larger holaspides (e.g. Fig. 4.4d, f) have terminal areas intermediate in length between this and those of late holaspid pygidia (Fig. 4.4c). Holmes *et al.* (2020) showed that holaspides of *Redlichia takooensis* Lu, 1950 from the Cambrian Series 2 (Stage 4) Emu Bay Shale of South Australia have a pygidium with two axial rings and bilobed terminal piece, pointing out that the second ring is often faint and difficult to discern. This also seems to be the case in *R. cf. versabunda*.

## 4.8 Discussion

### 4.8.1 Morphological comparisons with other redlichiine protaspides

In most known cases, protaspides of redlichiine trilobites have similar morphologies overall. Early stage protaspides are generally circular to ovoid and display an anteriorly expanding axis composed of five segments (LO–LA), with the anterior lobe being distinctly wider than L3 and often bilobed. The eye ridges extend laterally from the posterior of the frontal lobe (with which they appear partly continuous, separated by a weakly developed axial furrow) before curving towards the posterior, with the palpebral lobe reaching about exoskeletal mid-length (exsag.). The fixigenae are semicircular and convex, with the posterior border

furrow curving anterolaterally from near the occipital ring to meet the posterior of the palpebral lobe. In well-preserved specimens, bacculae can be discerned at the posterior of the fixigenae, at about the level of the occipital furrow. Distinct pits (or fossulae) are present in the angle created by the junction of the eye ridge and the frontal lobe. There is a distinct gap between the glabellar frontal lobe and the anterior cephalic margin that Laibl *et al.* (2018) called a 'preglabellar field' in *Ellipsostrenua granulosa*. In reality, this gap most likely represents a poorly defined anterior border (although there is a short but distinct preglabellar field in later protaspides of *R. cf. versabunda*). The librigenae appear to have been small, very narrow (tr.) and laterally (or anterolaterally) orientated. In most cases, a pair of small, laterally-directed fixigenal spines are present just behind the posterior facial suture, with a second pair of ventrally-orientated posterior fixigenal (or 'intergenal') spines present along the posterior margin. Many of these similarities were noted by Laibl *et al.* (2018) in comparing early protaspides of the ellipsocephaloids *Ichangia ichangensis*, *Estaingia bilobata* and *E. granulosa*; however, this general description also applies to redlichoid protaspides such as *Metaredlichia cylindrica* (Dai & Zhang, 2012b). Protaspides of the paradoxidid *Acadoparadoxides pinus* are also similar (Westergård, 1936; Whittington, 1957); however, related species such as *Eccaparadoxides pusillus* and *Hydrocephalus carens* (despite displaying similar features in general) have very large protaspides with greatly enlarged glabellas that were interpreted as possible instances of lecithotrophy by Laibl *et al.* (2017). Excluding minor allometric changes, later stage redlichiine protaspides are comparable to early stages, the major difference being the appearance of a trunk region with at least one pair of pleural spines.

There are currently very few redlichoid trilobites for which protaspid morphology is known in detail. Some of the best examples are those of *Metaredlichia cylindrica* figured by Dai & Zhang (2012b) from the Shuijingtuo Formation in the Hubei Province of China, who described a relatively complete post-embryonic ontogeny of this species based on protaspides and isolated cranidia. They also suggested that the superbly silicified specimens of 'genus and species indeterminate 1' of Zhang & Pratt (1999) from the Shuigoukou Formation (Henan Province, China) may be conspecific with *M. cylindrica*. This suggestion is strengthened by the identification of additional specimens of 'genus and species indeterminate 1' of Zhang & Pratt (1999) in the Shuijingtuo Formation of Shaanxi Province (China) by Zhang & Clarkson (2012).



Protaspides of *R. cf. versabunda* from the Ramsay Limestone closely resemble those of *M. cylindrica* (and the possibly conspecific ‘genus and species indeterminate 1’ of Zhang & Pratt, 1999). These species exhibit the standard morphology discussed above, although they differ in minor ways. The glabella of *M. cylindrica* has more divergent axial furrows and potentially longer posterior fixigenal spines in early protaspides compared with *R. cf. versabunda*, although these spines may be incomplete in available specimens of the latter species. The overall shape of the exoskeleton is also slightly different, with *M. cylindrica* appearing to be slightly longer (sag.) relative to width (tr.), but this may be a result of preservation in shale compared to limestone (see discussion below about overall size).

These redlichiid species also share several additional characteristics that are not shared across all redlichiine groups. Firstly, they exhibit a longitudinal medial glabellar furrow that subdivides the anterior glabellar lobes (L1–LA). Such a feature is shared with other redlichoids (where known), such as *Dolerolenus zoppii* (Meneghini, 1882) (Pillola, 1991), and is also present in paradoxidoids (Westergård, 1936; Whittington, 1957; Šnajdr, 1958), but is apparently absent in ellipsocephaloids (e.g. Zhang & Pratt, 1999; Laibl *et al.* 2018).

Secondly, these redlichiid protaspides bear additional paired fixigenal spines, situated between the anterior and posterior pairs, and orientated posterolaterally. Dai & Zhang (2012b) identified one such pair in *M. cylindrica*, while Zhang & Clarkson (2012) figured silicified specimens of ‘genus and species indeterminate 1’ (Zhang & Pratt, 1999; tentatively assigned to *M. cylindrica* by Dai & Zhang, 2012b) that clearly show a second additional pair close to the posterior fixigenal spines. It appears at least one additional pair of spines is present in *R. cf. versabunda* from the Ramsay Limestone (although these are not very clear; Figs 4.6e, f, 4.8a), probably corresponding with those identified in *M. cylindrica* (Dai & Zhang, 2012b: figs 1.10, 1.11, 4.1–4.3) and the more anterior pair in ‘genus and species indeterminate 1’ (Zhang & Clarkson, 2012: pl. 19, figs 4–7). These additional spines are also apparently absent in ellipsocephaloids (e.g. Zhang & Pratt, 1999; Laibl *et al.* 2018).

Finally, in *R. cf. versabunda* protaspides, the segmental boundaries of the cranidium indicated by the glabellar furrows appear to extend into the fixigenal area, a trait shared with other redlichoids and emuelloids (and also observed in olenelline meraspides), but lacking in paradoxidoids (including xystridurids) and ellipsocephaloids (see Paterson & Edgecombe, 2006 and references therein).

#### 4.8.2 Size comparisons with other redlichoid protaspides

Dai & Zhang (2012b) noted two size clusters of early stage protaspides lacking a trunk in *Metaredlichia cylindrica* (their ‘anaprotaspides’, ranging from 0.50–0.54 mm and 0.70–0.81 mm in length), as well as two size clusters of later stage protaspides (their ‘metaprotaspides’, ranging from 0.73–0.78 and 0.82–0.96 mm in length), which they interpreted as having one and two trunk segments, respectively. In this instance, the larger ‘anaprotaspid’ cluster overlapped substantially with the smaller ‘metaprotaspid’ cluster. Zhang & Pratt (1999) recognised three stages of early protaspides of their ‘genus and species indeterminate 1’ (all lacking a visible trunk): their ‘P0a’ (c. 0.35 mm in length), ‘P0b’ (c. 0.38 mm in length), and ‘P0c’ (c. 0.57 mm in length) stages, as well as a later stage protaspis with two axial rings in the trunk (their ‘P2’ stage: 0.62–0.75 mm in length). Additional specimens assigned to this taxon by Zhang & Clarkson (2012) identified an additional late stage protaspis with a single axial ring (their ‘P1’ stage), although no measurements were listed and only non-dorsal images provided. The size discrepancy between the different stage clusters of these taxa suggest that they may belong to different species, *contra* Dai & Zhang (2012b). This is not surprising given the apparent overall similarity between redlichoid protaspides, although in this case the size difference discussed above may be partly related to compression in mudstone compared with three-dimensional silicification.

Both Dai & Zhang (2012b) and Zhang & Pratt (1999) suggested that in the earliest protaspis stages of *M. cylindrica* and ‘genus and species indeterminate 1’, the ‘mid-fixigenal’ spines (i.e. those between the anterior and posterior spines) were absent, although this may be related to preservation. Based on size and morphology, it appears that the two protaspis stages of *R. cf. versabunda* recognised from the Ramsay Limestone most closely resemble the ‘P0c’ and ‘P2’ stages of ‘genus and species indeterminate 1’ of Zhang & Pratt (1999).

#### 4.8.3 Allometric change and pygidial segmentation throughout ontogeny

During the course of ontogeny, cranidia of *Redlichia cf. versabunda* from the Ramsay Limestone underwent a significant amount of allometric change (Fig. 4.8), particularly in

relation to the glabella. In protaspides, particularly in the early stage, the glabella is long, reaching close to the anterior margin, and expanding towards the anterior. Throughout the early meraspid period, the glabella shortens relative to the length of the cranidium and develops a conical shape, tapering towards the anterior. At the same time, a distinct preglabellar field with a medial plectrum develops. In the later meraspid period, the glabella extends again but maintains a conical shape, and the preglabellar field reduces until it is extremely short in holaspides. This pattern of glabella retraction and subsequent extension across ontogeny is common across a number of Cambrian trilobite groups, including olenellines, redlichiids, xystridurids and paradoxidids (see McNamara, 1986 and references therein). Interestingly, *Metaredlichia cylindrica* does not follow this pattern; rather, the glabella retains its clavate shape throughout ontogeny, with a short preglabellar field developing in holaspides; there is no retraction and subsequent extension of the glabella during the meraspid period. This is likely a pedomorphic trait, with ancestral juvenile glabellar morphology retained throughout development. This may also explain why the protaspides of *M. cylindrica* are much larger than those of equivalent stages in *R. cf. versabunda*.

#### 4.8.4 Phylogenetic implications

Redlichiid protaspides such as those of *Redlichia cf. versabunda* and *Metaredlichia cylindrica* are characterised by a longitudinal medial glabellar furrow, three or four pairs of fixigenal spines, and the degree of dorsal cephalic segmentation evident in the glabellar furrows continuing onto the fixigenal area. This last trait is also present in certain olenelloid meraspides (e.g., *Nephrolenellus geniculatus*; Webster, 2007), as well as many other redlichiine protaspides such as the gigantopygid *Zhangshania typica* (Li *et al.* 1990), the emuellids *Balcoracania dailyi* and *Emuella polymera* (Paterson & Edgecombe, 2006), and several redlichioid taxa (see Paterson *et al.* 2019). This trait is likely to be plesiomorphic for Trilobita, being present in a wide range of early Cambrian taxa, but is apparently lost in the more derived ellipsocephaloids and paradoxidoids (Paterson *et al.* 2019). The presence of

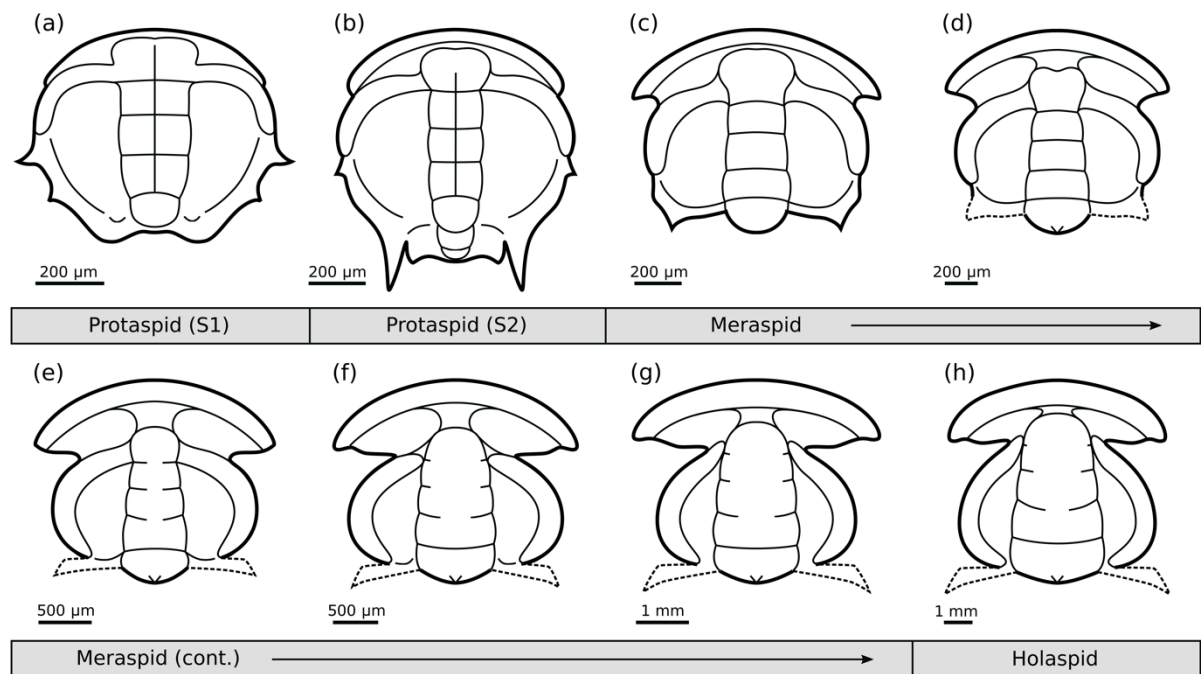


**Figure 4.8:** Reconstructions of various ontogenetic stages of *Redlichia cf. versabunda* from the Ramsay Limestone (Yorke Peninsula, South Australia). (a) Early stage protaspis. (b) Late stage protaspis. (c–g) Meraspid stages in order of increasing size. (h) Holaspis. Dashed lines represent uncertain morphology.

several fixigenal spines in redlichiid protaspides may also be plesiomorphic, as this morphology is possibly associated with the expression of dorsal segmentation in the cephalon, as indicated by the presence of transverse furrows in the fixigenal area (noted above). Unfortunately, detailed information on protaspides from more basal groups (e.g., emuellids) is lacking, so the polarity of this character cannot be easily established; however, it is important to note that the protaspides of more derived ellipsocephaloids display a reduced number of fixigenal spines (e.g., Zhang & Pratt, 1999; Dai & Zhang, 2012a; Laibl *et al.* 2018; Holmes *et al.* in press). The longitudinal medial glabellar furrow is present in some redlichioid and paradoxidoid protaspides, but is absent in ellipsocephaloids, emuellids and many other Cambrian taxa, suggesting this trait is homoplasious (Paterson *et al.* 2019). The retraction and subsequent extension of the glabella observed throughout the ontogeny of *R. cf. versabunda* is probably a plesiomorphic trait, being present in many early Cambrian trilobites, including some of the earliest known taxa (e.g., *Fallotaspis*: McNamara, 1986). Non-retraction of the glabella, or retraction without subsequent re-extension, have been suggested to reflect derived pedomorphic states (e.g., Hupé, 1953; McNamara, 1986).

## 4.9 Acknowledgements

We thank Brent Bowman for collection and preparation of the specimens described in this contribution. Thanks to Lukáš Laibl and an anonymous referee for their helpful reviews. This research was supported by an Australian Government Research Training Scheme (RTS) scholarship and the Constance Fraser Supplementary Scholarship from the University of Adelaide to JDH.

## 4.10 References

- Adrain JM** (2011) Class Trilobita Walch, 1771. In *Animal Biodiversity: An Outline of Higher-Level Classification and Survey of Taxonomic Richness* (ed. Z-Q Zhang). *Zootaxa* **3148**, 104–9.
- Ahlberg P** (1983) A Lower Cambrian trilobite fauna from Jämtland, central Scandinavian Caledonides. *GFF* **105**(4), 349–61.
- Bengtson S, Conway Morris S, Cooper BJ, Jell PA and Runnegar BN** (1990) Early Cambrian fossils from South Australia. *Memoirs of the Association of Australasian Palaeontologists* **9**, 1–364.
- Betts MJ, Paterson JR, Jacquet SM, Andrew AS, Hall PA, Jago JB, Jagodzinski EA, Preiss WV, Crowley JL, Brougham T, Mathewson CP, García-Bellido DC, Topper TP, Skovsted CB and Brock GA** (2018) Early Cambrian chronostratigraphy and geochronology of South Australia. *Earth-Science Reviews* **185**, 498–543.
- Brock GA and Cooper BJ** (1993) Shelly fossils from the early Cambrian (Toyonian) Wirrealpa, Aroona Creek, and Ramsay limestones of South Australia. *Journal of Paleontology* **67**(5), 758–87.
- Chatterton BDE, Siveter DJ, Edgecombe GD and Hunt AS** (1990) Larvae and relationships of the Calymenina (Trilobita). *Journal of Paleontology* **64**(2), 255–77.
- Chatterton BDE and Speyer SE** (1997) Ontogeny. In *Treatise on Invertebrate Paleontology, Part O, Revised. Arthropoda 1, Trilobita 1, (Introduction, Order Agnostida, Order Redlichiida)* (ed RL Kaesler), pp. 173–247. Boulder, Colorado and Lawrence, Kansas: Geological Society of America and University of Kansas Paleontological Institute.

- Dai T and Zhang X** (2012a) Ontogeny of the trilobite *Estaingia sinensis* (Chang) from the Lower Cambrian of South China. *Bulletin of Geosciences* **87**(1), 151–8.
- Dai T and Zhang X** (2012b) Ontogeny of the redlichiid trilobite *Metaredlichia cylindrica* from the lower Cambrian (Stage 3) of South China. *Journal of Paleontology* **86**(4), 646–51.
- Dai T and Zhang X** (2013) Ontogeny of the redlichiid trilobite *Eoredlichia intermediata* from the Chengjiang Lagerstätte, lower Cambrian, southwest China. *Lethaia* **46**(2), 262–73.
- Daily B** (1956) The Cambrian in South Australia. In *El sistema Cámbrico, su paleogeografía y el problema de su base* (ed J Rodgers), pp. 91–147. Mexico, 1956: 20th International Geological Congress.
- Daily B** (1957) Progress report on the Cambrian sequence met with in the Minlaton Stratigraphic Bore 1, Sect. 153, Hd. Ramsay, Yorke Peninsula, S. Aust. (unpublished).
- Daily B** (1968) Subsurface stratigraphy and palaeontology of the Cambrian sequence, Stansbury Town No. 1 well. *South Australian Department of Mines, open file envelope 48* (unpublished).
- Daily B** (1976) The Cambrian of the Flinders Ranges: 25th International Geological Congress, Excursion Guide 33A, pp. 15–19.
- Daily B** (1982) Guide to Excursion A. Archean Proterozoic and lower Palaeozoic Geology, Eyre Peninsula and the Flinders Ranges, South Australia. In *4th International Symposium on Antarctic Earth Sciences, Adelaide* pp. 37–72.
- Daily B** (1990) Cambrian stratigraphy of Yorke Peninsula. *Geological Society of Australia, Special Publication 16*, 215–29.
- Edgecombe GD, Speyer SE and Chatterton BDE** (1988) Protaspid larvae and phylogenetics of encrinurid trilobites. *Journal of Paleontology* **62**(5), 779–99.
- Etheridge R** (1905) Additions to the Cambrian fauna of South Australia. *Transactions of the Royal Society of South Australia* **29**, 246–51.
- Etheridge R** (1919) The Cambrian trilobites of Australia and Tasmania. *Transactions of the Royal Society of South Australia* **43**, 373–93.
- Foord AH** (1890) Description of fossils from the Kimberley district, Western Australia. *Geological Magazine* **7**(3), 98–106, 45–55.
- Fortey RA and Chatterton BDE** (1988) Classification of the trilobite suborder Asaphina. *Palaeontology* **31**(1), 165–222.

- Gravestock DI** (1995) Early and Middle Palaeozoic. In *The Geology of South Australia, Volume 2: The Phanerozoic* (eds JF Drexel and WV Preiss), pp. 3–61. *Geological Survey of South Australia, Bulletin*, **54**.
- Gravestock DI, Alexander EM, Demidenko YE, Esakova NV, Holmer LE, Jago JB, Lin T-R, Melnikova LM, Parkhaev PY, Rozanov AY, Ushatinskaya GT, Zang W-L, Zhegallo EA and Zhuravlev AY** (2001) The Cambrian biostratigraphy of the Stansbury Basin, South Australia. *Transactions of the Palaeontological Institute, Russian Academy of Sciences* **282**, 1–344.
- Gravestock DI and Shergold JH** (2001) Australian early and middle Cambrian sequence biostratigraphy with implications for species diversity and correlation. In *The ecology of the Cambrian radiation* (eds AY Zhuravlev and R Riding), pp. 105–36. New York: Columbia University Press.
- Hawle I and Corda AJC** (1847) Prodom einer Monographie der böhmischen Trilobiten. *Abhandlungen der Königl. Böhmischen Gessellschaft der Wissenschaften* **4**, 120–292.
- Holmes JD, Paterson JR and García-Bellido DC** (in press) The post-embryonic ontogeny of the early Cambrian trilobite *Estaingia bilobata* from South Australia: trunk development and phylogenetic implications. *Papers in Palaeontology*, doi: 10.1002/spp2.1323.
- Holmes JD, Paterson JR and García-Bellido DC** (2020) The trilobite *Redlichia* from the lower Cambrian Emu Bay Shale *Konservat-Lagerstätte* of South Australia: systematics, ontogeny and soft-part anatomy. *Journal of Systematic Palaeontology* **18**(4), 295–334.
- Horwitz RC and Daily B** (1958) Yorke Peninsula. In *The geology of South Australia* (eds MF Glaessner and LW Parkin), pp. 46–70. *Journal of the Geological Society of Australia* **5**.
- Hou J-B, Hughes NC, Yang J, Lan T, Zhang X-G and Dominguez C** (2017) Ontogeny of the articulated yiliangellinine trilobite *Zhangshania typica* from the lower Cambrian (Series 2, Stage 3) of southern China. *Journal of Paleontology* **91**(1), 86–99.
- Hughes NC, Hong PS, Hou J and Fusco G** (2017) The development of the Silurian trilobite *Aulacopleura koninckii* reconstructed by applying inferred growth and segmentation dynamics: a case study in Paleo-Evo-Devo. *Frontiers in Ecology and Evolution* **5**, 37.
- Hughes NC, Minelli A and Fusco G** (2006) The ontogeny of trilobite segmentation: a comparative approach. *Paleobiology* **32**(4), 602–27.
- Hupé P** (1953) Classification des trilobites. *Annales de Paléontologie*, **39**, 61–168.

- Jago JB, Gehling JG, Betts MJ, Brock GA, Dalgarno CR, García-Bellido DC, Haslett PW, Jacquet SM, Kruse PD, Langsford N, Mount TJ and Paterson JR** (2018) The Cambrian System in the Arrowie Basin, Flinders Ranges, South Australia. *Australian Journal of Earth Sciences*, doi: 10.1080/08120099.2018.1525431.
- Jago JB, Gehling JG, Paterson JR, Brock GA and Zang W.** (2012). Cambrian stratigraphy and biostratigraphy of the Flinders Ranges and the north coast of Kangaroo Island, South Australia. *Episodes* **35**(1), 247–255.
- Jago JB and Kruse PD** (2019) Significance of the middle Cambrian (Wuliuan) trilobite *Pagetia* from Yorke Peninsula, South Australia. *Australian Journal of Earth Sciences*, doi: 10.1080/08120099.2019.1643405.
- Jago JB and Zang W-L** (eds. 2006) *XI International Conference of the Cambrian Stage Subdivision Working Group: Field Guide*. Adelaide: Geological Society of Australia, South Australian Division, 59 pp.
- Jago JB, Zang W-L, Sun XW, Brock GA, Paterson JR and Skovsted CB** (2006) A review of the Cambrian biostratigraphy of South Australia. *Palaeoworld* **15**, 406–23.
- Kautsky F** (1945) Die Unterkambrische Fauna vom Aistjakk in Lappland (die larven von *Strenuella*). *Geologiska Föreningens i Stockholm Föerhandlingar* **67**, 129–211.
- Kruse PD** (1990) Cambrian palaeontology of the Daly Basin. *Northern Territory Geological Survey Report* **7**, 1–58.
- Kruse PD** (1998) Cambrian palaeontology of the eastern Wiso and western Georgina Basins. *Northern Territory Geological Survey Report* **9**, 1–68.
- Kruse PD, Laurie JR and Webby BD** (2004) Cambrian geology and palaeontology of the Ord Basin. *Memoirs of the Association of Australasian Palaeontologists* **30**, 1–58.
- Laibl L, Cederström P and Ahlberg P** (2018) Early post-embryonic development in *Ellipsostrenua* (Trilobita, Cambrian, Sweden) and the developmental patterns in Ellipsocephaloidea. *Journal of Paleontology* **92**(6), 1018–27.
- Laibl L, Esteve J and Fatka O** (2017) Giant postembryonic stages of *Hydrocephalus* and *Eccaparadoxides* and the origin of lecithotrophy in Cambrian trilobites. *Palaeogeography, Palaeoclimatology, Palaeoecology* **470**, 109–15.
- Laurie JR** (2006) Early middle Cambrian trilobites from Pacific Oil & Gas Baldwin 1 well, southern Georgina Basin, Northern Territory. *Memoirs of the Association of Australasian Palaeontologists* **32**, 127–204.



- Laurie JR** (2016) Whitehouse's *Redlichia* (Trilobita) specimens from the Georgina Basin, western Queensland. *Australasian Palaeontological Memoirs* **49**, 75–81.
- Li S-J, Kang C-L and Zhang X-G** (1990) Sedimentary environment and trilobites of lower Cambrian Yuxiansi Formation in Leshan district, Sichuan. *Bulletin of the Chengdu Institute of Geology and Mineral Resources, Chinese Academy of Geological Sciences* **12**, 37–56.
- Lu Y-H** (1940) On the ontogeny and phylogeny of *Redlichia intermediata* Lu (sp. nov.). *Bulletin of Geological Society of China* **3–4**, 333–42.
- Lu Y-H** (1950) On the genus *Redlichia* with description of its new species. *Geological Review* **15**, 157–70.
- Lu Y-H, Zhang W-T, Qian Y-Y, Zhu Z-L, Lin H-L, Zhou Z-Y, Qian Y, Zhang S-G and Yuan J-L** (1974) Cambrian trilobites. In *Handbook of Stratigraphy and Palaeontology of Southwest China* pp. 82–107. Beijing: Science Press.
- Ludbrook NH** (1965). Minlaton and Stansbury stratigraphic bores: subsurface stratigraphy and micropalaeontology. In *The Geology of the Yorke Peninsula* pp. 83–95. *Geological Survey of South Australia, Bulletin* **39** (Appendix).
- McNamara KJ** (1986) The role of heterochrony in the evolution of Cambrian trilobites. *Biological Reviews* **61**(2), 121–56.
- Meneghini G** (1882) Fauna Cambriana dell'Iglesiente in Sardegna. *Atti Soc. Toscana Scienze Naturali, Processi verbali* **4**, 7–9.
- Öpik AA** (1958) The Cambrian trilobite *Redlichia*: organization and generic concept. *Commonwealth of Australia, Bureau of Mineral Resources, Geology and Geophysics, Bulletin* **42**, 1–51.
- Öpik AA** (1968) The Ordian Stage of the Cambrian and its Australian Metadoxididae. *Commonwealth of Australia, Bureau of Mineral Resources, Geology and Geophysics, Bulletin* **92**, 133–70.
- Öpik AA** (1970) *Redlichia* of the Ordian (Cambrian) of Northern Australia and New South Wales. *Commonwealth of Australia, Bureau of Mineral Resources, Geology and Geophysics, Bulletin* **114**, 1–67.
- Öpik AA** (1975) Templetonian and Ordian xystridurid trilobites of Australia. *Commonwealth of Australia, Bureau of Mineral Resources, Geology and Geophysics, Bulletin* **121**, 1–84.

- Palmer AR and Rowell AJ** (1995) Early Cambrian trilobites from the Shackleton Limestone of the Central Transantarctic Mountains. *Paleontological Society Memoir* **45**, 1–28.
- Paterson JR** (2020) The trouble with trilobites: classification, phylogeny and the cryptogenesis problem. *Geological Magazine* **157**(1), 35–46.
- Paterson JR and Brock GA** (2007) Early Cambrian trilobites from Angorichina, Flinders Ranges, South Australia, with a new assemblage from the *Pararaia bunyeroensis* Zone. *Journal of Paleontology* **81**(1), 116–42.
- Paterson JR and Edgecombe GD** (2006) The early Cambrian trilobite family Emuellidae Pocock 1970: Systematic position and revision of Australian species. *Journal of Paleontology* **80**(3), 496–513.
- Paterson JR, Edgecombe GD and Lee MSY** (2019) Trilobite evolutionary rates constrain the duration of the Cambrian explosion. *Proceedings of the National Academy of Sciences (USA)* **116**, 4394–9.
- Paterson JR, Jago JB, Brock GA and Gehling JG** (2007) Taphonomy and palaeoecology of the emuellid trilobite *Balcoracania dailyi* (early Cambrian, South Australia). *Palaeogeography, Palaeoclimatology, Palaeoecology* **249**(3–4), 302–21.
- Percival IG and Kruse PD** (2014) Middle Cambrian brachiopods from the southern Georgina Basin of central Australia. *Memoirs of the Association of Australasian Palaeontologists* **45**, 349–402.
- Pillola GL** (1991) Trilobites du Cambrien inférieur du SW de la Sardaigne, Italie. *Palaeontographia Italica* **78**, 1–173.
- Pocock KJ** (1964) *Estaingia*, a new trilobite genus from the Lower Cambrian of South Australia. *Palaeontology* **7**, 45–71.
- Pocock KJ** (1970) The Emuellidae, a new family of trilobites from the lower Cambrian of South Australia. *Palaeontology* **13**(4), 522–62.
- Popov LE, Holmer LE, Hughes NC, Ghobadi Pour M and Myrow PM** (2015) Himalayan Cambrian brachiopods. *Papers in Palaeontology* **1**(4), 345–99.
- Schneider CA, Rasband WS and Eliceiri KW** (2012) NIH Image to ImageJ: 25 years of image analysis. *Nature methods* **9**(7), 671.
- Smith TE, Carr LK, Edwards DS, Hall L, Kelman AP, Laurie JR, le Poidevin S and Nicoll RS** (2013). Georgina Basin biozonation and stratigraphy, 2013. *Geoscience Australia Basin Biozonation and Stratigraphy Chart Series*, **41**.

- Šnajdr M** (1958) Trilobiti českého středního kambria [Trilobites of the Middle Cambrian of Bohemia]. *Rozpravy Ústředního ústavu geologického* **24**, 1–280.
- Teichert C** (1948) A simple device for coating fossils with ammonium chloride. *Journal of Paleontology* **22**(1), 102–4.
- Walch JEI** (1771) *Die Naturgeschichte der Versteinerungen zur Erläuterung der Knorr'schen Sammlung von Merkwürdigkeiten der Natur*. Nürnberg: Paul Jonathan Felstecker, 235 p.
- Walcott CD** (1905) Cambrian faunas of China. *Proceedings of the United States National Museum* **29**, 1–106.
- Webster M** (2007) Ontogeny and evolution of the early Cambrian trilobite genus *Nephrolenellus* (Olenelloidea). *Journal of Paleontology* **81**(6), 1168–93.
- Westergård AH** (1936) *Paradoxides oelandicus* beds of Öland. *Sveriges Geologiska Undersökning, Serie C* **394**, 1–66.
- Whitehouse FW** (1939) The Cambrian faunas of north-eastern Australia. Part 3 – The polymerid trilobites (with supplement No. 1). *Memoirs of the Queensland Museum* **11**(3), 179–282.
- Whittington HB** (1957) The ontogeny of trilobites. *Biological Reviews* **32**(4), 421–67.
- Whittington HB and Kelly SRA** (1997) Morphological terms applied to Trilobita. In *Treatise on Invertebrate Paleontology, Part O, Revised. Arthropoda 1, Trilobita 1, (Introduction, Order Agnostida, Order Redlichiida)* (ed RL Kaesler), pp. 313–29. Boulder, Colorado and Lawrence, Kansas: Geological Society of America and University of Kansas Paleontological Institute.
- Zhang W-T** (1953) Some Lower Cambrian trilobites from western Hupei. *Acta Palaeontologica Sinica* **1**(3), 121–49.
- Zhang W-T** (1957) Cambrian and Ordovician stratigraphy of the Gorge District of the Yangtze, Hupeh. *Kexue Tongbao* **5**, 145.
- Zhang W-T** (1985) Current biostratigraphic scheme of the Chinese Cambrian. *Palaeontologia Cathayana* **2**, 73–5.
- Zhang W-T** (2003) Cambrian biostratigraphy of China. In *Biostratigraphy of China* eds W-T Zhang, P-J Chen and AR Palmer), pp. 55–119. Beijing: Science Press.
- Zhang W-T, Lu Y-H, Zhu Z-L, Qian Y-Y, Lin H-L, Zhao Z-Y, Zhang S-G and Yuan J-L** (1980) Cambrian trilobite faunas of southwestern China. *Palaeontologia Sinica, new series B (no.16)* **159**, 1–497.

**Zhang W-T and Jell PA** (1987) *Cambrian trilobites of North China*. Beijing: Science Press.

**Zhang X-G and Clarkson ENK** (2012) Phosphatized eodiscoid trilobites from the Cambrian of China. *Palaeontographia Abteilung A* **297**(1–4), 1–121.

**Zhang X-G and Pratt BR** (1999) Early Cambrian trilobite larvae and ontogeny of *Ichangia ichangensis* Chang, 1957 (Protolenidae) from Henan, China. *Journal of Paleontology* **73**(1), 117–28.



## Chapter 5

The trilobite *Redlichia* from the lower Cambrian Emu Bay Shale  
*Konservat-Lagerstätte* of South Australia:  
systematics, ontogeny and soft-part anatomy

**Holmes, J.D., Paterson, J.R. & García-Bellido, D.C.** 2020. The trilobite *Redlichia* from the lower Cambrian Emu Bay Shale *Konservat-Lagerstätte* of South Australia: systematics, ontogeny and soft-part anatomy. *Journal of Systematic Palaeontology*, **18**: 295–334.

## Statement of Authorship

|                      |   |
|----------------------|---|
| Title of paper:      | The trilobite <i>Redlichia</i> from the lower Cambrian Emu Bay Shale <i>Konservat-Lagerstätte</i> of South Australia: systematics, ontogeny and soft-part anatomy   |
| Publications status  | Published   |
| Publication details: | Holmes, J.D., Paterson, J.R. & García-Bellido, D.C. 2020b. The trilobite <i>Redlichia</i> from the lower Cambrian Emu Bay Shale <i>Konservat-Lagerstätte</i> of South Australia: systematics, ontogeny and soft-part anatomy. <i>Journal of Systematic Palaeontology</i> 18: 295–334. |

### Principal author

|                                      |  |
|--------------------------------------|--|
| Name of principal author (candidate) | James D. Holmes  |
| Contribution to the paper            | Collected specimens, measured and photographed all specimens considered, conducted all analyses, wrote the manuscript, drew up all figures and acted as corresponding author.  |
| Overall percentage (%)               | 90   |
| Certification                        | This paper reports on original research I conducted during the period of my Higher Degree by Research candidature and is not subject to any obligations or contractual agreements with a third party that would constrain its inclusion in this thesis. I am the primary author of this paper. |
| Signature/date                       | 07/07/2020   |

### Co-author contributions

By signing the Statement of Authorship, each author certifies that:

- i. the candidate's stated contribution to the publication is accurate (as detailed above);
- ii. permission is granted for the candidate to include the publication in the thesis; and
- iii. the sum of all co-author contributions is equal to 100% less the candidate's stated contribution.

|                           |   |
|---------------------------|---|
| Name of co-author         | John R. Paterson  |
| Contribution to the paper | Collected specimens, supervised development of work and helped to evaluate and edit the manuscript. |
| Signature/date            | 13/7/2020   |

|                           |   |
|---------------------------|---|
| Name of co-author         | Diego C. García-Bellido   |
| Contribution to the paper | Collected specimens, supervised development of work and helped to evaluate and edit the manuscript. |
| Signature/date            | 8/7/2020  |

**LIBRARY NOTE:**

The following article on pages 91-130 has been removed due to copyright.

It is also available online to authorised users at:  
<https://doi.org/10.1080/14772019.2019.1605411>



## Chapter 6

Meraspid axial growth gradients in the early Cambrian ellipsocephaloid trilobite *Estaingia bilobata* from South Australia

Intended for submission to *Paleobiology*.

## Statement of Authorship

|                      |  |
|----------------------|--|
| Title of paper:      | Meraspid axial growth gradients in the early Cambrian ellipsocephaloid trilobite <i>Estaingia bilobata</i> from South Australia  |
| Publications status  | Unpublished and unsubmitted work written in manuscript style   |
| Publication details: | Holmes, J.D., Paterson, J.R. & García-Bellido, D.C. Meraspid axial growth gradients in the early Cambrian ellipsocephaloid trilobite <i>Estaingia bilobata</i> from South Australia. |

### Principal author

|                                      |  |
|--------------------------------------|--|
| Name of principal author (candidate) | James D. Holmes  |
| Contribution to the paper            | Collected specimens, measured and photographed all specimens considered, conducted all analyses, wrote the manuscript and drew up all figures.   |
| Overall percentage (%)               | 90   |
| Certification                        | This paper reports on original research I conducted during the period of my Higher Degree by Research candidature and is not subject to any obligations or contractual agreements with a third party that would constrain its inclusion in this thesis. I am the primary author of this paper. |
| Signature/date                       | 07/07/2020   |

### Co-author contributions

By signing the Statement of Authorship, each author certifies that:

- i. the candidate's stated contribution to the publication is accurate (as detailed above);
- ii. permission is granted for the candidate to include the publication in the thesis; and
- iii. the sum of all co-author contributions is equal to 100% less the candidate's stated contribution.

|                           |   |
|---------------------------|---|
| Name of co-author         | John R. Paterson  |
| Contribution to the paper | Collected specimens, supervised development of work and helped to evaluate and edit the manuscript. |
| Signature/date            | 13/7/2020   |

|                           |   |
|---------------------------|---|
| Name of co-author         | Diego C. García-Bellido   |
| Contribution to the paper | Collected specimens, supervised development of work and helped to evaluate and edit the manuscript. |
| Signature/date            | 8/7/2020  |

## 6.1 Abstract

Quantitative studies of trilobite growth require multiple high-quality specimens from each of a series of sequential developmental stages, and are often restricted to later portions of ontogeny due to poor representation of early instars. The Cambrian Series 2 (Stage 4) Emu Bay Shale from Kangaroo Island, South Australia, contains abundant specimens of the ellipsocephaloid trilobite *Estaingia bilobata*, including a complete meraspid ontogenetic series. Here we examine axial growth of exoskeletal body parts, in particular of the trunk region, from across the entire meraspid period of *E. bilobata* from the Emu Bay Shale. Initial examination of trunk segment growth rates across ontogeny revealed a growth gradient in the meraspid trunk of *E. bilobata*, similar to that identified in other trilobites. However, growth rates of exoskeletal elements (including the cephalon and trunk) appear to decrease as growth progresses, at odds with Dyar's rule (a constant pre- to post-moult size ratio), and with observations of other trilobites across shorter periods of meraspid ontogeny. We contrastively tested two hypotheses of trunk growth control in *E. bilobata*, the segmental gradient (SG) and trunk gradient (TG) hypotheses, under the condition of a decreasing trunk growth rate. Several models under each hypothesis were tested using non-linear least squares regression of relative trunk lengths and positions across sequential meraspid developmental stages. Results of the hypothesis testing are equivocal; the best models under the SG hypothesis perform better using relative segment lengths, whereas those under the TG hypothesis perform better using relative segment position. If the SG hypothesis is true, model support suggests that individual trunk segments maintained a constant allometric coefficient with respect to trunk length. However, if the TG hypothesis is true, results suggest that the trunk gradient changed, being steeper in earlier stages and decreasing across the meraspid period. Thus, the steeper meraspid and shallower holaspid gradients previously identified in the Silurian trilobite *Aulacopleura koninckii* may be a result of a dynamic growth gradient rather than separate static gradients. Extension of this work to the holaspid period of *E. bilobata*, and results of similar studies on other early Cambrian trilobites, will be important in determining the true controls of trunk development in this early arthropod.

## 6.2 Introduction

Trilobites are some of the most abundant early animal fossils with a record spanning almost the entire Palaeozoic, and are useful for answering questions about early animal evolution, including those relating to developmental processes (e.g. Fusco *et al.* 2012; Hughes *et al.* 2017; Paterson *et al.* 2019). Unlike most fossil groups, development in trilobites is well known due to their possession of a biomineralized exoskeleton throughout the majority of post-embryonic ontogeny (Hughes 2003). A considerable number of articulated trilobite ontogenies have been published, particularly in recent years (e.g. Dai & Zhang 2013; Dai *et al.* 2014; 2017; Du *et al.* 2019; 2020; Holmes *et al.* 2020; Hou *et al.* 2015; 2017). However, even with their exemplary record, obtaining the data required for detailed morphometric studies (such as those relating to segmental growth) is problematic, and as such these previous studies have been largely descriptive.

In order to move beyond simple description of developmental patterns, multiple high-quality specimens from sequential early developmental stages (usually meraspid degrees characterised by differing numbers of thoracic segments) are required from which to take accurate measurements. To obtain these, it is likely that several thousands of specimens would need to be examined for any one species, in order to obtain datasets of a useable sample size (e.g. Du *et al.* 2019; Fusco *et al.* 2014; Holmes *et al.* 2020; Hong *et al.* 2014). These should also be sourced from a single locality, within the narrowest stratigraphic interval possible, preferably several metres or less. These requirements have thus far limited detailed studies of development in trilobites to a single species: the 429 million-year-old *Aulacopleura koninckii* from the Silurian of the Czech Republic (for a review, see Hughes *et al.* 2017). Even for this species, analysis has focused on the latter part of the meraspid period (stages D9–D17, representing specimens with between nine and seventeen thoracic segments) and the holaspid period, due to a scarcity of specimens from earlier developmental stages. Extending these types of analyses to other trilobites, particularly those from the early Cambrian, will help to identify conserved patterns of growth control within the Trilobita, and potentially the ancestral developmental condition for the clade (Hughes *et al.* 2017).

In their investigation of segmental growth dynamics in *A. koninckii*, Fusco *et al.* (2014) identified a growth gradient in the trunk during the meraspid period for this trilobite (and

later during the holaspid period: Fusco *et al.* 2016), with the highest rates of growth at the posterior of the trunk, and lowest rates at the anterior. Based on this observation, they used several non-linear regression models to test the validity of two hypotheses for how trunk segment growth was controlled in *A. koninckii*: (1) the segmental gradient (SG) hypothesis, where each individual segment grew at a constant, predefined growth rate, and (2) the trunk gradient (TG) hypothesis, where the growth of individual segments was a result of their (changing) position within a continuous growth field represented by the trunk. Their findings suggested that the TG hypothesis had more support, and that trunk segment growth was controlled by a regional gradient.

Based on their observations across the latter part of the meraspid period, the analysis by Fusco *et al.* (2014) assumed a constant growth rate for the overall trunk across the period in question. Growth in arthropods (as in other ecdysozoans) occurs in a stepwise fashion as a result of their requirement to periodically moult their exoskeleton, and it has been shown that growth trajectories of external structures in arthropods are often characterised by a constant per-moult growth rate, the so-called Dyar's rule (Dyar 1890). In general, growth in trilobites has been shown to largely conform to Dyar's rule (Fusco *et al.* 2012), and this appears to be the case for the trunk of *A. koninckii*, at least for the latter half of the meraspid period; it should be noted, however, that the TG hypothesis suggests a decrease in segmental growth rates across ontogeny and therefore, if true, precludes Dyar's rule in the strict sense.

Recently collected material from the Cambrian Series 2 (Stage 4) Emu Bay Shale in South Australia includes very large numbers of the ellipsocephaloid trilobite *Estaingia bilobata* (Holmes *et al.* 2020). An abundance of specimens from most post-embryonic developmental stages makes this species an ideal candidate to explore aspects of growth control in an early Cambrian trilobite. Initial examination of segmental growth rates across the meraspid period for *E. bilobata* suggests a growth gradient (Fig. 6.1A) similar to that identified in *A. koninckii* (Fusco *et al.* 2014; 2016) and *Changaspis elongata* (Du *et al.* 2019). However, observations of mean (log) segment length across the various stages (Fig. 6.1B) suggests that growth of segments was faster in early stages and decreased in later stages, as did the overall trunk and cephalic growth rates (Fig. 6.1C, D), which is at odds with the expectations of Dyar's rule. These observations suggest the possibility of a constant segmental growth rate with respect to a changing trunk growth rate—an alternative form of

the SG hypothesis. The purpose of this paper is to explore the SG and TG hypotheses with respect to the observation of a changing trunk growth rate in *E. bilobata*, in order to determine the likely growth control mechanisms in this early arthropod.

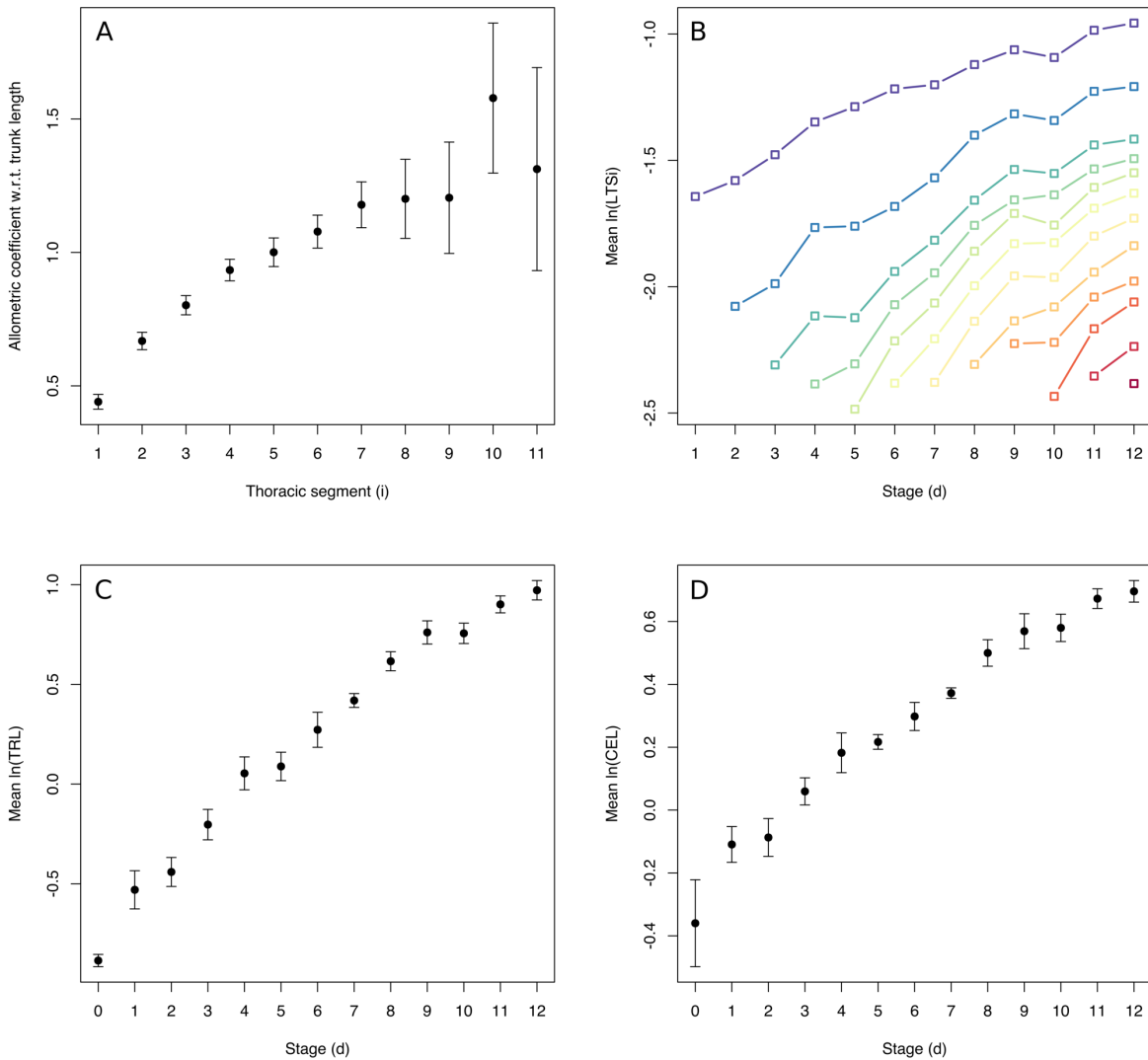


**Figure 6.1:** Various indicators of growth in the meraspid trunk of *Estaingia bilobata* from the Emu Bay Shale. (A) Allometric coefficients of thoracic segments (TS)1–11 with respect to overall trunk length. Segments with allometric coefficients less than one (TS1–4) decreased in length relative to the trunk across ontogeny, whereas those with allometric coefficients greater than one (TS6–11) increased in relative length. TS5 has an allometric coefficient of approximately one, meaning that the proportions of this segment with respect to the trunk remained approximately equal. (B) Mean log lengths of thoracic segments across meraspid ontogeny (TS1–12 from top left to bottom right). (C) Mean log trunk length across meraspid ontogeny. (D) Mean log cephalic length across meraspid ontogeny. The D0 meraspidites included were interpreted as being of the same developmental stage ( $n = 2$ ). Note that length in all body parts appears to increase at a decreasing rate, suggesting a gradual decrease in the growth rate across the period analysed (A–C).

## 6.3 Material and methods

### 6.3.1 Specimen data

Material considered in this study was collected between 2007 and 2019 from the Emu Bay Shale at Big Gully on the north coast of Kangaroo Island, and are housed in the South Australian Museum Palaeontological collections (specimen number prefix SAMP). There are 572 registered specimens of *Estaingia bilobata* in the collection, with many additional unregistered specimens associated with other fossils; the total number is estimated to be several thousand individuals. Recent efforts have focused on identifying and retaining complete, articulated meraspides from the thousands of specimens examined in the field. Specimens were collected from a c. 2-m section of dark, laminated mudstone, interspersed with centimetre-scale silt and fine sandstone intercalations, exposed in Buck and Daily quarries about 10–12 m above the base of the formation (Gehling *et al.* 2011; Paterson *et al.* 2016). Within this interval, the trilobite *Estaingia bilobata* occurs in abundance, being present on certain surfaces in densities of up to 630 individuals per m<sup>2</sup> (J. R. Paterson, unpub. data). It is suspected that fluctuations of the oxycline may have been responsible for ‘mass kill’ events, with the predominance of ‘dorsum down’ specimens (up to 90%: Drage *et al.* 2018) potentially an indication of oxygen stress prior to death. This is supported by a high ratio of carcasses compared to specimens interpreted to represent moult configurations (Drage *et al.* 2018; Gehling *et al.* 2011). Due to the discontinuous nature, faulting and fracturing of beds, it is not possible to obtain an accurate census of single bedding plane assemblages within the deposit. The Emu Bay Shale forms part of the Kangaroo Island Group, the various formations of which have been interpreted as representing different environmental expressions of a fan delta complex adjacent to a zone of active tectonic uplift to the immediate north of the Big Gully area (Gehling *et al.* 2011; Jago *et al.* 2020; Paterson *et al.* 2018).

The specimens of *Estaingia bilobata* considered here are from the so-called meraspid period, during which trunk segments were generated within and sequentially released from the pygidium to become fully articulating segments of the thorax. Holmes *et al.* (2020) presented data on 124 *E. bilobata* meraspides from the Emu Bay Shale for which the degree (a morphotype with the same number of thoracic segments) could be identified

with a high degree of confidence. They also interpreted each meraspid degree as representing a separate developmental stage or moult instar (except the first 'M0' meraspid degree with no thoracic segments that may have had multiple stages). In *E. bilobata* (as seems to be the case for most trilobites), a segment was released from the anterior of the pygidium into the thorax at each moult, such that successive stages are represented by instars with a steadily increasing number of thoracic segments (i.e. 1, 2, 3, etc.) (Fig. 6.2). The adult (or holaspid) period commenced when the animal attained the full complement of 13 thoracic segments. The identification of developmental stages by a measure independent of size (in this case the number of thoracic segments) provides what is called 'cross-sectional data' for segmental growth across the meraspid period of *E. bilobata*.

The growth gradient analyses conducted here are based on a subset of the specimens considered by Holmes *et al.* (2020) for which accurate thoracic segment length measurements could be taken ( $n = 102$ ). The number of specimens for each stage is as follows (Dx represents growth stages designated by number of thoracic segments x): 7 D1, 3 D2, 8 D3, 7 D4, 4 D5, 8 D6, 16 D7, 11 D8, 8 D9, 7 D10, 16 D11, 7 D12. Two D0 meraspides were also used to explore additional patterns of growth in the trunk of *E. bilobata*.

### 6.3.2 Measurements

Methodology for the collection of body-part length data largely follows Fusco *et al.* (2014). Photos of *Estiaingia bilobata* meraspides were taken with an Olympus SZX7 stereomicroscope with an Olympus SC50 camera attachment using the associated Olympus cellSens Standard v.1.17 software. Using the freeware vector-based drawing program Inkscape (v.0.92), a sagittal line along the entire body was drawn on each specimen, and lateral lines were drawn between points on either pleural lobe where each articulation bends sharply at the fulcrum. In *E. bilobata*, this corresponds to the most distal point of the inner, straight portion of each articulation. These modified images were imported into ImageJ (Schneider *et al.* 2012) and a series of landmarks placed along the sagittal line at the intersections with: the anterior cephalic margin, posterior pygidial margin, and one for each of the line intersections representing the articulations (Fig. 6.3; images were calibrated using the scale bar). These data were imported into the R statistical environment and used



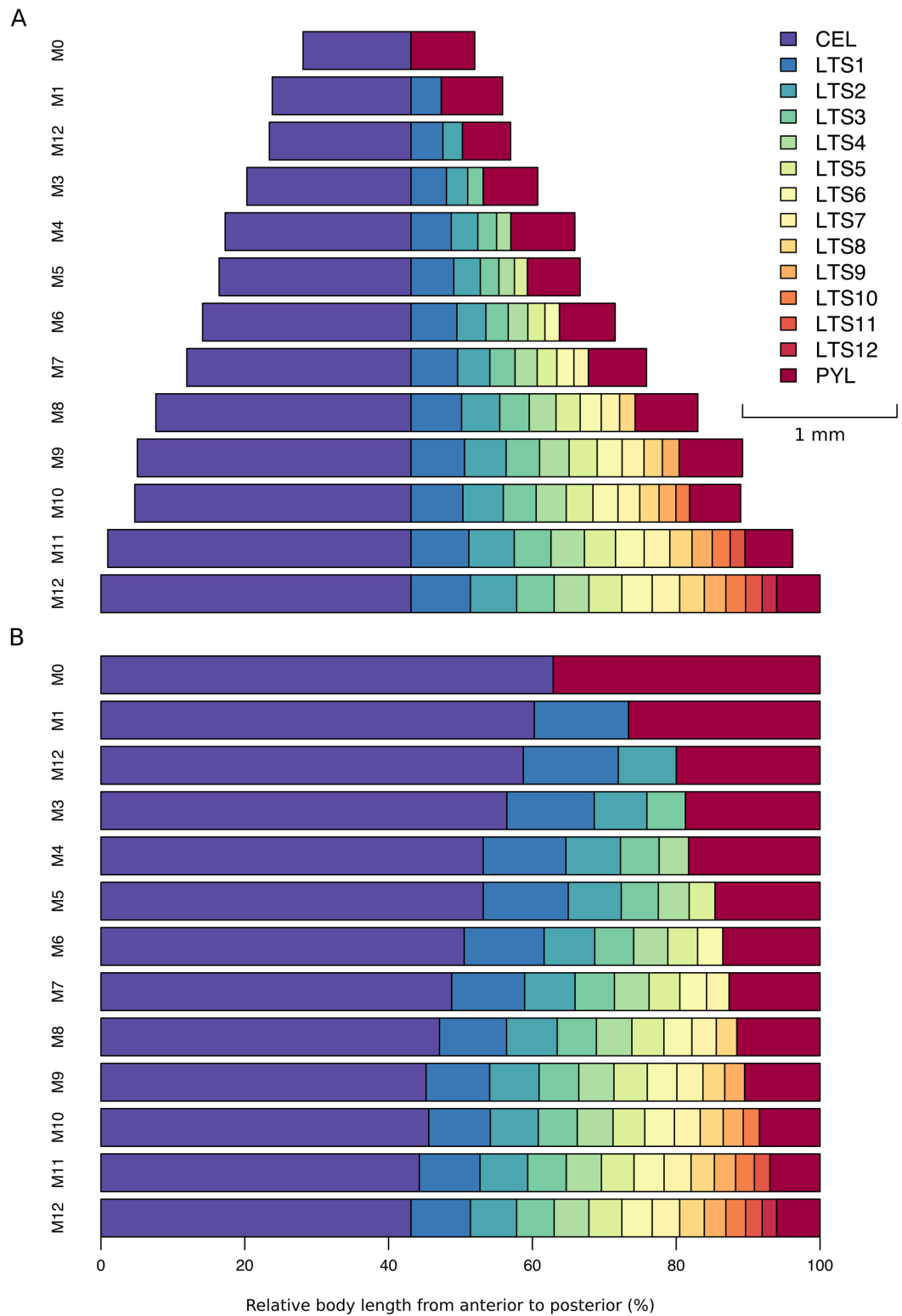
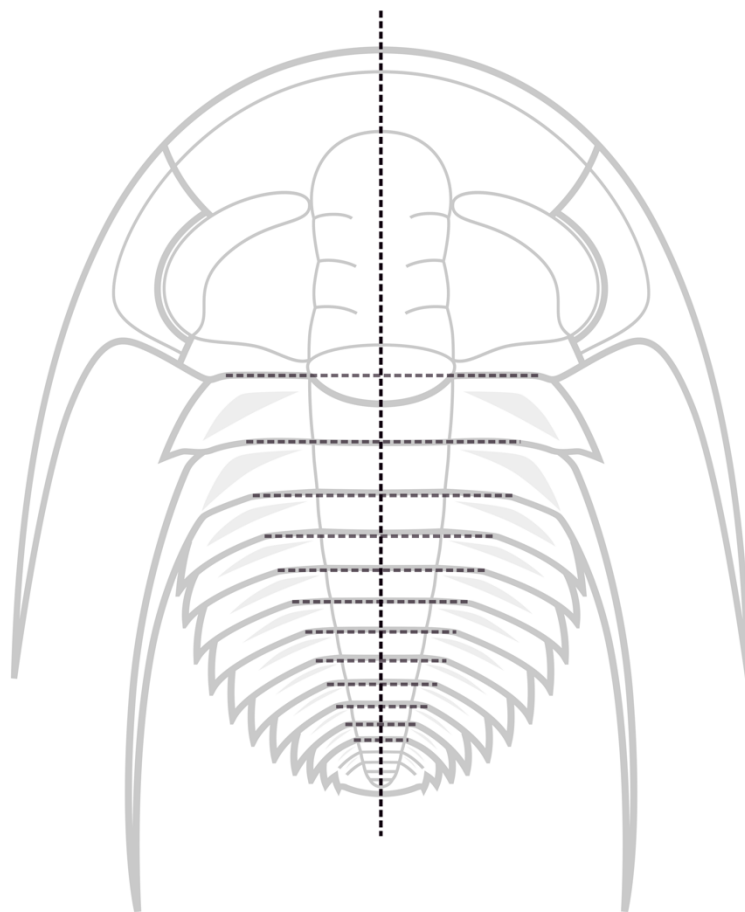


Figure 6.2: Axial lengths of different body parts of *Estaingia bilobata* from the Emu Bay Shale. (A) Absolute axial lengths. (B) Relative axial lengths. Abbreviations: *CEL* = cephalic length; *LTS<sub>i</sub>* = length of thoracic segment *i*; *PYL* = pygidial length.

to produce a dataset containing the lengths ( $i$ ) of all body parts at each stage ( $d$ ), and the position of the posterior of each thoracic segment relative to the cephalic/trunk boundary for all specimens (in our analysis this boundary corresponds to the intersection of the line drawn across the anterior of TS1 and the sagittal line, and is thus slightly anterior to the true posteriormost axial point of the cephalon). In turn, this was used to produce mean length for each body part at each stage, as well as mean length ( $RLS$ ) and mean position of the posterior boundary of each thoracic segment ( $RPS$ ) relative to trunk length. See the Supplementary Material (Chapter 10, section 10.3.1) for details on how these measures were calculated).



**Figure 6.3:** Lines constructed on photographs of *Estaingia bilobata* meraspides to obtain body part length measurements (D11 specimen). Landmarks were placed at the intersection of the sagittal line with each of the perpendicular lines (see main text for details), and at the intersections with the anterior cranial and posterior pygidial margins.

### 6.3.3 Initial growth gradient detection

Previous studies have used both the Average Growth Rate (AGR: Fusco *et al.* 2012) of thoracic segments across ontogeny to illustrate trunk growth gradients, as well as the allometric coefficients of thoracic segments with respect to trunk length (using mean values), to show that growth rates increase from more anterior to more posterior segments (Du *et al.* 2019; Fusco *et al.* 2014). In this case, AGR is an inappropriate measure due to the clear change (decrease) in growth rate of the various thoracic segments across meraspid ontogeny, in violation of Dyar's rule (Fig. 6.1B). As such, we use allometric coefficients of thoracic segments to illustrate growth gradients in the meraspid trunk of *E. bilobata*. Major axis regression was conducted on the log transformed lengths of each thoracic segment against trunk length (using actual rather than mean data, which allows for the calculation of meaningful confidence intervals). The slope of these regressions represent the allometric coefficients for each thoracic segment with respect to overall trunk length across the meraspid period. These show a clear growth gradient in the trunk, with anterior segments displaying lower allometric coefficients with respect to trunk length, and more posterior segments showing higher values (Fig. 6.1A). Thoracic segment five has an allometric coefficient approximately equal to one, meaning that once this segment was released into the thorax it maintained a similar relative length with respect to the trunk throughout ontogeny.

### 6.3.4 Model testing

The models used by Fusco *et al.* (2014) to contrastively test the SG and TG hypotheses incorporated a fixed trunk growth rate, based on their observations of the latter half of the meraspid period for the Silurian trilobite *Aulacopleura koninckii*. Under this scenario, the SG hypothesis expects a constant growth rate of individual segments once they are released into the thorax, with overall trunk growth dependent upon the autonomous growth of individual segments and the pygidium. This reflects the standard model of allometric growth, where the relationship in size between two body measurements is the result of differential constant growth rates (Huxley 1932). In contrast, the TG hypothesis under a

constant trunk growth rate predicts a decrease in segment growth rates across ontogeny, due to segments shifting their position from a more posterior to a more anterior position in the trunk as segments are added behind. Segments are thus sequentially exposed to decreasing values of the gradient (in this case a continuous growth field) that decays from posterior to anterior.

Based on our observations across the entire meraspid period of *E. bilobata*, it is clear that the trunk growth rate decreased as ontogeny progressed, as did the cephalic growth rate (Fig. 6.1C, D). Thus, to test these hypotheses under the condition of a changing trunk growth rate, new models needed to be devised. The model comparison framework used here is essentially the same as that of Fusco *et al.* (2014). Non-linear least squares regression was conducted in R with the *nls()* function, using the default Gauss-Newton algorithm. A range of models were screened based on the expectations of the two hypotheses (see below). For derivation of model fitting functions see the Supplementary Material (Chapter 10, section 10.3.2).

## 6.4 Results

The Segmental Gradient (SG) hypothesis under the condition of a changing (decreasing) trunk growth rate suggests that each segment grew at some pre-defined rate proportional to the overall, changing trunk growth rate. Under this hypothesis we tested two models for which the segmental gradient is a geometric progression ( $g(i) = a + b * e^{w*i}$ ) that decays from posterior to anterior: (1) the SG-R model, which sets the ratio of segment to trunk growth rates as constant; and (2) the SG-A model, which sets a constant allometric coefficient for the segments with respect to the trunk (i.e. a constant ratio of logged segment to trunk growth rates; see Supplementary Material, section 10.3.2). Initial results suggest that parameter  $w$  trends to zero, and the gradient function can be reduced to the linear function  $g(i) = a + b * i$  with no loss of fit. Thus, both SG models have two parameters and are fitted using relative thoracic segment length (*RLS*).

The Trunk Gradient hypothesis suggests that each segment grew at a rate specified by its position in the trunk at any one time; however, the condition of a changing trunk growth rate suggests that the gradient changes across ontogeny. We screened a number of

variants of a regional gradient (RG) model under this hypothesis for which the (continuous) trunk gradients are described by an exponential function ( $g(x) = a + be^{-w(1-x)}$ ) that decays from posterior to anterior. The RG model does not rely on segments as individual units; rather, it recognises segmental boundaries as landmark positions within a continuous growth field (the regional gradient). As such, it is best fitted using the relative position of posterior segmental boundaries (*RPS*). However, the model can be adapted to predict relative segment length (*RLS*), allowing direct comparison with the SG models. Thus, variants of the RG-1 model utilise *RLS*, and variants of the RG-2 model utilise *RPS*.

Several variants of the RG-1 and RG-2 models were tested. Firstly, the 'A' models are two-parameter models ( $b, w$ ) for which there is a single gradient that adapts to a (changing) trunk growth rate by not depending on it (i.e. it is scalable by the trunk growth rate as mentioned above). The 'B' models accommodate the possibility that the trunk growth rate may affect the shape and not only scaling of the gradient. To do this, the models can be increased to four parameter models, with  $b$  and  $w$  replaced with the linear functions  $b_0 + b^*d$  and  $w_0 + w^*d$ , allowing the gradient to vary with stage ( $d$ ). Finally, the 'C' models recognise that in this context, stage may be dependent on the trunk growth rate (*TRG*), and we can therefore substitute  $d$  with  $TRG_d$  so that the fitting parameters become  $b_0 + b^*TRG_d$  and  $w_0 + w^*TRG_d$ . In some cases, certain parameters had little effect on model performance and were removed from the models (Supp. Table 10.2).

Based on comparison with the corrected Akaike Information Criterion ( $AIC_c$ ; Table 6.1), it is clear that both the SG-A and RG-C models have much higher levels of support than other models. The SG-R model in particular has very low support; therefore, the possibility of a constant ratio of segment/trunk growth rates ( $r_S/r_T$ ) is discounted. Likewise, the low level of support for the RG-A1 model suggests that if the TG hypothesis is true, then the regional gradient changed not only in scale but also in shape, and that the inclusion of additional parameters to allow the gradients to vary in some way across ontogeny is important to the model fit. Between the two models that allow this variation, RG-C1 is clearly superior to RG-B1, suggesting that the observed trunk growth rate between stages ( $TRG_d$ ) is more important in explaining the observed data than stage ( $d$ ) alone. The SG-A model has slightly higher support than the RG-C1 model (evidential ratio  $[R] = 1.82$ , the weight of evidence of one model with respect to another calculated as their ratio of corrected Akaike weights,  $wAIC_c$ ); however, this does not reflect strong evidence to reject

one model in favour of the other. Both of these models show very similar predictions with respect to observed data (Fig. 6.4). The RG-C2 model (fitted using *RPS*) performs better than either the SG-A or RG-C1 models (fitted using *RLS*) based on pseudo R-squared values (99.86 compared with 99.58 and 99.60 respectively: Supp. Table 10.2, Supp. Fig. 10.2); however, a direct comparison with AICc is not appropriate based on their differing response variables. Nevertheless, higher support for this two-parameter model does lend support to the TG hypothesis in general.

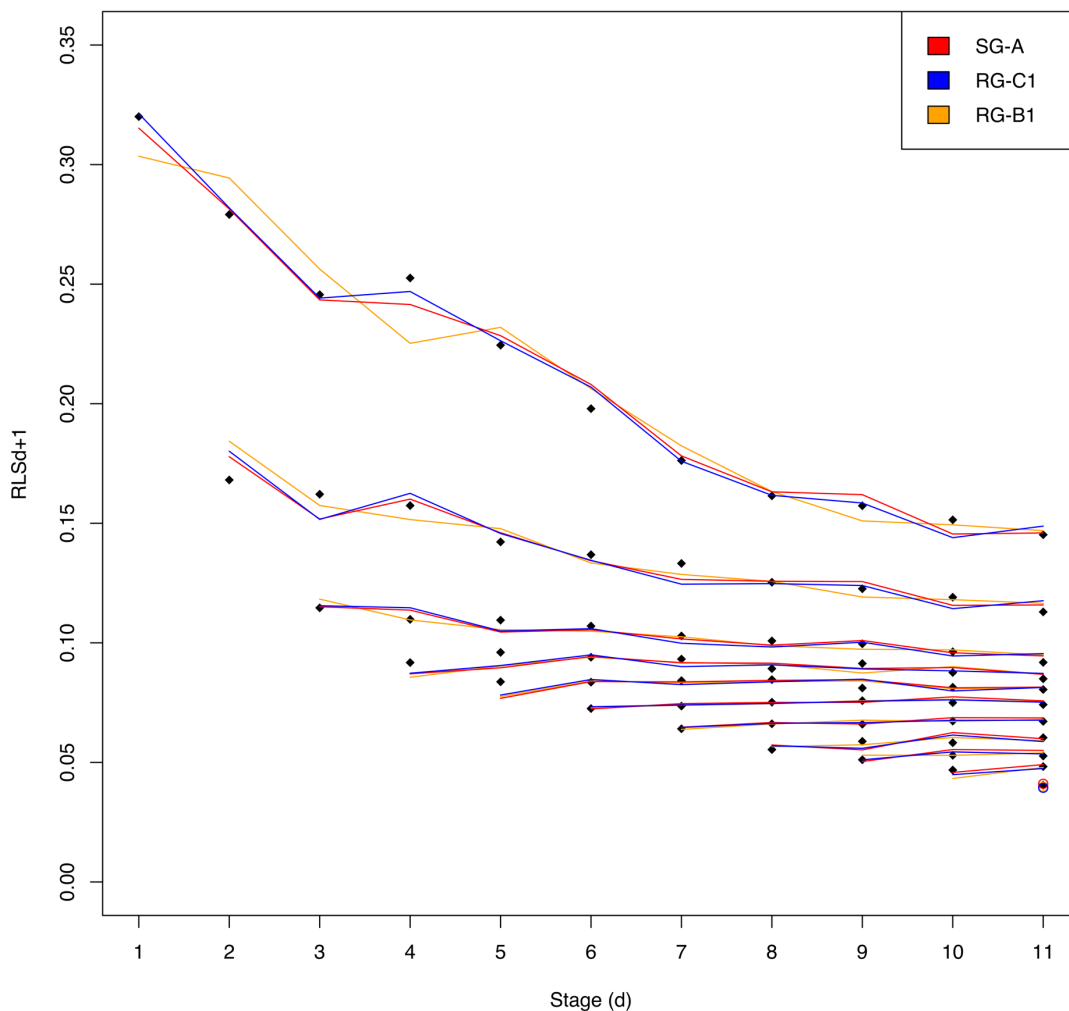


**Figure 6.4:** Fitting of the best supported models under the Segmental Gradient (SG) and Trunk Gradient (TG) hypotheses to observed *RLS* data. The SG-A and RG-C1 models have the highest support, and the predictions of these models are very similar. The RG-B1 model has considerably lower support and is shown here for comparison.

**Table 6.1:** AIC<sub>c</sub> comparison of the models utilising relative thoracic segment length (*RLS*). AIC<sub>c</sub> = AIC<sub>c</sub> score;  $\Delta$ AIC<sub>c</sub> = difference in AIC<sub>c</sub> score between the model in question and the model with the lowest score; wAIC<sub>c</sub> = probability of being the correct model amongst the set of competing models.

| Model | No. of parameters | AIC <sub>c</sub> | $\Delta$ AIC <sub>c</sub> | wAIC <sub>c</sub> |
|-------|-------------------|------------------|---------------------------|-------------------|
| SG-A  | 2                 | -545.16          | 0.00                      | 0.65              |
| RG-C1 | 4                 | -543.97          | 1.20                      | 0.35              |
| RG-B1 | 4                 | -481.14          | 64.02                     | 0.00              |
| RG-A1 | 2                 | -478.01          | 67.15                     | 0.00              |
| SG-R  | 2                 | -367.05          | 178.12                    | 0.00              |

## 6.5 Discussion

### 6.5.1 Trunk growth patterns in *Estaingia bilobata*

The availability of well-preserved specimens from across the entire meraspid period has allowed the clear identification of decreasing growth rates for both the cephalon and trunk, as well as individual trunk segments (Fig. 6.1B–D). The rate of decrease appears to be highest in earlier stages and reduces in later stages, mirroring the pattern of morphological change seen across the same period (Holmes *et al.* 2020). Under the condition of a static trunk growth rate (rather than the dynamic growth rate shown here), Fusco *et al.* (2014) concluded that the TG hypothesis had more support in explaining trunk segment growth in the Silurian trilobite *Aulacopleura koninckii*, and that segmental growth was under some form of regional rather than segment-specific control (the SG hypothesis). They noted that the TG models outperformed the SG models, as the latter were unable to account for the slight decrease in segmental growth rates observed across ontogeny. However, if the trunk growth rate in trilobites is not constant (as is clearly the case for *E. bilobata*), but instead decreases across ontogeny (as tends to be the case in other departures from Dyar's rule: Hartnoll 1982), this conclusion may not be valid. The trunk growth rate across the period analysed by Fusco *et al.* (2014) does appear to be highly consistent with a static growth rate (see their fig. S6); however, inclusion of the smaller number of trunk length observations for *A. koninckii* across the early meraspid period, as well as the lower rate of growth in the

holaspid trunk (Fusco *et al.* 2016: fig. 5), suggests the possibility of a dynamically changing (decreasing) trunk growth rate across not only the meraspid period, but potentially across the entire ontogeny of this trilobite. This is also supported by the predicted length of holaspid body parts by the generative model of Hopkins (2020) being consistently higher than observed data, suggesting that growth rates may have also decreased across the holaspid period. Thus, a changing (decreasing) trunk growth rate in *A. koninckii* might suggest support for the SG hypothesis as defined herein, with the decreasing trunk growth rate being proportional to the slight decrease in observed segmental growth rates.

In contrast to other body parts, the growth rate of the pygidium for the majority of the meraspid period in *E. bilobata* (stages D0–10) was essentially zero (non-significant OLS regression coefficient for stages D0–10, two-tailed Student's *t*-test,  $n = 81$ ,  $p > 0.92$ : Figs 6.2A, 6.5A, Supp. Table 10.3). There is a slight decrease in pygidial size in stages D11–12, possibly associated with the onset of the epimorphic phase (i.e., the termination of trunk segment generation) at stage D10, which equates to a slightly negative average growth rate across the entire meraspid period (significant OLS regression coefficient for stages D0–12, two-tailed Student's *t*-test,  $n = 104$ ,  $p < 0.001$ : Fig. 6.5B, Supp. Table 10.3). The maintenance of a pygidium with a constant absolute length across the meraspid period is also seen in *A. koninckii* (Fusco *et al.* 2016), but apparently not in *Changaspis elongata* (Du *et al.* 2019). However, pygidial morphology and the boundary between the thorax and pygidium in the latter is somewhat unclear, and this trilobite also supposedly had a very large amount of within-stage size variation, something that is not seen in either *E. bilobata* or *A. koninckii*.

In *E. bilobata*, segments decrease sequentially from anterior to posterior throughout the meraspid period. This is in contrast to *A. koninckii*, where segments increase in length from TS1 to about TS4–5, before decreasing towards the posterior. In *C. elongata*, the longest segment is often TS2; however, TS1–2 are often similar lengths. These observations may be a result of different 'initial conditions', resulting from differential development of segments within the transitory pygidia of early growth stages (most likely protaspides or M0 meraspides). Interestingly, it would appear that if the same conditions of trunk segment generation occurred in very early stages of *A. koninckii* as in later stages, it would not be possible to produce the pattern of segment lengths discussed above. Incidentally, the generative model of Hopkins (2020) was only able to produce a trunk with sequentially decreasing trunk segment lengths for *A. koninckii*. This suggests that the development of



these segments, probably within the protaspid and M0 transitory pygidia, were potentially subject to different growth controls at early stages of their development than segments that appeared later.

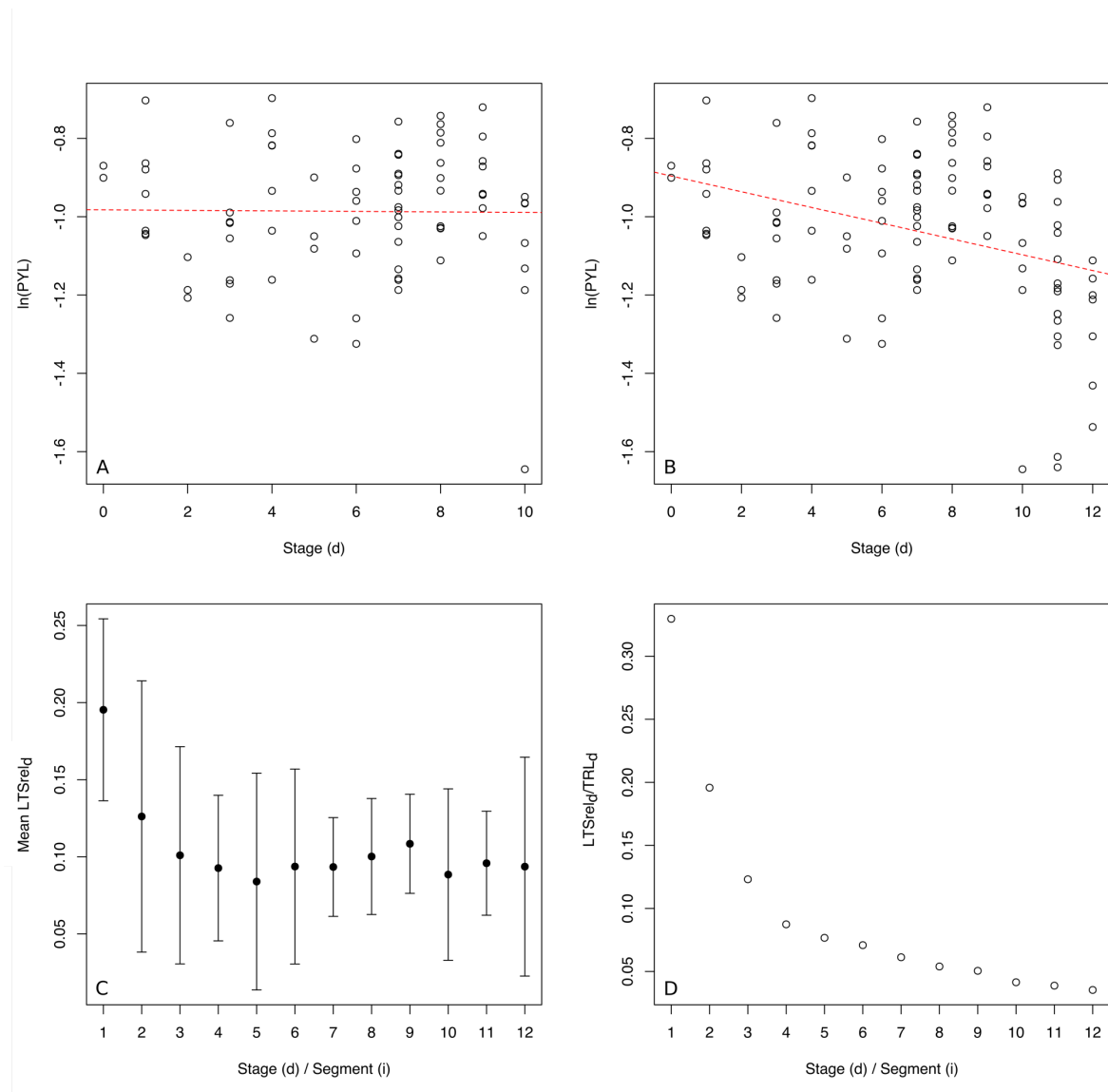


**Figure 6.5:** Growth patterns in the trunk of *Estaingia bilobata*. (A) OLS regression of log pygidial length [ $\ln(PYL)$ ] against stages D0–10; the growth rate of the pygidium is not significantly different to zero across this period (see Supp. Table 10.3). (B) OLS regression of  $\ln(PYL)$  against stages D0–D12; the growth rate is slightly negative (significantly less than zero). (C) Mean length of the released segment at each stage ( $LTS_{rel_d}$ ); there is an initial decrease in length before stabilising across the remainder of the meraspid period. Bars represent standard errors. (D) Proportion of the released segment ( $LTS_{rel_d}$ ) at each stage across the meraspid period relative to mean trunk length ( $TRL_d$ ).

In *E. bilobata*, segments TS3–12 were approximately the same length when released from the pygidium. In contrast, TS1 and TS2 (particularly the former) are much larger (Fig. 6.5C). As a result, the length of the released segment at each stage does not show an obvious proportional relationship to either the trunk or the pygidium. Rather, it shows a smooth, exponential decrease relative to trunk length (Fig. 6.5D). The length of the released segment in *A. koninckii* is also complex, with no obvious relationship to trunk or pygidial length (G. Fusco pers. comm., June 2020). It is possible that the release of segments is somehow connected to the maintenance of a constant pygidial length across the meraspid period.

### 6.5.2 Implications of model support

Based on the results presented here, it is not possible to determine with certainty whether the SG or TG hypothesis represents the true model of growth control in *Estaingia bilobata*. The SG-A model, representing a constant allometric coefficient for the segments with respect to the trunk across ontogeny, is ranked slightly higher than the RG-C1 model based on  $AIC_c$ . The alternative RG-C2 model that utilises the more appropriate *RPS* (relative position of segmental boundaries) dataset for this model has a higher level of support based on pseudo- $R^2$  values, but is not directly comparable with the models that utilise the *RLS* (relative segment length) dataset. Despite this, relative support for the various models tested here can help to constrain the possible controls on trunk segment growth for this trilobite.

Within the SG models, it is clear that the maintenance of a constant allometric coefficient for each segment with respect to the trunk is the preferred model. Within the TG models, RG-C (which uses  $TRG_d$  as an input parameter) clearly outperforms RG-B (which uses stage [ $d$ ]). This shows that variations in the overall trunk growth rate across ontogeny, that are a result of random sampling variation between stages (i.e. the deviations from a hypothetical fitted curve in Fig. 6.1C), are important in explaining the observations of relative segment length and position in *E. bilobata* meraspides. In other words, the relative segment lengths do not appear to be a function of stage, but rather of the growth rate. In reality, it is likely that the trunk growth rate would approximate a smooth curve,

corresponding to a series of steadily decreasing (relative) growth gradients (e.g. Fig. 6.6A). In essence, this is how the RG-B models fit the data; however, these models are unable to adapt to the random sampling variation mentioned above. The growth gradients predicted by the RG-C models fluctuate as a result of this same sampling variation, allowing these models to fit the observed data better (Fig. 6.6B).

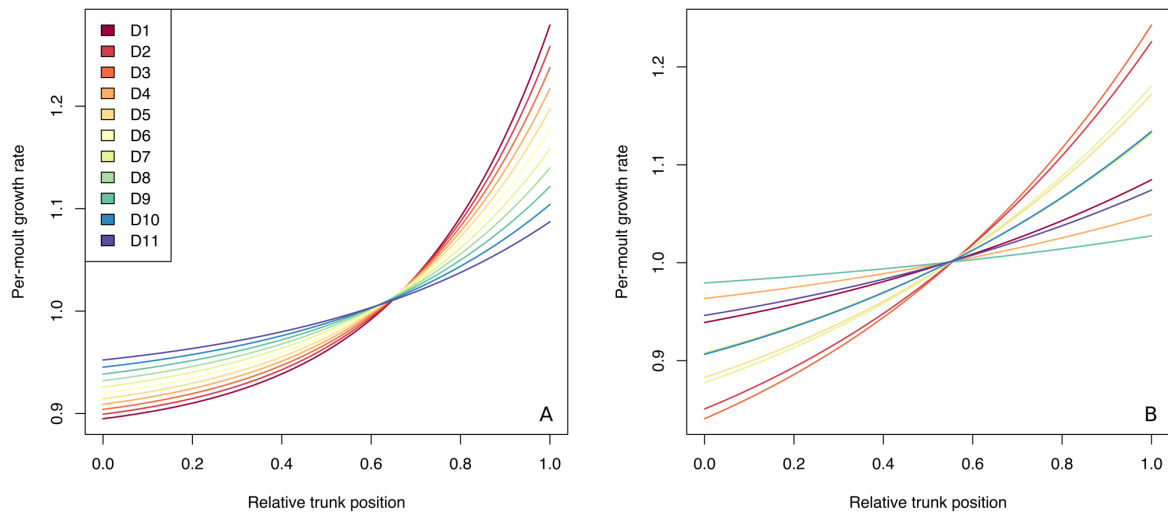


**Figure 6.6:** Predicted relative growth gradients under the Trunk Gradient (TG) hypothesis. (A) RG-B2 model. (B) RG-C2 model. The RG-C2 model allows the growth gradients to fluctuate in line with variations in the trunk growth rate ( $TRG_d$ ), which are largely a result of sampling variation in trunk length ( $TRL_d$ ) between stages. In reality, the gradients would likely form a series of decreasing gradients corresponding to a steadily decreasing growth rate, similar to those shown in A.

## 6.6 Conclusions

The general decrease in the gradient across ontogeny predicted by the TG models is similar to that seen between the differing ‘static’ gradients predicted by the TG hypothesis between the meraspid and holaspid periods of *Aulacopleura koninckii* (Fusco *et al.* 2016: fig. 7). This suggests the possibility that growth may have been controlled by a gradient that continuously changed across the entire ontogeny of these early arthropods. Future investigations into the growth of trunk segments within the holaspid period of *Estaingia bilobata* will help to determine: (a) if the TG hypothesis is the most likely explanation for

trunk segment growth in this trilobite, and (b) assuming this is the case, if there was a change in the gradient associated with the meraspid/holaspid transition, or if the gradient changed continuously across ontogeny. Results from similar studies on other trilobites, particularly those from the early Cambrian, will also help to confirm the observations made here.

## 6.7 References

- Dai, T. & Zhang, X.** 2013. Ontogeny of the redlichiid trilobite *Eoredlichia intermediata* from the Chengjiang Lagerstätte, lower Cambrian, southwest China. *Lethaia*, **46**: 262–273.
- Dai, T., Zhang, X. & Peng, S.** 2014. Morphology and ontogeny of *Hunanocephalus ovalis* (trilobite) from the Cambrian of South China. *Gondwana Research*, **25**: 991–998.
- Dai, T., Zhang, X.-L., Peng, S.-C. & Yao, X.-Y.** 2017. Intraspecific variation of trunk segmentation in the oryctocephalid trilobite *Duyunaspis duyunensis* from the Cambrian (Stage 4, Series 2) of South China. *Lethaia*, **50**: 527–539.
- Drage, H.B., Holmes, J.D., Daley, A.C. & García-Bellido, D.C.** 2018. An exceptional record of Cambrian trilobite moulting behaviour preserved in the Emu Bay Shale, South Australia. *Lethaia*, **51**: 473–492.
- Du, G.-Y., Peng, J., Wang, D.-Z., Wang, Q.-J., Wang, Y.-F. & Zhang, H.** 2019. Morphology and developmental traits of the trilobite *Changaspis elongata* from the Cambrian Series 2 of Guizhou, South China. *Acta Palaeontologica Polonica*, **64**: 797–813.
- Du, G.-Y., Peng, J., Wang, D.-Z., Wen, R.-Q. & Liu, S.** 2020. Morphology and trunk development of the trilobite *Arthricocephalus chauveaui* from the Cambrian Series 2 of Guizhou, South China. *Historical Biology*, **32**: 174–186.
- Dyar, H.G.** 1890. The number of molts of lepidopterous larvae. *Psyche*, **5**: 420–422.
- Fusco, G., Garland Jr., T., Hunt, G. & Hughes, N.C.** 2012. Developmental trait evolution in trilobites. *Evolution*, **66**: 314–329.
- Fusco, G., Hong, P.S. & Hughes, N.C.** 2014. Positional specification in the segmental growth pattern of an early arthropod. *Proceedings of the Royal Society of London B*, **281**: 20133037.

- Fusco, G., Hong, P.S. & Hughes, N.C.** 2016. Axial growth gradients across the postprotaspid ontogeny of the Silurian trilobite *Aulacopleura koninckii*. *Paleobiology*, **42**: 426-438.
- Gehling, J.G., Jago, J.B., Paterson, J.R., García-Bellido, D.C. & Edgecombe, G.D.** 2011. The geological context of the Lower Cambrian (Series 2) Emu Bay Shale Lagerstätte and adjacent stratigraphic units, Kangaroo Island, South Australia. *Australian Journal of Earth Sciences*, **58**: 243-257.
- Hartnoll, R.G.** 1982. Growth. Pp. 111–196 in E. Bliss (ed) *The biology of Crustacea. Vol. 2*. Academic Press, New York.
- Holmes, J.D., Paterson, J.R. & García-Bellido, D.C.** 2020. The post-embryonic ontogeny of the early Cambrian trilobite *Estaingia bilobata* from South Australia: trunk development and phylogenetic implications. *Papers in Palaeontology*: doi:10.1002/spp2.1323.
- Hong, P.S., Hughes, N.C. & Sheets, H.D.** 2014. Size, shape, and systematics of the Silurian trilobite *Aulacopleura koninckii*. *Journal of Paleontology*, **88**: 1120–1138.
- Hopkins, M.J.** 2020. A simple generative model of trilobite segmentation and growth. *PaleorXiv version 3, peer-reviewed by PCI Paleo*: doi.org/10.31233/osf.io/zt31642.
- Hou, J.-B., Hughes, N.C., Lan, T., Yang, J. & Zhang, X.-G.** 2015. Early postembryonic to mature ontogeny of the oryctocephalid trilobite *Duodingia duodingensis* from the lower Cambrian (Series 2) of southern China. *Papers in Palaeontology*, **1**: 497–513.
- Hou, J.-B., Hughes, N.C., Yang, J., Lan, T., Zhang, X.-G. & Dominguez, C.** 2017. Ontogeny of the articulated yiliangellinine trilobite *Zhangshania typica* from the lower Cambrian (Series 2, Stage 3) of southern China. *Journal of Paleontology*, **91**: 86–99.
- Hughes, N.C.** 2003. Trilobite body patterning and the evolution of arthropod tagmosis. *Bioessays*, **25**: 386–395.
- Hughes, N.C., Hong, P.S., Hou, J. & Fusco, G.** 2017. The development of the Silurian trilobite *Aulacopleura koninckii* reconstructed by applying inferred growth and segmentation dynamics: a case study in Paleo-Evo-Devo. *Frontiers in Ecology and Evolution*, **5**: 37.
- Huxley, J.S.** 1932. *Problems of Relative Growth*. MacVeagh, London.
- Jago, J.B., Bentley, C.J., Paterson, J.R., Holmes, J.D., Lin, T.R. & Sun, X.W.** 2020. The stratigraphic significance of early Cambrian (Series 2, Stage 4) trilobites from the Smith Bay Shale near Freestone Creek, Kangaroo Island. *Australian Journal of Earth Sciences*: doi:10.1080/08120099.2020.1749882.

- Paterson, J.R., Edgecombe, G.D. & Lee, M.S.Y.** 2019. Trilobite evolutionary rates constrain the duration of the Cambrian explosion. *Proceedings of the National Academy of Sciences of the USA*, **116**: 4394–4399.
- Paterson, J.R., Gaines, R.R., García-Bellido, D.C. & Jago, J.B.** 2018. The Emu Bay Shale fan delta complex: palaeoenvironmental conditions affecting the community structure of a unique Cambrian *Lagerstätte*. P. 59 in *International Conference on Ediacaran and Cambrian Sciences, Programme and Abstracts*, 196 pp. 12–16 August, Xi'an, China.
- Paterson, J.R., García-Bellido, D.C., Jago, J.B., Gehling, J.G., Lee, M.S.Y. & Edgecombe, G.D.** 2016. The Emu Bay Shale Konservat-Lagerstätte: a view of Cambrian life from East Gondwana. *Journal of the Geological Society, London*, **173**: 1–11.
- Schneider, C.A., Rasband, W.S. & Eliceiri, K.W.** 2012. NIH Image to ImageJ: 25 years of image analysis. *Nature methods*, **9**: 671.

## **Chapter 7**


### Ontogeny and phylogeny of Cambrian trilobites

Intended for submission to *Journal of Paleontology* (or similar)

## Statement of Authorship

|                      |  |
|----------------------|--|
| Title of paper:      | Ontogeny and phylogeny of Cambrian trilobites  |
| Publications status  | Unpublished and unsubmitted work written in manuscript style                                       |
| Publication details: | Holmes, J.D., Paterson, J.R. & García-Bellido, D.C. Ontogeny and phylogeny of Cambrian trilobites. |


### Principal author

|                                      |  |
|--------------------------------------|--|
| Name of principal author (candidate) | James D. Holmes  |
| Contribution to the paper            | Conceived the study, conducted all analyses, wrote the manuscript and drew up all figures.   |
| Overall percentage (%)               | 90   |
| Certification                        | This paper reports on original research I conducted during the period of my Higher Degree by Research candidature and is not subject to any obligations or contractual agreements with a third party that would constrain its inclusion in this thesis. I am the primary author of this paper. |
| Signature/date                       | (  07/07/2020   |

### Co-author contributions

By signing the Statement of Authorship, each author certifies that:

- i. the candidate's stated contribution to the publication is accurate (as detailed above);
- ii. permission is granted for the candidate to include the publication in the thesis; and
- iii. the sum of all co-author contributions is equal to 100% less the candidate's stated contribution.

|                           |   |
|---------------------------|---|
| Name of co-author         | John R. Paterson  |
| Contribution to the paper | Supervised development of work and helped to evaluate and edit the manuscript.                  |
| Signature/date            |  13/7/2020 |

|                           |  |
|---------------------------|--|
| Name of co-author         | Diego C. García-Bellido  |
| Contribution to the paper | Supervised development of work and helped to evaluate and edit the manuscript. |
| Signature/date            | 8/7/2020   |



## 7.1 Abstract

Ontogenetic characters have long been considered important in unravelling the phylogenetic relationships within Trilobita. In particular, the morphology of the earliest biomineralized larval stage, the protaspis, has been used to help diagnose a number of major groups within this extinct clade of marine arthropods. However, despite well over 100 years of research—including many studies devoted to ontogeny—our understanding of broad trilobite relationships remains poor. A series of recent studies have revealed a wealth of new ontogenetic data for a range of trilobites, particularly from the early Cambrian of China and South Australia, including detailed information of protaspid morphologies and developmental patterns relating to segmentation and articulation. This new information provides the opportunity to investigate ontogenetic patterns in Cambrian trilobites in a phylogenetic context not previously possible. Here we conduct a phylogenetic analysis of a series of Cambrian trilobites for which detailed ontogenetic character information is known, in order to assess their phylogenetic signal and their importance in understanding the relationships between different groups. The majority of taxa included are from the Order Redlichiida, including members of the superfamilies Olenelloidea, Redlichioidea, Paradoxidoidea and Ellipsocephaloidea, with the remainder from the Order Corynexochida. Results suggests that certain groups exhibit distinct combinations of ontogenetic character traits, and that these characters are important in contributing to the resolution of phylogenetic hypotheses. Certain characters such as the development of the glabella across ontogeny are best interpreted in light of multiple instances of paedomorphism. The suspected paraphyly of the suborder Redlichiina is reaffirmed.

## 7.2 Introduction

Despite being one of the most well-studied and diverse fossil groups, represented by over 22,000 described species, the broad relationships between major groups of trilobites remain something of a mystery (Paterson 2020). Ontogenetic characters have long been considered important in unravelling the phylogenetic relationships within this group of ancient arthropods (e.g. Raw 1927; Stubblefield 1926), and some recognised groups are partly diagnosed by ontogenetic traits, in particular, the morphology of the earliest widely-recognised larval stage, known as the protaspis: e.g. the orders Phacopida (Whittington 1957), Asaphida (Fortey & Chatterton 1988) and Proetida (Fortey & Owens 1975).

In a review of trilobite systematics Fortey (2001) noted a 'distinct shortage' (p. 1145) of ontogenies known from the Cambrian, and suggested that the discovery of new examples would likely be critical in resolving issues relating to higher level taxonomic relationships, such as the identification of Cambrian sister taxa to later (post-Cambrian) clades, and the status of certain groups suspected to be paraphyletic (e.g. Redlichiina and 'Ptychopariida'). Since this review, a number of papers describing complete Cambrian trilobite ontogenies have been published, revealing previously unknown patterns of growth and articulation (e.g. Dai & Zhang 2013; Dai *et al.* 2014; 2017; Du *et al.* 2019; 2020; Holmes *et al.* 2020; Hou *et al.* 2015; 2017). These have been accompanied by studies revealing detailed information on protaspid morphologies (e.g. Dai & Zhang 2012a; 2012b; Holmes *et al. in review*; Laibl *et al.* 2017; 2018; Zhang & Clarkson 2012). These new data provide the opportunity to examine the ontogenetic characters of Cambrian trilobites in a more detailed phylogenetic context than has previously been possible. Here we conduct a phylogenetic analysis based on the recently published Cambrian trilobite phylogeny of Paterson *et al.* (2019), focusing on taxa for which detailed ontogenetic information is known, and interpret the results in relation to ontogenetic character patterns.

### 7.3 Methodology

The Cambrian trilobite dataset used in this study is based on a modified version of that presented by Paterson *et al.* (2019). Ten species for which detailed ontogenetic data are known were retained in the dataset, and six additional species added (see Supp. Table 10.4). Preference was given to the small number of species for which complete, articulated ontogenies are known; however, instances of such preservation are rare, and these have only been reported as compressed fossils in fine-grained siliciclastics. As such, they often provide little (or no) data on protaspid morphology. Therefore, we have also included additional taxa preserved as disarticulated sclerites in limestones (including phosphatized material) for which detailed information is known of early ontogenetic stages, particularly protaspides. The majority of taxa considered here belong to the Order Redlichiida, with all the superfamilies recognised by Adrain (2011) being represented (except Fallotaspidoidea), including ellipsocephaloids, emuelloids, paradoxidoids, olenelloids and redlichoids. The remaining three taxa are from the Order Corynexochida, all from the family Oryctocephalidae.

For simplicity, we used only the discrete characters of Paterson *et al.* (2019) and excluded meristic/continuous characters. Due to the removal of the majority of species from the dataset of Paterson *et al.* (2019), many of the original characters were no longer applicable to the trilobites analysed herein, and were subsequently removed; autapomorphic characters and character states were also excluded. Several existing characters were modified, and certain codings changed to reflect new information. Five additional ontogenetic characters were introduced, for a total of 53 characters. A full list of characters and characters states, and how these compare with those of Paterson *et al.* (2019), is provided in the Supplementary Material (Section 10.4.2).

We subjected this dataset to a simple parsimony analysis using PAUP\* (Swofford 2001) with a branch-and-bound search and all characters equally weighted. Trees were rooted using two olenelloid trilobites as the outgroup (*Olenellus gilberti* and *Nephrolenellus geniculatus*). This is justified by the fact that olenelloids (and olenellines more generally) exhibit a number of traits that are often assumed to be plesiomorphic for Trilobita (such as the lack of dorsal ecdysial sutures and the absence of a calcified protaspid stage). Characters

were then mapped on the tree and interpreted, with particular emphasis placed on the phylogenetic signal of ontogenetic characters. A bootstrap 50% majority-rule consensus tree based on 1000 replicates was produced to assess clade support. The parsimony analysis was repeated with the removal of all ontogenetic characters to gauge their overall contribution to the topology of the tree(s) produced.

Terminology in general follows Whittington and Kelly (1997) and we follow the taxonomic classification of Adrain (2011).

## 7.4 Results

The parsimony analysis with all characters included produced a single most parsimonious tree of 111 steps (Fig. 7.1). The tree shows a paraphyletic Redlichiida/Redlichiina, with the emuelloids representing the most basal redlichiines, which are a sister clade to a group containing a monophyletic Oryctocephalidae (including *Duodingia duodingensis*, *Duyunaspis duyunensis* and *Oryctocarella duyunensis*), and a larger clade of redlichiine superfamilies. Within the latter, the Redlichioidea forms a distinct clade, with the gigantopygid *Zhangshania typica* representing the sister taxon to a clade of redlichiids: *Metaredlichia cylindrica*, *Eoredlichia intermediata* and *Redlichia cf. versabunda*. The redlichiods are the sister group to a clade containing representatives of the superfamilies Ellipsocephaloidea and Paradoxidoidea. The ellipsocephaloids form the most derived group within this clade, where the estaingiid *Estaingia bilobata* sits outside a grouping of the estaingiid *Ichangia ichangensis* and the ellipsocephalid *Ellipsostrenua granulosa*. The paradoxidoids form a paraphyletic group basal to this, with *Xystridura templetonensis* forming the sister taxon to the ellipsocephaloids, and *Eccaparadoxides pusillus* sitting at the base.

The bootstrap 50% majority-rule consensus tree exhibited an identical topology and thus bootstrap values were transposed onto the most parsimonious tree for ease of reference (Fig. 7.1). In general, bootstrap values of nodes defining the major groupings basal to the more derived redlichiine clade are quite high, suggesting that this section of the tree is quite robust. Generally lower values within this group suggest more uncertainty, particularly with respect to the position of the paradoxidoids.

The parsimony analysis with ontogenetic characters excluded produced two most parsimonious trees (each of 88 steps) from which a strict consensus tree was produced (Supp. Fig. 10.3). This results in the more derived redlichiine clade collapsing to form a polytomy with four branches (the redlichoids, ellipsocephaloids, *X. templetonensis* and *E. pusillus*), suggesting that ontogenetic characters are important in providing support for certain groupings.

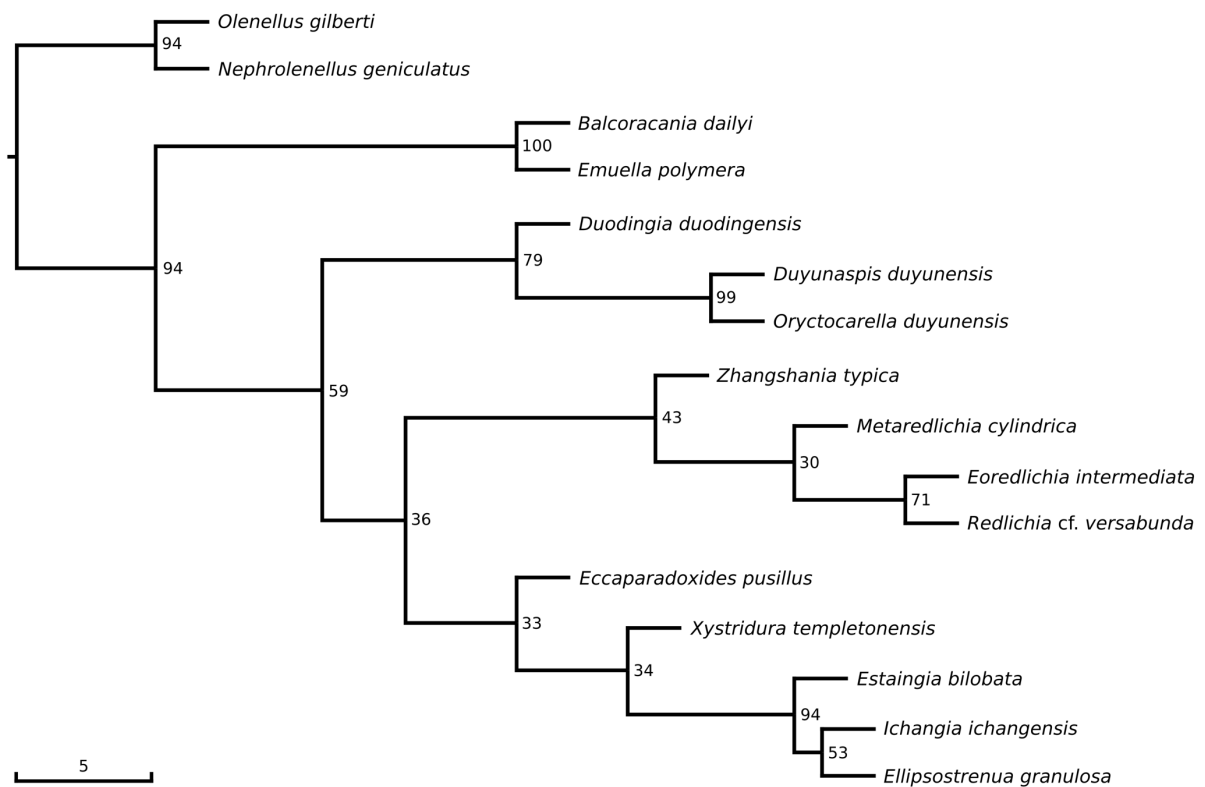


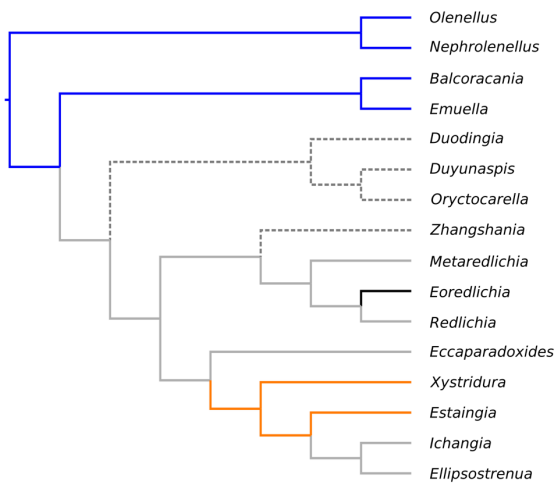
**Figure 7.1:** Single most parsimonious tree of 16 Cambrian trilobites for which detailed ontogenetic information is known. Numbers at nodes are bootstrap values transposed from a bootstrap consensus tree with identical topology. Terminal branch lengths not to scale.

## 7.5 Discussion

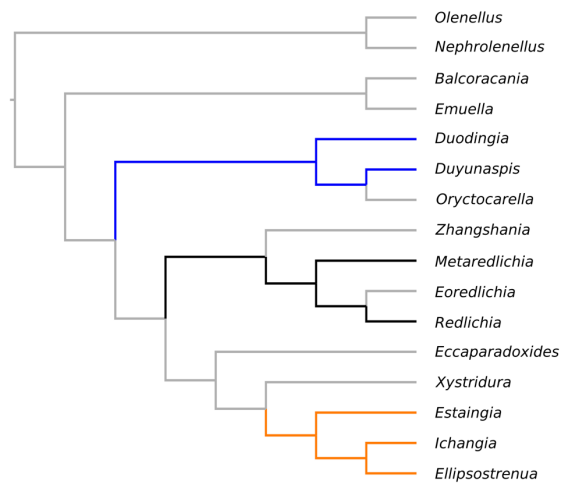
The results show that ontogenetic characters influence the broad relationships produced by a phylogenetic analysis, and provide support for certain groupings across the tree. These characters appear to show a mixed phylogenetic signal, with some showing clear patterns of

shared traits within and across certain clades, and others making more sense in light of multiple acquisitions of certain character states, particularly with regard to heterochronic processes.

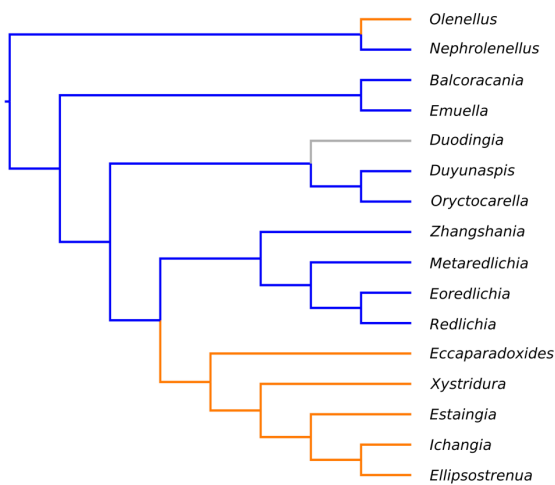
A. Development of thoracic macropleurae



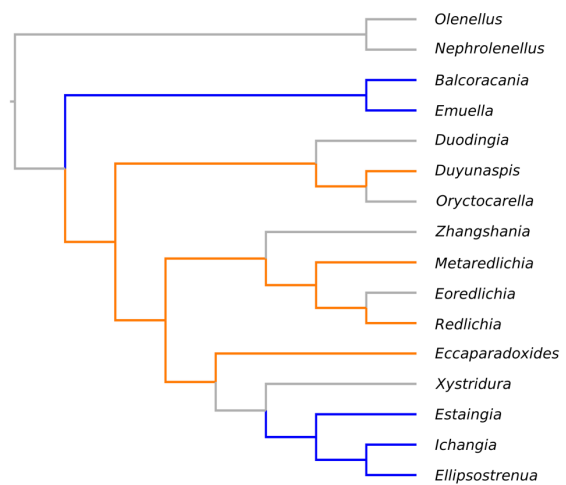
B. Number of fixigenal spine pairs



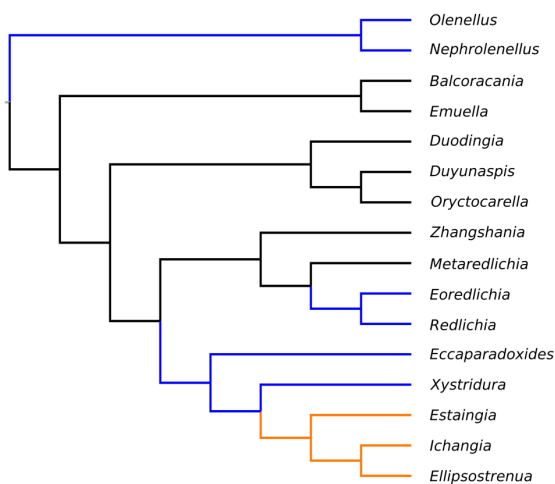
C. Transverse furrows on interocular cheeks



D. Longitudinal medial glabellar furrow



E. Glabellar development



F. Pygidial segmentation pattern

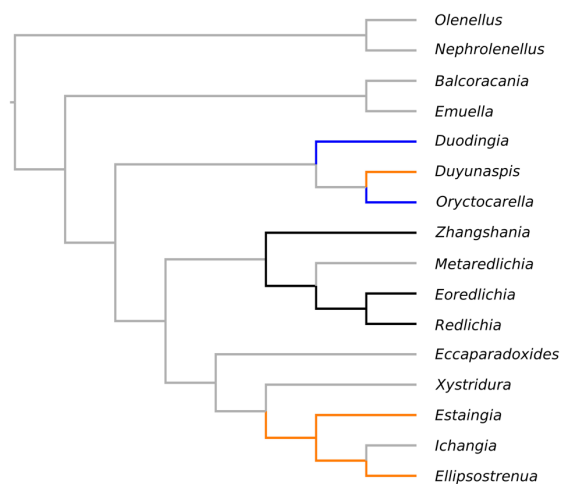


**Figure 7.2 (previous page):** Single most parsimonious tree of Cambrian trilobites with various ontogenetic characters mapped (trees are unscaled). Each tree represents a single character, with blue, black and orange representing character states, grey lines representing uncertainty, and grey dashed lines representing a non-applicable character for that taxon/grouping. Genus names listed refer only to the species above and are presented as such for easy reference. (A) Development of thoracic macropleurae across the meraspid/holaspid periods (character 48): blue = macropleurae retained in late holaspides; black = macropleurae occasionally retained in late holaspides; orange = macropleurae lost in late holaspides. (B) Number of pairs of fixigenal spines in protaspides (character 50): blue = less than two; black = more than two; orange = two. (C) Transverse furrows on interocular cheeks in protaspides and/or early meraspides (character 45): blue = present; orange = absent. (D) Longitudinal medial glabellar furrow in protaspides (character 44): blue = absent; orange = present. (E) Development of glabella across ontogeny (character 53): blue = retracts and then extends across meraspid period; black = retracts slightly in holaspides or does not retract; orange = retracts in meraspides and remains retracted. (F) Pattern of pygidial segmentation during meraspid period (character 51): blue = initial accumulation phase then similar number of segments through to holaspid period; black = micropygous pygidium retained throughout meraspid period; orange = progresses through accumulation and depletion phases.

In the context of the topology presented here (Fig. 7.1), the presence and retention of macropleurae throughout ontogeny is associated with more basal taxa, with both olenelloids and emuelloids displaying this feature (Fig 7.2A). In reality, this trait was almost certainly independently derived. In emuellids, the fifth and sixth thoracic segments are fused, with the sixth being macropleural, and the opisthothorax positioned immediately to the posterior of this. In olenelloids, the third segment is macropleural (when present) and decoupled from the prothorax/opisthothorax boundary. Although this trait may be independently derived in these two groups, the propensity to develop this feature appears to have been widespread in more basal taxa. Similar phylogenetic relationships are retrieved from the analyses of Paterson *et al.* (2019), where other macropleurae-bearing taxa such as *Bathynotus* and *Onaraspis* also group with the emuellids.

Where known, members of the paradoxidoid/ellipsocephaloid clade bear macropleurae during early ontogenetic stages that are lost in later holaspides (Fig. 7.2A); this is the case for *Eccaparadoxides pusillus*, *Estaingia bilobata* and *Xystridura templetonensis*. In *Estaingia bilobata*, the first and second thoracic segments bear

macropleural spines in the early meraspid period; these are lost from the first segment at about degree five, while those on the second segment are retained until the earliest holaspid period (Holmes *et al.* 2020). Although it is uncertain if such a pattern of spine loss occurs in the other members of the paradoxidoid/ellipsocephaloid group included in this analysis, it does occur in the paradoxidoids *Xystridura saintsmithi* and *Hydrocephalus carens*, as well as the ellipsocephaloid *Hamatolenus vincenti* and probably *Ellipsocephalus hoffi* (see Laibl *et al.* 2015). *Eccaparadoxides pradoanus* also bears macropleural spines on the first and second segments in earlier stages, but these are apparently lost simultaneously (Esteve 2014). Within the redlichiods, *Eoredlichia intermediata* displays the same pattern of macropleural spine disappearance from the first followed by the second segment during the meraspid period as *E. bilobata*, although macropleural spines in the former are occasionally retained into the holaspid period. It is uncertain if other redlichiod taxa show a similar pattern, although macropleurae are absent throughout the ontogeny of the gigantopygid *Zhangshania typica*. None of the oryctocephalids exhibit macropleurae at any stage of their development.

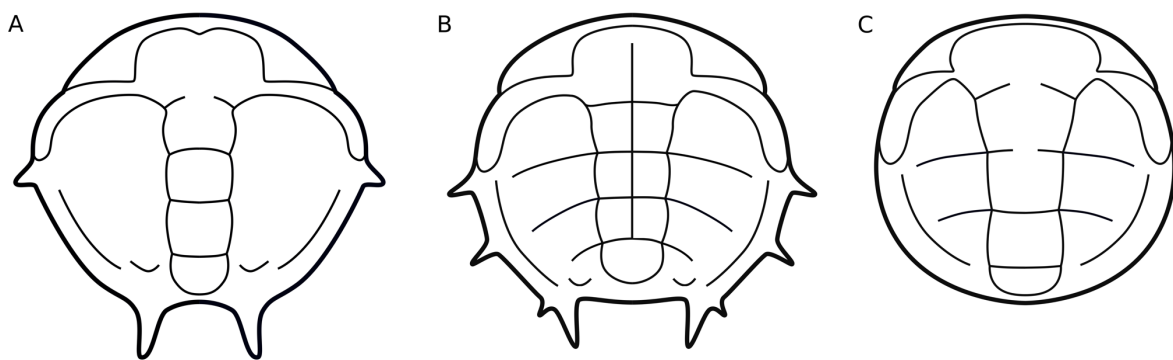


**Figure 7.3:** Protaspides exemplifying features of major early Cambrian trilobite groups. A, *Ellipsostrenua granulosa* (Ellipsocephalidae, Ellipsocephaloidea), modified from Laibl *et al.* (2018). B, genus and species indeterminate 1 of Zhang and Pratt (1999) (Redlichiida, Redlichioidea), based also on material from Zhang and Clarkson (2012). These protaspides were tentatively assigned to *Metaredlichia cylindrica* by Dai and Zhang (2012). C, *Duodingia duodingensis* (Oryctocephalidae, Corynexochida), modified from Hou *et al.* (2015).



Where morphology is well known, protaspides of ellipsocephaloids bear two pairs of fixigenal spines (Fig. 7.2B): an anterior pair located just behind the posterior branch of the facial suture, and a second, larger pair located towards the posterior of the exoskeleton (Fig. 7.3A). The redlichiids *Metaredlichia cylindrica* and *Redlichia cf. versabunda* also exhibit these two pairs, and at least one additional pair of spines positioned between these along the posterolateral margin (Dai & Zhang 2012a; Holmes *et al. in review*). Superbly preserved phosphatized specimens figured by Zhang and Pratt (1999) and tentatively assigned to *M. cylindrica* by Dai and Zhang (2012a) show these clearly, and several specimens figured by Zhang and Clarkson (2012: pl. 19, figs 4–7) also exhibit a fourth pair (Fig. 7.3B). Paradoxidids show a mixed signal in relation to this trait. *Eccaparadoxides pusillus* appears to show two pairs, as in ellipsocephaloids (as has been interpreted for *Paradoxides rugulosus*; Whittington 1957). However, *Hydrocephalus carens* appears to show these, plus an additional pair (Laibl *et al.* 2017). This is consistent with the somewhat uncertain position of this group between the redlichioids and the ellipsocephaloids based on bootstrap support values (Fig. 7.1), and suggests that paradoxidids may reflect transitional forms that potentially gave rise to the *Xystridura*/ellipsocephaloid clade. The number of fixigenal spine pairs in xystridurid protaspides is not known, and is also unclear in emuellids. Information on protaspid stages in the three oryctocephalids considered here is less detailed, though they appear to lack fixigenal spines (Fig. 7.3C). In summary, this trait appears to show clear phylogenetic signal, with ellipsocephaloids showing two pairs of fixigenal spines, redlichioids showing three or four pairs, and oryctocephalids potentially having no spines.

The emuelloids, oryctocephalids and redlichioids all display transverse furrows on the interocular cheeks in protaspides or early meraspides (Fig. 7.2C). This trait is also present in *Nephrolenellus geniculatus* (but not *Olenellus gilberti*) (Webster 2007; Webster 2015). This is likely a plesiomorphic trait, being lost in the paradoxidoid/ellipsocephaloid clade. The presence of a longitudinal medial glabellar furrow in protaspides shows a more mixed signal (Fig. 7.2D). It is present in the oryctocephalids and redlichioids, as well as in *Eccaparadoxides pusillus*, but is absent in the ellipsocephaloids and emuelloids. This may also be a plesiomorphic trait that has been lost multiple times; however, the polarity of this character is uncertain given the lack of calcified protaspides in olenellines.

In many Cambrian trilobites, the anterior of the frontal glabellar lobe reaches the anterior border in protaspides. During the early meraspid period, the frontal lobe retracts

(resulting in the appearance of a distinct preglabellar field), before extending again later in the meraspid period. Variations of this pattern occur in olenellids (e.g. *Olenellus*, *Nephrolenellus*), redlichiids (e.g. *Redlichia*), paradoxidids (e.g. *Paradoxides*, *Eccaparadoxides*) and xystridurids (e.g. *Xystridura*). This pattern was discussed in detail by McNamara (1986) in the context of discussing the role of heterochrony in Cambrian trilobites. He identified five stages of glabellar development: stasis, retraction, protraction, expansion and development. Stasis, retraction and protraction refer (respectively) to the initial state (where the frontal lobe reaches the anterior border), the retraction during the early meraspid period, and the subsequent protraction (or extension) during the later meraspid period. These three stages occur in some of the earliest trilobites such as *Fallotaspis*, as well as the younger *Redlichia* (Holmes *et al. in review*; McNamara 1986). It is possible, therefore, that this represents a plesiomorphic state. The subsequent expansion stage involves a distinct inflation of the frontal lobe (as seen in *Xystridura*, for example; Öpik 1975), with the development stage resulting in a greatly enlarged frontal lobe (such as in the Phacopida).

In the taxa considered here, the initial retraction and subsequent extension of the frontal glabellar lobe occurs in the olenellids, as well as in the redlichiids *R. cf. versabunda* and *E. intermediata*, and the paradoxidoids *E. pusillus* and *X. templetonensis* (Fig. 7.2E). In the emuellids, the oryctocephalids, and the redlichoids *Z. typica* and *M. cylindrica*, the glabella remained in the stasis stage throughout ontogeny, and did not retract. These likely represent multiple instances of paedomorphosis, with glabella development not progressing beyond the stasis stage in any of these taxa (though there is a very slight retraction in *M. cylindrica* and *B. dailyi*). This has been suggested previously for Corynexochida, such as the oryctocephalids considered here (Hupé 1953). The presence of bilobed frontal lobes in emuellid holaspides—a feature seen in many redlichiine protaspides—supports this as being the retention of a juvenile trait in the adult. These taxa also show more transversally-orientated glabellar furrows resulting from not progressing through the retraction and protraction stages of glabellar development. In the ellipsocephaloids considered here, the development of the glabella reached the retraction stage and did not re-extend; this pattern has also been attributed to paedomorphosis and occurs in a wide range of taxa (McNamara 1986).

The pattern of pygidial segmentation across the meraspid period (where known) appears to show a strong signal (Fig. 7.2F). The ellipsocephaloid *Estaingia bilobata* underwent a clear accumulation and depletion phase with respect to the meraspid pygidium, as also appears to have been the case for *Ellipsostrenua granulosa* (Holmes *et al.* 2020; Laibl *et al.* 2018). In contrast, the redlichiods *Z. typica*, *E. intermediata* and *R. cf. versabunda* had micropygous pygidia with a small number of segments throughout the meraspid period. The pygidia of the oryctocephalids *Duodingia duodingensis* and *Oryctocarella duyunensis* had an initial accumulation phase, followed by a long equilibrium phase with a similar number of segments through to the holaspid period. In contrast, *Duyunaspis duyunensis* appears to have gone through an accumulation and depletion phase similar to the ellipsocephaloids.

## 7.6 Conclusions

- Ellipsocephaloid ontogeny (where known) is characterised by: protaspides with two pairs of fixigenal spines, but without a longitudinal medial glabellar furrow or transverse furrows on the interocular cheeks; distinct accumulation and depletion phases in the meraspid pygidium; and glabellar development that reached the retraction stage.
- Redlichiod ontogeny is characterised by: protaspides with three or four pairs of fixigenal spines, a longitudinal medial glabellar furrow, and transverse furrows on the interocular cheeks; and a micropygous pygidium throughout the meraspid period.
- Paradoxidoid ontogeny shows a mixture of traits, reflecting their transitional position between the redlichiods and ellipsocephaloids.
- Redlichiine taxa in general (excluding emuellids) tend to exhibit macropleural spines on the first and second thoracic segments early in ontogeny that are usually lost during the meraspid period; initially on the first segment, then on the second. Some taxa (e.g. *Zhangshania*) do not exhibit macropleurae. More basal taxa (e.g. olenelloids and emuellids) exhibit macropleural spines throughout their ontogeny.

- Oryctocephalid ontogeny is characterised by: protaspides with no obvious fixigenal spines; an accumulation phase of the meraspid pygidium with or without a depletion phase; and a lack of macropleurae throughout all stages. As with redlichoids, a longitudinal medial glabellar furrow and transverse furrows on the interocular cheeks are present.
- Glabellar development is variable across the taxa considered here. Olenelloids, paradoxidoids and some redlichids (e.g. *Redlichia*) exhibit glabellar development reaching at least the protraction stage. Emuellids, oryctocephalids and some other redlichids (*Metaredlichia cylindrica* and *Zhangshania typica*) remain in the stasis stage (or retract very slightly), likely reflecting multiple instances of paedomorphic development.
- Including many of the ontogenetic characters discussed here in broad scale phylogenetic analyses may be of limited use given the lack of detailed ontogenetic data for many taxa. Nevertheless, these characters remain important sources of taxonomic information, and we should question if our phylogenetic hypotheses make sense in light of what we know of ontogenetic patterns within the groups under discussion.

## 7.7 References

- Adrain, J.M.** 2011. Class Trilobita Walch, 1771. *Zootaxa*, **3148**: 104–109.
- Dai, T. & Zhang, X.** 2012a. Ontogeny of the redlichid trilobite *Metaredlichia cylindrica* from the lower Cambrian (Stage 3) of South China. *Journal of Paleontology*, **86**: 646–651.
- Dai, T. & Zhang, X.** 2012b. Ontogeny of the trilobite *Estaingia sinensis* (Chang) from the Lower Cambrian of South China. *Bulletin of Geosciences*, **87**: 151-158.
- Dai, T. & Zhang, X.** 2013. Ontogeny of the redlichid trilobite *Eoredlichia intermediata* from the Chengjiang Lagerstätte, lower Cambrian, southwest China. *Lethaia*, **46**: 262–273.
- Dai, T., Zhang, X. & Peng, S.** 2014. Morphology and ontogeny of *Hunanocephalus ovalis* (trilobite) from the Cambrian of South China. *Gondwana Research*, **25**: 991–998.

- Dai, T., Zhang, X.-L., Peng, S.-C. & Yao, X.-Y.** 2017. Intraspecific variation of trunk segmentation in the oryctocephalid trilobite *Duyunaspis duyunensis* from the Cambrian (Stage 4, Series 2) of South China. *Lethaia*, **50**: 527–539.
- Du, G.-Y., Peng, J., Wang, D.-Z., Wang, Q.-J., Wang, Y.-F. & Zhang, H.** 2019. Morphology and developmental traits of the trilobite *Changaspis elongata* from the Cambrian Series 2 of Guizhou, South China. *Acta Palaeontologica Polonica*, **64**: 797–813.
- Du, G.-Y., Peng, J., Wang, D.-Z., Wen, R.-Q. & Liu, S.** 2020. Morphology and trunk development of the trilobite *Arthricocephalus chauveau* from the Cambrian Series 2 of Guizhou, South China. *Historical Biology*, **32**: 174–186.
- Esteve, J.** 2014. Intraspecific variability in paradoxid trilobites from the Purujosa trilobite assemblage (middle Cambrian, northeast Spain). *Acta Palaeontologica Polonica*, **59**: 215–240.
- Fortey, R.A.** 2001. Trilobite systematics: the last 75 years. *Journal of Paleontology*, **75**: 1141–1151.
- Fortey, R.A. & Chatterton, B.D.E.** 1988. Classification of the trilobite suborder Asaphina. *Palaeontology*, **31**: 165–222.
- Fortey, R.A. & Owens, R.M.** 1975. Proetida – a new order of trilobites. *Fossils and Strata*, **4**: 227–239.
- Holmes, J.D., Paterson, J.R. & García-Bellido, D.C.** 2020. The post-embryonic ontogeny of the early Cambrian trilobite *Estaingia bilobata* from South Australia: trunk development and phylogenetic implications. *Papers in Palaeontology*: doi.org/10.1002/spp2.1323.
- Holmes, J.D., Paterson, J.R., Jago, J.B. & García-Bellido, D.** *in review*. Ontogeny of the trilobite *Redlichia* from the lower Cambrian (Series 2, Stage 4) Ramsay Limestone of South Australia. *Geological Magazine*.
- Hou, J.-B., Hughes, N.C., Lan, T., Yang, J. & Zhang, X.-G.** 2015. Early postembryonic to mature ontogeny of the oryctocephalid trilobite *Duodingia duodingensis* from the lower Cambrian (Series 2) of southern China. *Papers in Palaeontology*, **1**: 497–513.
- Hou, J.-B., Hughes, N.C., Yang, J., Lan, T., Zhang, X.-G. & Dominguez, C.** 2017. Ontogeny of the articulated yiliangellinine trilobite *Zhangshania typica* from the lower Cambrian (Series 2, Stage 3) of southern China. *Journal of Paleontology*, **91**: 86–99.
- Hupé, P.** 1953. Classification des trilobites. *Annales de Paléontologie*, **39**: 1–110.

- Laibl, L., Cederström, P. & Ahlberg, P.** 2018. Early post-embryonic development in *Ellipsostrenua* (Trilobita, Cambrian, Sweden) and the developmental patterns in Ellipsocephaloidea. *Journal of Paleontology*, **92**: 1018–1027.
- Laibl, L., Esteve, J. & Fatka, O.** 2017. Giant postembryonic stages of *Hydrocephalus* and *Eccaparadoxides* and the origin of lecithotrophy in Cambrian trilobites. *Palaeogeography, Palaeoclimatology, Palaeoecology*, **470**: 109–115.
- Laibl, L., Fatka, O., Budil, P., Ahlberg, P., Szabad, M., Vokáč, V. & Kozák, V.** 2015. The ontogeny of *Ellipsocephalus* (Trilobita) and systematic position of Ellipsocephalidae. *Alcheringa*, **39**: 477–487.
- McNamara, K.J.** 1986. The role of heterochrony in the evolution of Cambrian trilobites. *Biological Reviews*, **61**: 121–156.
- Öpik, A.A.** 1975. Templetonian and Ordian Xystridurid Trilobites of Australia. *Commonwealth of Australia, Bureau of Mineral Resources, Geology and Geophysics, Bulletin*, **121**: 1–84.
- Paterson, J.R.** 2020. The trouble with trilobites: classification, phylogeny and the cryptogenesis problem. *Geological Magazine*, **157**: 35–46.
- Paterson, J.R., Edgecombe, G.D. & Lee, M.S.Y.** 2019. Trilobite evolutionary rates constrain the duration of the Cambrian explosion. *Proceedings of the National Academy of Sciences of the USA*, **116**: 4394–4399.
- Raw, F.** 1927. The ontogenies of trilobites and their significance. *American Journal of Science*, **14**: 7–35.
- Stubblefield, C.J.** 1926. Notes on the development of a trilobite, *Shumardia pusilla* (Sars). *Linnean Society of London, Zoological Journal*, **36**: 345–372.
- Swofford, D.L.** 2001. PAUP\*: Phylogenetic Analysis Using Parsimony (\*and Other Methods), Version 4. Sinauer Associates, Sunderland, Massachusetts.
- Webster, M.** 2007. Ontogeny and evolution of the early Cambrian trilobite genus *Nephrolenellus* (Olenelloidea). *Journal of Paleontology*, **81**: 1168–1193.
- Webster, M.** 2015. Ontogeny and intraspecific variation of the early Cambrian trilobite *Olenellus gilberti*, with implications for olenelline phylogeny and macroevolutionary trends in phenotypic canalization. *Journal of Systematic Palaeontology*, **13**: 1–74.
- Whittington, H.B.** 1957. The ontogeny of trilobites. *Biological Reviews*, **32**: 421–467.

- Whittington, H.B. & Kelly, S.R.A.** 1997. Morphological terms applied to Trilobita. Pp. 313–329 in R.L. Kaesler (ed) *Treatise on Invertebrate Paleontology, Part O, Revised. Arthropoda 1, Trilobita 1, (Introduction, Order Agnostida, Order Redlichiida)*. Geological Society of America and University of Kansas Paleontological Institute, Boulder, Colorado and Lawrence, Kansas.
- Zhang, X.-G. & Clarkson, E.N.K.** 2012. Phosphatized eodiscoid trilobites from the Cambrian of China. *Palaeontographia Abteilung A*, **297**: 1–121.
- Zhang, X.-G. & Pratt, B.R.** 1999. Early Cambrian trilobite larvae and ontogeny of *Ichangia ichangensis* Chang, 1957 (Protolenidae) from Henan, China. *Journal of Paleontology*, **73**: 117–128.





## **Chapter 8**

### Conclusions

## 8.1 Summary and future directions

This thesis highlights the exceptionally detailed preservation of early Cambrian trilobites from South Australia. The complete growth series of *Estaingia bilobata* from the Emu Bay Shale *Lagerstätte* described in Chapter 3 is one of the most complete ontogenies known for any trilobite, and provides a basis for the more detailed morphometric analyses of Chapter 6 (Holmes *et al.* 2020a). Likewise, specimens of *Redlichia cf. versabunda* described from the Ramsay Limestone in Chapter 4 include some of the best-preserved protaspides known (Holmes *et al. in review*). Together, these provide a significant amount of new information that adds to a growing list of Cambrian trilobite ontogenies published in recent years (e.g. Dai & Zhang 2013; Dai *et al.* 2014; 2017; Du *et al.* 2018; 2020; Hou *et al.* 2015; 2017), the data from which are used in Chapter 7 to explore patterns of Cambrian trilobite ontogenetic development in a phylogenetic context. This last paper reaffirms the importance of ontogenetic characters in furthering our understanding of trilobite evolutionary relationships.

The comprehensive study of the trilobite *Redlichia* from the Emu Bay Shale *Lagerstätte* presented in Chapter 5 again highlights the exceptional preservation of this deposit (Holmes *et al.* 2020b), as well as the importance of comprehensive descriptive works in providing raw data for larger analyses, including recognising and quantifying variation seen within individual trilobite species (Paterson 2020). This chapter extends the work of Chapter 4 by examining ontogenetic development in later holaspid forms of *Redlichia*, and shows that considerable allometric change occurred even in the adult phase of this trilobite. The description and reconstruction of the biramous appendages of the giant species *Redlichia rex* is of particular importance, and includes the identification of an exopodite with a tripartite structure that has implications for the broader relationships between trilobites and related arthropodan groups. The disarticulated nature and very large size of these appendages has allowed highly accurate 3D reconstruction, including the dorsoproximal portion of the protopodite where the appendage would have attached to the body—morphology that is otherwise poorly known in trilobites (e.g. Hou *et al.* 2009; Whittington 1975; 1980; Whittington & Almond 1987; but see Zeng *et al.* 2017). This is extremely important in terms of functionality and will allow the appendages to be modelled in future using methods such as Finite Element Analysis (FEA) to understand their

capabilities. The irregular saw-tooth gnathobasic spines of *R. rex* are similar to the suspected durophages *Sidneyia inexpectans* and *Wisangocaris barbarahardyae* and future work will test whether this trilobite was also capable of shell-crushing (Bicknell *et al.* 2018a; 2018b; Jago *et al.* 2016). The presence of injured trilobites (Bicknell & Paterson 2018) and of coprolites containing trilobite fragments in the Emu Bay Shale (previously attributed to *Anomalocaris*) may represent indirect evidence of this (Daley *et al.* 2013).

The results of the morphometric analyses conducted on *Estaingia bilobata*, firstly in Chapter 3 and followed by the more quantitative work of Chapter 6, clearly shows that our understanding of trilobite growth is incomplete. These results suggest that when data are known from across the entirety of post-embryonic ontogeny, Dyar's rule of a constant growth rate may not necessarily be an appropriate model for trilobite growth, especially in very early growth phases (Chatterton & Speyer 1997; Fusco *et al.* 2004; 2012). Furthermore, despite the inconclusive results of Chapter 6 in relation to the different hypotheses of trunk growth control in *E. bilobata*, the identification of decreasing trunk and cephalic growth rates across ontogeny suggests that previous conclusions of trunk growth control in *Aulacopleura koninckii* may need to be revisited (Fusco *et al.* 2014; 2016). Incorporation of data from the holaspid period of *E. bilobata* in future studies will refine the results presented herein, and will help to determine if the pattern of gradual change identified across the meraspid period continued in holaspides, or whether there was a more abrupt change at the meraspid/holaspid transition (Fusco *et al.* 2016). The extension of these methods to other trilobites, particularly those from the early Cambrian, will help to determine the variation and evolution of development within this important early animal group. Results of such studies may also be important in confirming patterns identified in *E. bilobata*.

Finally, the comparison of *Redlichia cf. versabunda* from the Ramsay Limestone in South Australia with material from the Cambrian succession in northern Australian has potentially important biostratigraphic implications (Chapter 6), being only the second (tentative) trilobite species level correlation between the two successions (the other being *Pagetia cf. edura* from the Coobowie Limestone, also from Yorke Peninsula: Jago & Kruse 2019). Focused studies on the uppermost part of the southern succession, and lowermost part of the northern succession (close to the Cambrian Series 2/Miaolingian boundary), and reviews of the work of Öpik (1958; 1970; 1975), will help to resolve the disjunct between

these successions, and assist in the development of a complete, integrated model of Cambrian sedimentation and palaeontology in Australia.

No significant problems were encountered during the course of this project.

## 8.2 References

- Bicknell, R.D.C., Ledogar, J.A., Wroe, S., Gutzler, B.C., Watson III, W.H. & Paterson, J.R.** 2018a. Computational biomechanical analyses demonstrate similar shell-crushing abilities in modern and ancient arthropods. *Proceedings of the Royal Society B*, **285**: 20181935.
- Bicknell, R.D.C. & Paterson, J.R.** 2018. Reappraising the early evidence of durophagy and drilling predation in the fossil record: implications for escalation and the Cambrian Explosion. *Biological Reviews*, **93**: 754–784.
- Bicknell, R.D.C., Paterson, J.R., Caron, J.-B. & Skovsted, C.B.** 2018b. The gnathobasic spine microstructure of recent and Silurian chelicerates and the Cambrian arthropodan *Sidneyia*: Functional and evolutionary implications. *Arthropod Structure & Development*, **47**: 12–24.
- Chatterton, B.D.E. & Speyer, S.E.** 1997. Ontogeny. Pp. 173–247 in R.L. Kaesler (ed) *Treatise on Invertebrate Paleontology, Part O, Revised. Arthropoda 1, Trilobita 1, (Introduction, Order Agnostida, Order Redlichiida)*. Geological Society of America and University of Kansas Paleontological Institute, Boulder, Colorado and Lawrence, Kansas.
- Dai, T. & Zhang, X.** 2013. Ontogeny of the redlichiid trilobite *Eoredlichia intermediata* from the Chengjiang Lagerstätte, lower Cambrian, southwest China. *Lethaia*, **46**: 262–273.
- Dai, T., Zhang, X. & Peng, S.** 2014. Morphology and ontogeny of *Hunanocephalus ovalis* (trilobite) from the Cambrian of South China. *Gondwana Research*, **25**: 991–998.
- Dai, T., Zhang, X.-L., Peng, S.-C. & Yao, X.-Y.** 2017. Intraspecific variation of trunk segmentation in the oryctocephalid trilobite *Duyunaspis duyunensis* from the Cambrian (Stage 4, Series 2) of South China. *Lethaia*, **50**: 527–539.

- Daley, A.C., Paterson, J.R., Edgecombe, G.D., García-Bellido, D.C., Jago, J.B.** 2013. New anatomical information on *Anomalocaris* from the Cambrian Emu Bay Shale of South Australia and a reassessment of its inferred predatory habits. *Palaeontology*, **56**: 971–990.
- Du, G.-Y., Peng, J., Wang, D.-Z., Wang, Q.-J., Wang, Y.-F. & Zhang, H.** 2019. Morphology and developmental traits of the trilobite *Changaspis elongata* from the Cambrian Series 2 of Guizhou, South China. *Acta Palaeontologica Polonica*, **64**: 797–813.
- Du, G.-Y., Peng, J., Wang, D.-Z., Wen, R.-Q. & Liu, S.** 2020. Morphology and trunk development of the trilobite *Arthrocephalus chauveaui* from the Cambrian Series 2 of Guizhou, South China. *Historical Biology*, **32**: 174–186.
- Fusco, G., Garland Jr., T., Hunt, G. & Hughes, N.C.** 2012. Developmental trait evolution in trilobites. *Evolution*, **66**: 314–329.
- Fusco, G., Hong, P.S. & Hughes, N.C.** 2014. Positional specification in the segmental growth pattern of an early arthropod. *Proceedings of the Royal Society of London B*, **281**: 20133037.
- Fusco, G., Hong, P.S. & Hughes, N.C.** 2016. Axial growth gradients across the postprotaspid ontogeny of the Silurian trilobite *Aulacopleura koninckii*. *Paleobiology*, **42**: 426–438.
- Fusco, G., Hughes, N.C., Webster, M. & Minelli, A.** 2004. Exploring developmental modes in a fossil arthropod: growth and trunk segmentation of the trilobite *Aulacopleura koninckii*. *The American Naturalist*, **163**: 167–183.
- Holmes, J.D., Paterson, J.R. & García-Bellido, D.C.** 2020a. The post-embryonic ontogeny of the early Cambrian trilobite *Estaingia bilobata* from South Australia: trunk development and phylogenetic implications. *Papers in Palaeontology*: doi:10.1002/spp2.1323.
- Holmes, J.D., Paterson, J.R. & García-Bellido, D.C.** 2020b. The trilobite *Redlichia* from the lower Cambrian Emu Bay Shale *Konservat-Lagerstätte* of South Australia: systematics, ontogeny and soft-part anatomy. *Journal of Systematic Palaeontology*, **18**: 295–334.
- Holmes, J.D., Paterson, J.R., Jago, J.B. & García-Bellido, D.** *in review*. Ontogeny of the trilobite *Redlichia* from the lower Cambrian (Series 2, Stage 4) Ramsay Limestone of South Australia. *Geological Magazine*.
- Hou, J.-B., Hughes, N.C., Lan, T., Yang, J. & Zhang, X.-G.** 2015. Early postembryonic to mature ontogeny of the oryctocephalid trilobite *Duodingia duodingensis* from the lower Cambrian (Series 2) of southern China. *Papers in Palaeontology*, **1**: 497–513.

- Hou, J.-B., Hughes, N.C., Yang, J., Lan, T., Zhang, X.-G. & Dominguez, C.** 2017. Ontogeny of the articulated yiliangellinine trilobite *Zhangshania typica* from the lower Cambrian (Series 2, Stage 3) of southern China. *Journal of Paleontology*, **91**: 86–99.
- Hou, X., Clarkson, E.N.K., Yang, J., Zhang, X., Wu, G. & Yuan, Z.** 2009. Appendages of early Cambrian *Eoredlichia* (Trilobita) from the Chengjiang biota, Yunnan, China. *Earth and Environmental Science Transactions of the Royal Society of Edinburgh*, **99**: 213–223.
- Jago, J.B., García-Bellido, D.C. & Gehling, J.G.** 2016. An early Cambrian chelicerate from the Emu Bay Shale, South Australia. *Palaeontology*, **59**: 549–562.
- Jago, J.B. & Kruse, P.D.** 2019. Significance of the middle Cambrian (Wuliuan) trilobite *Pagetia* from Yorke Peninsula, South Australia. *Australian Journal of Earth Sciences*: doi:10.1080/08120099.2019.1643405.
- Öpik, A.A.** 1958. The Cambrian trilobite *Redlichia*: organization and generic concept. *Commonwealth of Australia, Bureau of Mineral Resources, Geology and Geophysics, Bulletin*, **42**: 1–51.
- Öpik, A.A.** 1970. *Redlichia* of the Ordian (Cambrian) of Northern Australia and New South Wales. *Commonwealth of Australia, Bureau of Mineral Resources, Geology and Geophysics, Bulletin*, **114**: 1–67.
- Öpik, A.A.** 1975. Templetonian and Ordian Xystridurid Trilobites of Australia. *Commonwealth of Australia, Bureau of Mineral Resources, Geology and Geophysics, Bulletin*, **121**: 1–84.
- Paterson, J.R.** 2020. The trouble with trilobites: classification, phylogeny and the cryptogenesis problem. *Geological Magazine*, **157**: 35–46.
- Whittington, H.B.** 1975. Trilobites with appendages from the Middle Cambrian, Burgess Shale, British Columbia. *Fossils and Strata*, **4**: 97–136.
- Whittington, H.B.** 1980. Exoskeleton, moult stage, appendage morphology, and habits of the Middle Cambrian trilobite *Olenoides serratus*. *Palaeontology*, **23**: 171–204.
- Whittington, H.B. & Almond, J.E.** 1987. Appendages and habits of the upper Ordovician trilobite *Triarthrus eatoni*. *Philosophical Transactions of the Royal Society B: Biological Sciences*, **317**: 1–46.
- Zeng, H., Zhao, F., Yin, Z. & Zhu, M.** 2017. Appendages of an early Cambrian metadoxidid trilobite from Yunnan, SW China support mandibulate affinities of trilobites and artiopods. *Geological Magazine*, **154**: 1306–1328.

## **Chapter 9**

### **Appendix 1: Supplementary Papers**

The following papers represent contributions published during the candidature that are not included in the thesis for examination purposes. For brevity, only first pages are included.

**9.1 Comparisons between Cambrian Lagerstätten assemblages  
using multivariate, parsimony and Bayesian methods**

James D. Holmes, Diego C. García-Bellido and Michael S. Y. Lee





## Comparisons between Cambrian Lagerstätten assemblages using multivariate, parsimony and Bayesian methods

James D. Holmes<sup>a,\*</sup>, Diego C. García-Bellido<sup>a,b</sup>, Michael S.Y. Lee<sup>b,c</sup>

<sup>a</sup> School of Biological Sciences, University of Adelaide, Adelaide, SA 5005, Australia

<sup>b</sup> South Australian Museum, North Terrace, Adelaide, SA 5000, Australia

<sup>c</sup> School of Biological Sciences, Flinders University, Adelaide, SA 5001, Australia

### ARTICLE INFO

#### Article history:

Received 21 April 2017

Received in revised form 28 August 2017

Accepted 24 October 2017

Available online 01 December 2017

Handling Editor: J.G. Meert

#### Keywords:

Chengjiang

Burgess Shale

Emu Bay Shale

BST

Palaeobiogeography

### ABSTRACT

Exceptional fossil deposits exhibiting soft-part preservation, or *Konservat-Lagerstätten*, are prevalent in Cambrian rocks and provide detailed information on fossil assemblages not available from conventional deposits. It has long been recognised that many of these assemblages exhibit certain taxonomic similarities, with many elements seemingly having cosmopolitan distributions. These types of assemblages, particularly those of Cambrian age, have become known as Burgess Shale-type (BST) biotas, named for the famous deposit in the Canadian Rocky Mountains where fossils preserved in this way were first discovered. This study provides the first broad-scale analysis of the assemblage relationships between all major BST biotas. We compiled a database of the presences and absences of over 600 genera within 12 Lagerstätten from Laurentia, Siberia, South China and East Gondwana, ranging in age from Cambrian Series 2 through Series 3 (late-early to middle Cambrian; c. 518–502 Ma), and analysed this using a variety of quantitative methods in order to investigate the relationships between these sites. Non-metric multidimensional scaling (NMDS) ordination, cluster analysis and Parsimony Analysis of Endemism (PAE) were used to group localities and examine relationships. We also used Bayesian inference and illustrate the benefits of this approach to biogeographic studies. Results suggest that both space and time have important effects on the taxonomic constitution of BST biotas, and that the similarity of these assemblages appears to increase from Series 2 through Series 3, largely driven by increases in cosmopolitanism of biomineralised taxa such as trilobites and brachiopods. There is also evidence of higher-level taxonomic turnover across this period. Endemic taxa help amplify these patterns, despite their frequent exclusion from biogeographic analyses.

© 2017 International Association for Gondwana Research. Published by Elsevier B.V. All rights reserved.

## 1. Introduction

### 1.1. Background

Cambrian *Konservat-Lagerstätten* – fossil deposits exhibiting exceptional preservation of soft parts – offer great insight into the diversity and ecology of early communities following the ‘Cambrian explosion’ (Conway Morris, 1985). As well as providing enhanced biological information about individual organisms, they also provide a more faithful representation of the full diversity and relative abundances of taxa present within these communities. This information should allow us to undertake not only more informative and unbiased ecological analysis of these early communities, but also to examine their biogeographic relationships based on shared taxa. The former has been undertaken for

several Cambrian Lagerstätten (e.g. Conway Morris, 1986; Ivantsov et al., 2005; Caron and Jackson, 2008; Dornbos and Chen, 2008; Zhao et al., 2010, 2014); the latter has also been pursued (e.g. Hendricks and Lieberman, 2007; Hendricks et al., 2008; Hendricks, 2013) and is the focus of the present contribution.

It is well known that many Cambrian Lagerstätten share common faunal elements. A substantial number of genera found within these assemblages exhibit largely cosmopolitan distributions, e.g. the sponges *Choaia*, *Hazelia*, *Leptomitus* and *Protospongia*, sponge-like *Chancelloria*, cnidarian *Byronia*, brachiopods *Lingulella* and *Nisusia*, anomalocaridid *Anomalocaris*, lobopodian *Hallucigenia*, the euarthropods *Canadaspis*, *Isoxys*, *Leanchoilia*, *Liangshanella*, *Naraoia* and *Tuzoia*, priapulid *Selkirkia*, and the enigmatic taxa *Haplophrentis*, *Wiwaxia*, *Eldonia* and *Dinomischus*. It is likely that at least some of these had larval stages capable of long distance dispersal via ocean currents (García-Bellido et al., 2007; Han et al., 2008; Zhao et al., 2011). These taxa are not particularly informative in a biogeographic sense, as their broad distributions provide little evidence when attempting to draw conclusions about relationships between localities; however, their shared presences suggest that we are looking at similar types of communities. These have

\* Corresponding author.

E-mail addresses: [james.holmes@adelaide.edu.au](mailto:james.holmes@adelaide.edu.au) (J.D. Holmes), [diego.garcia-bellido@adelaide.edu.au](mailto:diego.garcia-bellido@adelaide.edu.au) (D.C. García-Bellido), [mike.lee@samuseum.sa.gov.au](mailto:mike.lee@samuseum.sa.gov.au) (M.S.Y. Lee).

**9.2 An exceptional record of Cambrian trilobite moulting behaviour preserved in the  
Emu Bay Shale, South Australia**

Harriet B. Drage, James D. Holmes, Diego C. García-Bellido and Allison C. Daley



# An exceptional record of Cambrian trilobite moulting behaviour preserved in the Emu Bay Shale, South Australia

HARRIET B. DRAGE , JAMES D. HOLMES , DIEGO C. GARCÍA-BELLIDO  AND ALLISON C. DALEY 

## LETHAIA



Drage, H.B., Holmes, J.D., García-Bellido, D.C. & Daley, A.C. 2018: An exceptional record of Cambrian trilobite moulting behaviour preserved in the Emu Bay Shale, South Australia. *Lethaia*, Vol. 51, pp. 473–492.

Trilobites dominate the Emu Bay Shale (EBS) assemblage (Cambrian Series 2, Stage 4, South Australia) in terms of numbers, with *Estaingia bilobata* Pocock 1964 being extremely abundant, and the larger *Redlichia takooensis* Lu 1950, being common. Many specimens within the EBS represent complete moulted exoskeletons, which is unusual for Cambrian fossil deposits. The abundance of complete moults provides an excellent record that has allowed the recognition of various recurrent moult configurations for both species, enabling the inference of movement sequences required to produce such arrangements. Moult configurations of *E. bilobata* are characterized by slight displacement of the joined rostral plate and librigenae, often accompanied by detachment of the cranidium, suggesting ecdysis was achieved by anterior withdrawal via opening of the cephalic sutures. Moulting in *R. takooensis* often followed the same method, but configurations show greater displacement of cephalic sclerites, suggesting more vigorous movement by the animal during moulting. Both species also show rare examples of Salter's configuration, with the entire cephalon anteriorly inverted, and several other unusual configurations. These results indicate that moulting in trilobites was a more variable process than originally thought. In contrast, other Cambrian Konservat-Lagerstätten with an abundance of trilobites (e.g. Wheeler Shale, USA, and Mount Stephen Trilobite Beds, Canada) show larger numbers of 'axial shields' and isolated sclerites, often interpreted as disarticulated exuviae. This points to a higher level of disturbance from factors, such as animal activity, depositional processes or water movement, compared to that of the EBS, where quiescent conditions and intermittent seafloor anoxia contributed to an unparalleled trilobite moulting record. □ *Burgess Shale, Cambrian, ecdysis, Emu Bay Shale, Lagerstätten, moult configuration, trilobite.*

Harriet B. Drage ✉ [harriet.drage@zoo.ox.ac.uk], Department of Zoology, University of Oxford, South Parks Road Oxford OX1 3PS, UK; Oxford University Museum of Natural History, Parks Road Oxford OX1 3PZ, UK; James D. Holmes [james.holmes@adelaide.edu.au], Diego C. García-Bellido [diego.garcia-bellido@adelaide.edu.au], School of Biological Sciences, University of Adelaide, Adelaide, South Australia 5005, Australia; South Australian Museum, Adelaide, South Australia 5000, Australia; Allison C. Daley [allison.daley@unil.ch], Institute of Earth Sciences, University of Lausanne, Géopolis, Lausanne CH-1015, Switzerland; manuscript received on 15/08/2017; manuscript accepted on 14/12/2017.

Trilobite exoskeleton moulting behaviour is highly variable in comparison with what has been observed for other Cambrian arthropods and for modern groups (Daley & Drage 2016). Trilobites moulted throughout their lifetime to develop, grow and repair, and in doing so left various 'moult configurations' preserved in the fossil record. Data suggest that trilobite moulting behaviour and the resulting configurations were both inter- and intraspecifically variable (Daley & Drage 2016), and this variability appears to be consistent among trilobites with less derived morphologies (unlike more specialized groups such as the Phacopina, Daley & Drage 2016). Other Cambrian arthropods (although with less heavily calcified exoskeletons) moulted using more consistent standardized behaviours, producing a

uniform location for the 'exuvial gape' (where the animal exits the old exoskeleton). For example, the anterior exuvial gape can be observed in an exceptional specimen of *Marrella splendens* Walcott 1909 from the Burgess Shale preserved midway through moulting (García-Bellido & Collins 2004). More recent arthropods also show consistent moulting behaviour, such as in many decapod crustaceans where moults can be identified by their characteristic Open Moult Position with dorsal carapace displaced from the abdomen (see Daley & Drage 2016). In contrast, studies of trilobite moulting have demonstrated the significant variability of the exuvial gape location (e.g. McNamara & Rudkin 1984; McNamara 1986; Brandt 2002; Budil & Bruthansová 2005; Paterson *et al.* 2007; Daley & Drage 2016). The

**9.3 Taxa, turnover and taphofacies: a preliminary analysis of facies-assemblage relationships in the Ediacara Member (Flinders Ranges, South Australia)**

Lily M. Reid, James D. Holmes, Justin L. Payne, Diego C. García-Bellido and James B. Jago



## Taxa, turnover and taphofacies: a preliminary analysis of facies-assemblage relationships in the Ediacara Member (Flinders Ranges, South Australia)

L. M. Reid<sup>a</sup> , J. D. Holmes<sup>b</sup> , J. L. Payne<sup>a</sup> , D. C. García-Bellido<sup>b,c</sup> , and J. B. Jago<sup>a</sup>

<sup>a</sup>School of Natural and Built Environments, University of South Australia, Mawson Lakes, SA 5095, Australia; <sup>b</sup>School of Biological Sciences, University of Adelaide, Adelaide, SA 5005, Australia; <sup>c</sup>South Australian Museum, Adelaide, SA 5000, Australia

### ABSTRACT

The Ediacara Member of the Flinders Ranges (South Australia) preserves body and trace fossils of the Ediacara biota. Fossils span five lithofacies representative of a range of shallow-marine environments and are preserved as *in situ* and transported material. Previous work has demonstrated a relationship between paleoenvironment and taxa at the Nilpena fossil site. We expand the analysis to include facies-taxa data from a further nine localities across the Flinders Ranges to assess if the taxa-paleoenvironment relationship is site specific or valid at a regional scale. The new analysis demonstrates that the distribution of taxa within the lithofacies, as a proxy for paleoenvironment, is non-random. This preliminary analysis presents a beta diversity-like spatial turnover across the range of shallow marine Ediacaran environments, and demonstrates taxonomic assemblages are specific to given paleoenvironmental zones. These assemblages are consistent over a broad spatial extent and also a presumed temporal distribution. This specificity indicates that a marked sensitivity to environmental parameters was present in these communities, as demonstrated by the non-random distribution of taxa and spatial turnover of biotic assemblage throughout the gradational environments of the Ediacara Member. This study highlights the variability and heterogeneity that is a characteristic of shallow marine settings, and offers a novel approach to the future investigation of the relationship between Ediacaran environments and taxa assemblages.

### ARTICLE HISTORY

Received 31 January 2018  
Accepted 8 May 2018

### KEYWORDS

Ediacara; Ediacara Member; Flinders Ranges; paleoecology; spatial turnover; taphofacies


### Introduction

The Ediacara biota encompasses a diverse group of body and trace fossils that collectively represent the earliest evidence of a range of stem and possible crown group metazoans, and arguably the earliest communities of macroorganisms on Earth (Droser, Tarhan, & Gehling, 2017a). In South Australia, the Ediacara Member of the Rawnsley Quartzite denotes the restricted stratigraphic interval that contains a unique, abundant and highly diverse assemblage of Ediacaran fossils. Historically, the Ediacara Member has been interpreted based on an evolving series of lithofacies models, which seek to classify and interpret the sedimentological characteristics of the shallow marine paleoenvironments they represent (see Gehling, 1983, 2000; Gehling & Droser, 2012; Goldring & Curnow, 1967; Jenkins, Ford, & Gehling, 1983; Tarhan, Droser, Gehling, & Dzaugis, 2017).

The variable distribution of taxa throughout the Ediacara Member was recognised early in the exploration of Ediacaran localities. Wade (1970) noted the restriction of the biota to specific stratigraphic horizons and presented taxonomic data on collected material from a range of sites (Wade 1970, table 1). A study undertaken at the Nilpena

locality (Figure 1) was the first to indicate the presence and significance of Ediacara biota body fossils throughout the entirety of the Ediacara Member (Gehling & Droser, 2013). The ripple-top, shallow marine horizons were previously considered to be the primary fossiliferous beds. Gehling and Droser (2013) highlighted the occurrence of both transported and *in situ* fossils in two distinct sediment packages that had been previously considered sparingly fossiliferous at best (Gehling, 2000; Goldring & Curnow, 1967). This study revealed the facies specificity (and conversely generalist behaviour) of a number of taxa. It supported findings by Grazhdankin (2004) for similar taxa assemblages in near-equivalent environments at sites in Russia, which suggested a remarkable level of environmental specificity was present within the Ediacara biota. While the analysis of a single locality allows evaluation of the relationships between taxa and paleoenvironment, the regional implications are limited by the possibility of site-specific relationships. By investigating broader relationships between geographic range, lithofacies and taxa assemblage we demonstrate the relationships found at Nilpena are repeatable by including a number of Ediacara Member sites. This analysis also allows the proposal of best practices

CONTACT L. M. Reid  lily.reid@mymail.unisa.edu.au  
Editorial handling: Stephen Hore

 Supplemental data for this article can be accessed <https://doi.org/10.1080/08120099.2018.1488767>

© 2018 Geological Society of Australia

**9.4 The stratigraphic significance of early Cambrian (Series 2, Stage 4) trilobites from the  
Smith Bay Shale near Freestone Creek, Kangaroo Island**

James B. Jago, Christopher J. Bentley, John. R. Paterson, James D. Holmes,  
Tian-Rui Lin and Xiao-Wen Sun

# The stratigraphic significance of early Cambrian (Series 2, Stage 4) trilobites from the Smith Bay Shale near Freestone Creek, Kangaroo Island

J. B. Jago<sup>a</sup> , C. J. Bentley<sup>b</sup> , J. R. Paterson<sup>c</sup> , J. D. Holmes<sup>d</sup> , T. R. Lin<sup>e</sup> and X. W. Sun<sup>f</sup>

<sup>a</sup>School of Natural and Built Environments, University of South Australia, Mawson Lakes, Australia; <sup>b</sup>Clare, Australia; <sup>c</sup>Palaeoscience Research Centre, School of Environmental and Rural Science, University of New England, Armidale, Australia; <sup>d</sup>School of Biological Sciences, University of Adelaide, Adelaide, Australia; <sup>e</sup>The School of Earth Sciences and Engineering, Nanjing University, Nanjing, PR China; <sup>f</sup>Sun Petroleum Geoservices, Melbourne, Australia

## ABSTRACT

The fossiliferous lower Cambrian (Series 2) successions along the north coast of Kangaroo Island, South Australia—known collectively as the Kangaroo Island Group—can be divided into two main areas: a western succession located between Snelling Beach and Smith Bay, which comprises the Mt McDonnell Formation (base), Stokes Bay Sandstone and Smith Bay Shale; and an eastern succession that extends from Emu Bay to Point Marsden, represented by exposures of the White Point Conglomerate (base), Marsden Sandstone, Emu Bay Shale and Boxing Bay Formation (top), with an overlap in the Cape d'Estaing/Emu Bay area. Some previous interpretations of the Kangaroo Island Group stratigraphy suggest that the western succession stratigraphically underlies the eastern succession. Most of the previously reported and described Cambrian fossils come from the eastern succession, especially the internationally significant Emu Bay Shale *Konservat-Lagerstätte*. Here we report the trilobites *Redlichia takooensis* and *Balcoracania dailyi* from the Smith Bay Shale near Freestone Creek, indicating that the eastern and western successions are at least partly contemporaneous. The present investigation indicates that the Smith Bay Shale of the western succession can be correlated with the stratigraphic interval represented by the Marsden Sandstone and the overlying Emu Bay Shale of the eastern succession. The Kangaroo Island Group was deposited as part of a fan delta system with the eastern succession representing the proximal part, and the western succession representing the distal part of the fan delta. The lack of substantial conglomerate units within the Kangaroo Island Group to the west of Cape d'Estaing suggests that the tectonic uplift that led to the deposition of the White Point Conglomerate was concentrated in the area immediately to the north of Emu Bay.

## ARTICLE HISTORY

Received 18 February 2020  
Accepted 21 March 2020

## KEYWORDS

Cambrian; Kangaroo Island; South Australia; Smith Bay Shale; trilobites; *Redlichia*; *Balcoracania*; fan delta system



## Introduction

The lower Cambrian (Series 2) succession on the north coast of Kangaroo Island, South Australia (Figure 1), has international significance owing to the presence of the Cambrian Stage 4 Emu Bay Shale *Konservat-Lagerstätte* at Big Gully (Paterson *et al.*, 2016, and references therein). This fossil locality was discovered by Brian Daily in 1954 on the shore platform about 8 km northeast of Emu Bay (Jago & Cooper, 2011), with the first descriptions of the soft-bodied fossils by Glaessner (1979).

The Cambrian exposures were previously considered by Belperio *et al.* (1998), Daily (1956), Daily *et al.* (1979), Gravestock and Gatehouse (1995) and James and Clark (2002) to comprise a stratigraphically continuous succession of six formations known as the Kangaroo Island Group: Mt McDonnell Formation (base), Stokes Bay Sandstone, Smith Bay Shale, White Point Conglomerate,

Emu Bay Shale and Boxing Bay Formation (top). Gehling *et al.* (2011) established a new unit, the Marsden Sandstone, between the White Point Conglomerate and the Emu Bay Shale, with the Emu Bay Shale resting unconformably on the Marsden Sandstone. Gehling *et al.* (2011) also erected the Rouge Mudstone Member, a 3 m thick calcareous mudstone, at the base of the Marsden Sandstone and provided correlations with the Cambrian successions on Yorke and Fleurieu peninsulas (Figure 2). The Marsden Sandstone was previously considered as the finer-grained upper part of the White Point Conglomerate (see Daily *et al.*, 1980).

The previously considered 'lower' formations (Mt McDonnell Formation, Stokes Bay Sandstone, Smith Bay Shale) are best exposed in the area between Snelling Beach and Emu Bay, although a fault bounded area around Cape d'Estaing largely comprises the White Point Conglomerate (Figure 3); lateral equivalents of the Marsden

CONTACT J. R. Paterson  [jpater20@une.edu.au](mailto:jpater20@une.edu.au)  Palaeoscience Research Centre, School of Environmental and Rural Science, University of New England, Armidale, NSW, 2351, Australia  
Editorial handling: Anita Andrew

© 2020 Geological Society of Australia





## **Chapter 10**

### Appendix 2: Supplementary Material

## 10.1 Supplementary material for Chapter 3

### 10.1.1 Dataset of *Estaingia bilobata* cranial (Cr.) length and width measurements. CeS

(Cephalic Size) is calculated as the arithmetic mean of log cranial length and width.

| SAM P-number | Cr. length | Cr. width | CeS    | Degree |
|--------------|------------|-----------|--------|--------|
| 44564        | 0.71       | 0.91      | -0.218 | 0      |
| 57597        | 0.74       | 1.01      | -0.146 | 0      |
| 57580        | 0.78       | 1.04      | -0.105 | 0      |
| 57621        | 0.8        | 1.2       | -0.020 | 0      |
| 57595        | 0.89       | 1.23      | 0.045  | 1      |
| 46020.1      | 0.9        | 1.14      | 0.013  | 1      |
| 15274        | 0.92       | 1.27      | 0.078  | 1      |
| 57658        | 1.02       | 1.41      | 0.182  | 1      |
| 57608        | 1.05       | 1.31      | 0.159  | 1      |
| 57614        | 1.05       | 1.45      | 0.210  | 1      |
| 57611        | 1.06       | 1.33      | 0.172  | 1      |
| 57588        | 0.96       | 1.21      | 0.075  | 2      |
| 14751        | 0.98       | 1.26      | 0.105  | 2      |
| 57584        | 1.05       | 1.34      | 0.171  | 2      |
| 57594        | 1.07       | 1.57      | 0.259  | 3      |
| 57670        | 1.15       | 1.34      | 0.216  | 3      |
| 57603        | 1.17       | 1.53      | 0.291  | 3      |
| 57583        | 1.19       | 1.44      | 0.269  | 3      |
| 57607        | 1.2        | 1.51      | 0.297  | 3      |
| 57671        | 1.22       | 1.46      | 0.289  | 3      |
| 49645        | 1.23       | 1.48      | 0.300  | 3      |
| 57676        | 1.32       | 1.62      | 0.380  | 3      |
| 46348.1      | 1.1        | 1.36      | 0.201  | 4      |
| 46099        | 1.19       | 1.61      | 0.325  | 4      |
| 57612        | 1.21       | 1.52      | 0.305  | 4      |
| 47009        | 1.33       | 1.67      | 0.399  | 4      |
| 46142        | 1.35       | 1.65      | 0.400  | 4      |
| 57655        | 1.4        | 1.7       | 0.434  | 4      |
| 52791        | 1.4        | 1.55      | 0.387  | 4      |
| 57650        | 1.45       | 1.95      | 0.520  | 4      |
| 57606        | 1.33       | 1.77      | 0.428  | 5      |
| 57682        | 1.38       | 1.58      | 0.390  | 5      |
| 57613        | 1.39       | 1.79      | 0.456  | 5      |
| 57589        | 1.41       | 1.78      | 0.460  | 5      |
| 57585        | 1.34       | 1.5       | 0.349  | 6      |
| 57586        | 1.39       | 1.67      | 0.421  | 6      |
| 57659        | 1.43       | 1.87      | 0.492  | 6      |
| 57622        | 1.5        | 1.9       | 0.524  | 6      |
| 57620        | 1.51       | 1.85      | 0.514  | 6      |
| 57649        | 1.52       | 1.96      | 0.546  | 6      |
| 57618        | 1.55       | 2.25      | 0.625  | 6      |
| 46120        | 1.55       | 1.99      | 0.563  | 6      |
| 57615        | 1.59       | 2         | 0.578  | 6      |
| 44572        | 1.63       | 2.05      | 0.603  | 6      |
| 57664        | 1.64       | 1.97      | 0.586  | 6      |
| 57605        | 1.52       | 2.09      | 0.578  | 7      |
| 57593        | 1.54       | 1.92      | 0.542  | 7      |

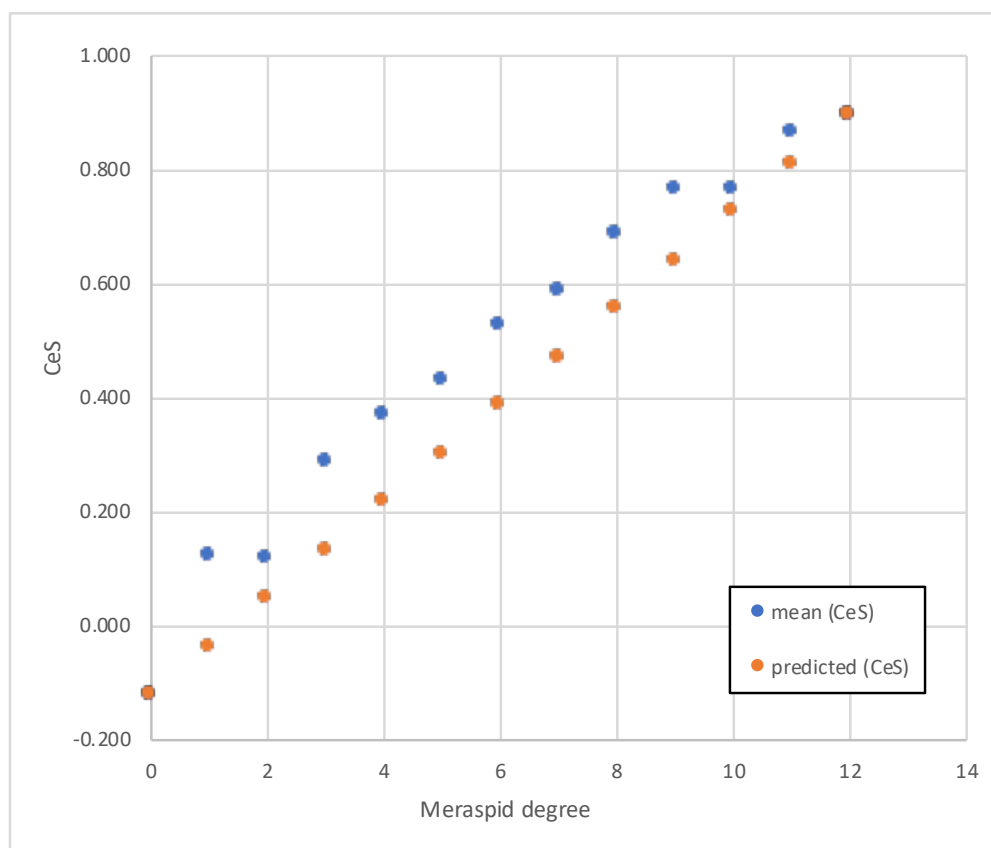
|                |      |      |       |    |
|----------------|------|------|-------|----|
| <b>57667</b>   | 1.55 | 1.88 | 0.535 | 7  |
| <b>57669</b>   | 1.55 | 1.91 | 0.543 | 7  |
| <b>57632</b>   | 1.56 | 2.01 | 0.571 | 7  |
| <b>57602</b>   | 1.57 | 1.96 | 0.562 | 7  |
| <b>46020.2</b> | 1.58 | 1.89 | 0.547 | 7  |
| <b>57616</b>   | 1.62 | 2.08 | 0.607 | 7  |
| <b>57587</b>   | 1.63 | 2.06 | 0.606 | 7  |
| <b>57642</b>   | 1.63 | 1.96 | 0.581 | 7  |
| <b>57591</b>   | 1.64 | 2.02 | 0.599 | 7  |
| <b>57631</b>   | 1.64 | 2.04 | 0.604 | 7  |
| <b>57656</b>   | 1.64 | 1.91 | 0.571 | 7  |
| <b>57623</b>   | 1.65 | 2.18 | 0.640 | 7  |
| <b>49700</b>   | 1.65 | 2.07 | 0.614 | 7  |
| <b>46131</b>   | 1.68 | 2.26 | 0.667 | 7  |
| <b>46219</b>   | 1.68 | 2.11 | 0.633 | 7  |
| <b>57582</b>   | 1.69 | 2.07 | 0.626 | 8  |
| <b>57617</b>   | 1.69 | 2.04 | 0.619 | 8  |
| <b>15472</b>   | 1.69 | 1.99 | 0.606 | 8  |
| <b>46093</b>   | 1.69 | 2.07 | 0.626 | 8  |
| <b>46206</b>   | 1.71 | 2.15 | 0.651 | 8  |
| <b>57628</b>   | 1.78 | 2.3  | 0.705 | 8  |
| <b>44424</b>   | 1.81 | 2.22 | 0.695 | 8  |
| <b>57653</b>   | 1.82 | 2.07 | 0.663 | 8  |
| <b>57663</b>   | 1.84 | 2.08 | 0.671 | 8  |
| <b>49586</b>   | 1.87 | 2.11 | 0.686 | 8  |
| <b>57668</b>   | 1.88 | 2.44 | 0.762 | 8  |
| <b>57601</b>   | 1.89 | 2.55 | 0.786 | 8  |
| <b>57637</b>   | 1.91 | 2.13 | 0.702 | 8  |
| <b>57610</b>   | 1.93 | 2.21 | 0.725 | 8  |
| <b>57677</b>   | 1.93 | 2.26 | 0.736 | 8  |
| <b>44052</b>   | 2.01 | 2.22 | 0.748 | 8  |
| <b>57641</b>   | 1.8  | 2.36 | 0.723 | 9  |
| <b>57681</b>   | 1.8  | 2.29 | 0.708 | 9  |
| <b>57626</b>   | 1.82 | 2.29 | 0.714 | 9  |
| <b>43824</b>   | 1.83 | 2.33 | 0.725 | 9  |
| <b>50298</b>   | 1.85 | 2.27 | 0.717 | 9  |
| <b>57636</b>   | 1.86 | 2.27 | 0.720 | 9  |
| <b>57625</b>   | 2    | 2.48 | 0.801 | 9  |
| <b>57633</b>   | 2.01 | 2.34 | 0.774 | 9  |
| <b>57619</b>   | 2.06 | 2.41 | 0.801 | 9  |
| <b>57665</b>   | 2.06 | 2.32 | 0.782 | 9  |
| <b>15544</b>   | 2.26 | 2.88 | 0.937 | 9  |
| <b>57666</b>   | 1.78 | 2.3  | 0.705 | 10 |
| <b>57640</b>   | 1.81 | 2.19 | 0.689 | 10 |
| <b>57679</b>   | 1.89 | 2.43 | 0.762 | 10 |
| <b>48253</b>   | 1.89 | 2.29 | 0.733 | 10 |
| <b>57630</b>   | 1.94 | 2.37 | 0.763 | 10 |
| <b>57680</b>   | 1.99 | 2.5  | 0.802 | 10 |

|                |      |      |       |    |
|----------------|------|------|-------|----|
| <b>57598</b>   | 2    | 2.36 | 0.776 | 10 |
| <b>57644</b>   | 2    | 2.55 | 0.815 | 10 |
| <b>44526</b>   | 2.09 | 2.54 | 0.835 | 10 |
| <b>46253</b>   | 1.93 | 2.4  | 0.766 | 11 |
| <b>57609</b>   | 2.06 | 2.38 | 0.795 | 11 |
| <b>57629</b>   | 2.07 | 2.29 | 0.778 | 11 |
| <b>57635</b>   | 2.07 | 2.67 | 0.855 | 11 |
| <b>57647</b>   | 2.08 | 2.69 | 0.861 | 11 |
| <b>57654</b>   | 2.08 | 2.6  | 0.844 | 11 |
| <b>57627</b>   | 2.11 | 2.53 | 0.837 | 11 |
| <b>49684</b>   | 2.11 | 2.86 | 0.899 | 11 |
| <b>57590</b>   | 2.17 | 2.4  | 0.825 | 11 |
| <b>57639</b>   | 2.19 | 2.71 | 0.890 | 11 |
| <b>46071</b>   | 2.22 | 2.4  | 0.836 | 11 |
| <b>57678</b>   | 2.25 | 2.67 | 0.897 | 11 |
| <b>57684</b>   | 2.27 | 2.63 | 0.893 | 11 |
| <b>44637</b>   | 2.33 | 2.83 | 0.943 | 11 |
| <b>43991</b>   | 2.35 | 2.96 | 0.970 | 11 |
| <b>46107</b>   | 2.36 | 2.93 | 0.967 | 11 |
| <b>57675</b>   | 2.11 | 2.77 | 0.883 | 12 |
| <b>57624</b>   | 2.13 | 2.47 | 0.830 | 12 |
| <b>57592</b>   | 2.18 | 2.55 | 0.858 | 12 |
| <b>49643</b>   | 2.19 | 2.69 | 0.887 | 12 |
| <b>45956</b>   | 2.23 | 2.42 | 0.843 | 12 |
| <b>57596</b>   | 2.26 | 2.94 | 0.947 | 12 |
| <b>46348.2</b> | 2.26 | 2.79 | 0.921 | 12 |
| <b>57662</b>   | 2.33 | 2.79 | 0.936 | 12 |
| <b>46063</b>   | 2.33 | 2.69 | 0.918 | 12 |
| <b>57638</b>   | 2.43 | 2.68 | 0.937 | 12 |

Average(M0) -0.122  
 Average(M12) 0.896

AGI 0.084840665  
**AGR 1.08854361**  
**IDC 0.828436423**

| degree | mean (CeS) | actual      | predicted  | predicted (CeS) | variation |
|--------|------------|-------------|------------|-----------------|-----------|
| 0      | -0.122     | 0.884925075 | 0.88492507 | -0.122          | 0.000     |
| 1      | 0.123      | 1.13054477  | 0.96327954 | -0.037          | -0.160    |
| 2      | 0.117      | 1.124150748 | 1.04857178 | 0.047           | -0.070    |
| 3      | 0.288      | 1.333329435 | 1.14141611 | 0.132           | -0.155    |
| 4      | 0.371      | 1.449764321 | 1.24248122 | 0.217           | -0.154    |
| 5      | 0.433      | 1.542529589 | 1.35249499 | 0.302           | -0.131    |
| 6      | 0.527      | 1.694439916 | 1.47224978 | 0.387           | -0.141    |
| 7      | 0.588      | 1.800734487 | 1.60260809 | 0.472           | -0.117    |
| 8      | 0.688      | 1.989779527 | 1.74450879 | 0.556           | -0.132    |
| 9      | 0.764      | 2.146566749 | 1.89897390 | 0.641           | -0.123    |
| 10     | 0.764      | 2.147410481 | 2.06711591 | 0.726           | -0.038    |
| 11     | 0.866      | 2.377526113 | 2.25014581 | 0.811           | -0.055    |
| 12     | 0.896      | 2.449381843 | 2.44938184 | 0.896           | 0.000     |



## 10.2 Supplementary material for Chapter 5

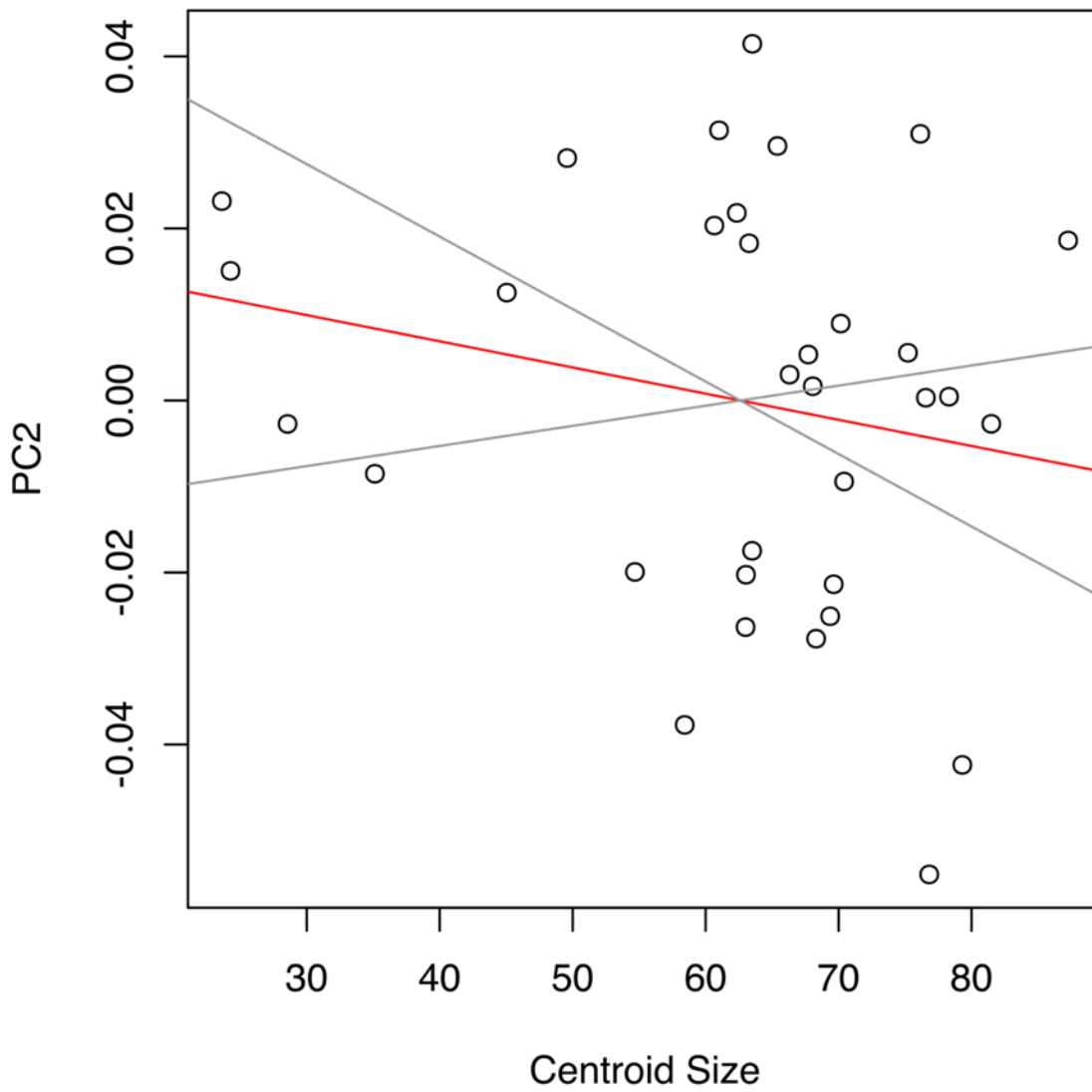


**Figure 10.1:** Major axis regression of PC2 against centroid size. The relationship is not significant ( $R^2 = 0.04$ ,  $p = 0.134$ ).

### 10.3 Supplementary material for Chapter 6

#### 10.3.1 Measurement definitions and abbreviations

|               |  |
|---------------|--|
| $CEL(s)$      | Cephalic length (of specimens $s$ )  |
| $TRL(s)$      | Trunk length   |
| $PYL(s)$      | Pygidium length  |
| $LTS_i(s)$    | Length of thoracic segment $i$   |
| $LTS_{rel_d}$ | Length of the most recently released segment at stage $d$  |
| $PTS_i(s)$    | Distance of posterior of thoracic segment $i$ from cephalon/trunk boundary   |
| $RLS_{i,d}$   | Mean relative length of segment $i$ at stage $d$ . Calculated as: $\Sigma[LTS_i(s)/TRL(s)]$  |
| $RPS_{i,d}$   | Mean relative position of posterior of segment $i$ relative to cephalon/trunk boundary at stage $d$ . Calculated as: $\Sigma[PTS_i(s)/TRL(s)]$ |
| $TRL_d$       | Mean trunk length at stage $d$   |
| $TRL_{d+1}$   | Mean trunk length at stage $d+1$   |
| $TRG_d$       | Mean trunk growth rate at stage $d$ . Calculated as: $TRL_{d+1}/TRL_d$   |

#### 10.3.2 Fitting functions and implementation

Fitting function derivation is based on the methodology of Fusco *et al.* (2014) and the following closely mimics Section 3 of their Electronic Supplementary Material.

##### **Segmental Gradient (SG) hypothesis:**

The SG hypothesis under the condition of a changing trunk growth rate suggests that each thoracic segment grows at a rate proportional to the overall trunk growth rate. Where  $r_S$  is the growth rate of a thoracic segment  $S$ , and  $r_T$  is the growth rate of the trunk  $T$ , the ratios  $r_S/r_T$  and  $\ln(r_S)/\ln(r_T)$  are constant under the condition of a static trunk growth rate.

However, if growth rates are expected to change only one of the ratios above can remain

constant. Thus, the models below test two options for which the segment growth can be proportional to trunk growth.

The **SG-R** model sets a **constant growth ratio of segment  $i$  with respect to trunk growth ratio**. The segmental gradient  $g(i)$  is a decaying geometric progression from the posterior of the thorax:  $g(i) = a + b \cdot e^{w \cdot i}$

*Fitting procedure:*

Dependent variable:  $RLS_{i,d+1}$

Independent variables:  $i$ ;  $RLS_{i,d}$ ;  $TRG_d = TRL_{d+1}/TRL_d$

Fitting parameters (3):  $a$ ,  $b$ ,  $w$

Fitting function:  $RLS_{i,d+1} = g(i) \cdot TGR_d \cdot RLS_{i,d}$

The **SG-A** model set a **constant allometric coefficient of segment  $i$  with respect to the trunk**. The segmental gradient  $g(i)$  is a decaying geometric progression from the posterior of the thorax:  $g(i) = a + b \cdot e^{w \cdot i}$

*Fitting procedure:*

Dependent variable:  $RLS_{i,d+1}$

Independent variables:  $i$ ;  $RLS_{i,d}$ ;  $TRG_d = TRL_{d+1}/TRL_d$

Fitting parameters (3):  $a$ ,  $b$ ,  $w$

Fitting function:  $RLS_{i,d+1} = TGR_d^{g(i)} \cdot RLS_{i,d}$

Results:

Preliminary analysis suggests that parameter  $w$  trends to 0 in both the SG-A and -B models and thus has no effect on the results. A reduced 2-parameter model using the simplified fitting function  $g(i) = a + b \cdot i$  showed no loss of fit.

**Table 10.1:** Parameter estimates and pseudo-R<sup>2</sup> values for the SG models.

| Model (n=66)        | a       | b       | Pseudo-R <sup>2</sup> |
|---------------------|---------|---------|-----------------------|
| <b>SG-R (2 par)</b> | 0.75847 | 0.02321 | 93.7370               |
| <b>SG-A (2 par)</b> | -0.6678 | 0.1351  | 99.5786               |



### Trunk Gradient (TG) hypothesis:

To allow for the possibility of a changing trunk growth rate it is possible to derive a fitting function that does not depend on the trunk growth rate ( $r_T$ ), but is rather solely based on the relative position of segmental markers. To do this, we use a modified version of the *TGexp* model of Fusco *et al.* (2014) where the growth rate along the trunk is defined by an exponential function that decays from posterior to anterior (reflecting higher growth rates towards the posterior). For any point ( $x$ ) within the closed interval  $[0,1]$  (representing the relative anterior/posterior position within the trunk) the growth gradient is defined by the function:

$$(1) \quad g(x) = a + be^{-w(1-x)}$$

From this, the average growth of a trunk section to position  $x[0,x]$  is:

$$(2) \quad G(x) = \int_0^x g(y)dy = a + \frac{-be^{-w} + be^{-w(1-x)}}{wx}$$

Instead of setting  $G(1) = r$  (where  $r$  is the static growth rate of Fusco *et al.* 2014), we set  $G(1) = 1$ , and solve for  $a$ , giving us:

$$(3) \quad a = 1 - \frac{b - be^{-w}}{w}$$

Substituting (3) into (1) gives us the relative gradient:

$$(4) \quad g(x) = 1 - \frac{b - be^{-w}}{w} + be^{-w(1-x)}$$

And its integral in  $x[0,x]$   $G(x)$  provides the fitting function:

$$(5) \quad G(x) = x + b \frac{-x - (1-x)e^{-w} + e^{-w(1-x)}}{w} = Z(x)$$

The absolute gradients can be found by multiplying  $g(x)$  and  $G(x)$  by  $r_T$  = trunk growth rate.

The **RG** model sets a local per-stage growth rate at each point along the trunk as an exponential function. For any point  $x$  in the closed interval  $[0,1]$  of relative anterior-posterior trunk positions, **the growth gradient is a decaying exponential function from the posterior**. Model fitting procedures are as follows:

**RG-(A,B,C)1**

*Fitting procedure (RLS):*

Dependent variable:  $RLS_{i,d+1}$

Independent variables:  $TRG; RPS_{i,d}$

Fitting function:  $RLS_{i,d+1} = Z(RPS_{i,d}) - Z(RPS_{i-1,d})$

**RG-(A,B,C)2**

*Fitting procedure (RPS):*

Dependent variable:  $RPS_{i,d+1}$

Independent variables:  $TRG; RPS_{i,d}$

Fitting function:  $RPS_{i,d+1} = Z(RPS_{i,d})$

Results:

**Table 10.2:** Parameter estimates and pseudo-R<sup>2</sup> values for the various RG models. Removing parameters  $w0$  and  $w$  from the *RG-C* models does not have a large effect on model support. Removing these parameters from the *RG-C1* model showed some loss of fit; however, removing these from the *RG-C2* model had essentially no effect.

| Model (n = 66)       | b0      | b        | w0      | w        | Pseudo-R <sup>2</sup> |
|----------------------|---------|----------|---------|----------|-----------------------|
| <b>RG-A1</b>         |         | 0.2967   |         | 2.7796   | 98.8342               |
| <b>RG-A2</b>         |         | 0.3129   |         | 1.0627   | 99.5855               |
| <b>RG-B1</b>         | 0.44604 | -0.02148 | 5.21755 | -0.43446 | 98.9633               |
| <b>RG-B2</b>         | 0.42590 | -0.02417 | 3.26603 | -0.12850 | 99.6683               |
| <b>RG-C1 (4 par)</b> | -2.099  | 2.082    | -17.130 | 16.352   | 99.5998               |
| <b>RG-C1 (2 par)</b> | -2.071  | 2.07     |         |          | 99.5226               |
| <b>RG-C2 (4 par)</b> | -1.4946 | 1.5865   | -0.5076 | 1.3831   | 99.8631               |
| <b>RG-C2 (2 par)</b> | -1.512  | 1.595    |         |          | 99.8630               |

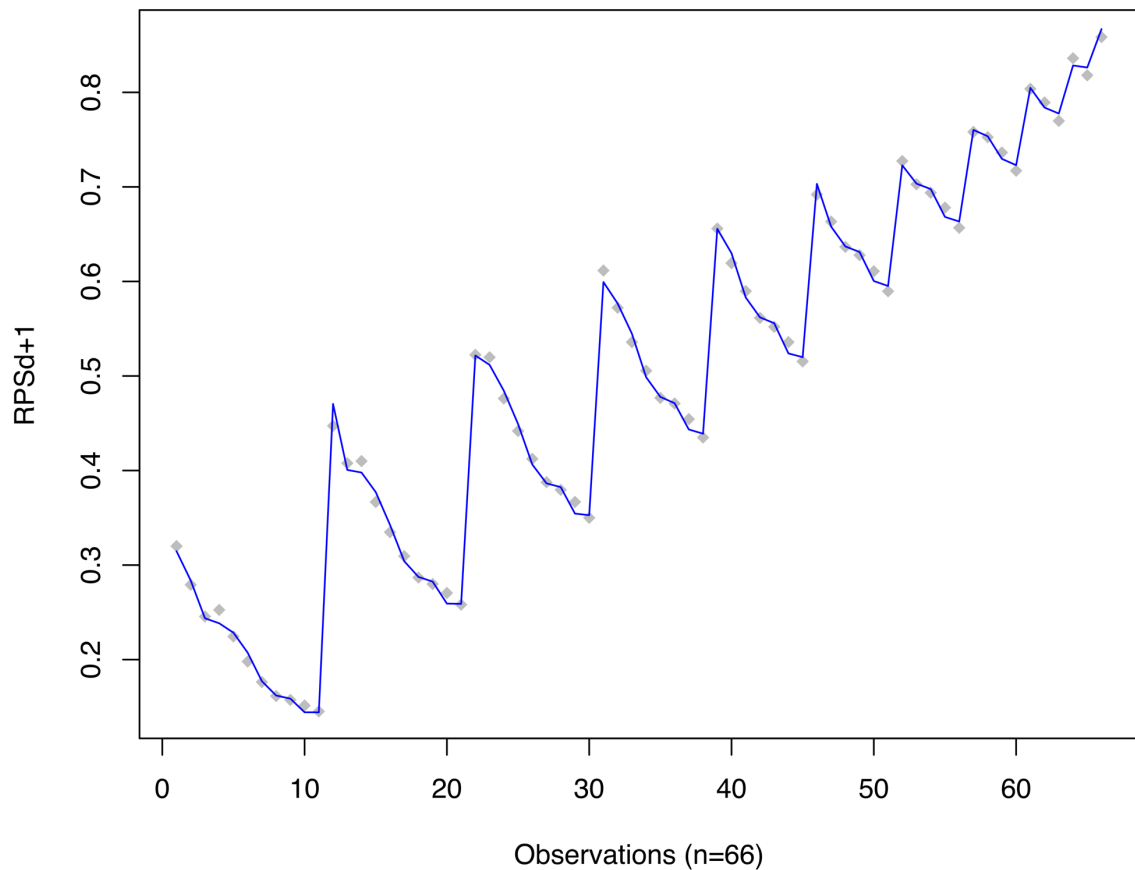


**Figure 10.2:** Fitting of the best supported (RG-C2) model to observed *RPS* data. Observed data = grey diamonds; RG-C2 model = blue. To make visualisation easier, this plot shows in 2D what is actually a 3D relationship, with observations of each segment (TS1–11) at each stage (D1–D11) shown sequentially (the x-axis refers to the total number of observations,  $n = 66$ ).

**Table 10.3:** OLS regression (slope only) coefficients and significance values for [*PYL* ~ stage (D0–D10)] and [*PYL* ~ stage (D0–D12)] representing pygidial growth rates across meraspid ontogeny.

| Slope coef.  | Estimate   | Std. Error | t value | Pr(> t ) |
|--------------|------------|------------|---------|----------|
| Stage D0–D10 | -0.0006577 | 0.0065238  | -0.101  | 0.92     |
| Stage D0–D12 | -0.020121  | 0.005439   | -3.699  | 0.00035  |

### 10.3.3 References

**Fusco, G., Hong, P.S. & Hughes, N.C.** 2014. Positional specification in the segmental growth pattern of an early arthropod. *Proceedings of the Royal Society of London B*, **281**: 20133037.

### 10.3.4 Dataset of thoracic segment lengths ( $LTS_i$ ) and relative position of posterior boundaries ( $PTS_i$ ) at each stage $d$ for all specimens.

| id      | d | CEL       | TRL       | PYL       | LTS1      | LTS2      | LTS3      | LTS4      | LTS5      | LTS6      | LTS7      | LTS8      | LTS9      | LTS10     | LTS11     | LTS12     |
|---------|---|-----------|-----------|-----------|-----------|-----------|-----------|-----------|-----------|-----------|-----------|-----------|-----------|-----------|-----------|-----------|
| 157_2   | 0 | 0.7476022 | 0.4063558 | NA        | NA        | NA        | NA        | NA        | NA        | NA        | NA        | NA        | NA        | NA        | NA        | NA        |
| 44564   | 0 | 0.6510492 | 0.4190430 | NA        | NA        | NA        | NA        | NA        | NA        | NA        | NA        | NA        | NA        | NA        | NA        | NA        |
| 141_1   | 1 | 0.9832853 | 0.3900033 | 0.2080024 | 0.2080024 | 0.2080024 | 0.2080024 | 0.2080024 | 0.2080024 | 0.2080024 | 0.2080024 | 0.2080024 | 0.2080024 | 0.2080024 | 0.2080024 | 0.2080024 |
| 144     | 1 | 0.9540634 | 0.6390383 | 0.4150301 | 0.2240089 | 0.2240089 | 0.2240089 | 0.2240089 | 0.2240089 | 0.2240089 | 0.2240089 | 0.2240089 | 0.2240089 | 0.2240089 | 0.2240089 | 0.2240089 |
| 147     | 1 | 0.9052872 | 0.7231998 | 0.4951010 | 0.2281074 | 0.2281074 | 0.2281074 | 0.2281074 | 0.2281074 | 0.2281074 | 0.2281074 | 0.2281074 | 0.2281074 | 0.2281074 | 0.2281074 | 0.2281074 |
| 15274   | 1 | 0.8224767 | 0.5493642 | 0.3522400 | 0.1971243 | 0.1971243 | 0.1971243 | 0.1971243 | 0.1971243 | 0.1971243 | 0.1971243 | 0.1971243 | 0.1971243 | 0.1971243 | 0.1971243 | 0.1971243 |
| 312     | 1 | 0.9423587 | 0.6126745 | 0.4217404 | 0.1909476 | 0.1909476 | 0.1909476 | 0.1909476 | 0.1909476 | 0.1909476 | 0.1909476 | 0.1909476 | 0.1909476 | 0.1909476 | 0.1909476 | 0.1909476 |
| 46020   | 1 | 0.8750091 | 0.4970040 | 0.3510057 | 0.1460000 | 0.1460000 | 0.1460000 | 0.1460000 | 0.1460000 | 0.1460000 | 0.1460000 | 0.1460000 | 0.1460000 | 0.1460000 | 0.1460000 | 0.1460000 |
| 84      | 1 | 0.8072236 | 0.5280152 | 0.3550127 | 0.1730029 | 0.1730029 | 0.1730029 | 0.1730029 | 0.1730029 | 0.1730029 | 0.1730029 | 0.1730029 | 0.1730029 | 0.1730029 | 0.1730029 | 0.1730029 |
| 14751   | 1 | 0.8808252 | 0.6887452 | 0.3317981 | 0.2195837 | 0.2195837 | 0.2195837 | 0.2195837 | 0.2195837 | 0.2195837 | 0.2195837 | 0.2195837 | 0.2195837 | 0.2195837 | 0.2195837 | 0.2195837 |
| 21_1    | 2 | 0.9722268 | 0.6361328 | 0.2990602 | 0.2010398 | 0.1373645 | 0.1360331 | 0.1360331 | 0.1360331 | 0.1360331 | 0.1360331 | 0.1360331 | 0.1360331 | 0.1360331 | 0.1360331 | 0.1360331 |
| 27      | 2 | 0.8991135 | 0.6082376 | 0.3051328 | 0.1980909 | 0.1980909 | 0.1980909 | 0.1980909 | 0.1980909 | 0.1980909 | 0.1980909 | 0.1980909 | 0.1980909 | 0.1980909 | 0.1980909 | 0.1980909 |
| 135_1   | 3 | 1.0542732 | 0.7051815 | 0.2840634 | 0.2300782 | 0.2300782 | 0.2300782 | 0.2300782 | 0.2300782 | 0.2300782 | 0.2300782 | 0.2300782 | 0.2300782 | 0.2300782 | 0.2300782 | 0.2300782 |
| 140     | 3 | 1.0730615 | 0.9034141 | 0.3630055 | 0.2556345 | 0.2556345 | 0.2556345 | 0.2556345 | 0.2556345 | 0.2556345 | 0.2556345 | 0.2556345 | 0.2556345 | 0.2556345 | 0.2556345 | 0.2556345 |
| 15      | 3 | 1.0621525 | 0.8610929 | 0.3718414 | 0.2175891 | 0.2175891 | 0.2175891 | 0.2175891 | 0.2175891 | 0.2175891 | 0.2175891 | 0.2175891 | 0.2175891 | 0.2175891 | 0.2175891 | 0.2175891 |
| 387     | 3 | 0.9710577 | 0.7614473 | 0.3100097 | 0.2247221 | 0.2247221 | 0.2247221 | 0.2247221 | 0.2247221 | 0.2247221 | 0.2247221 | 0.2247221 | 0.2247221 | 0.2247221 | 0.2247221 | 0.2247221 |
| 389     | 3 | 1.0873606 | 0.7992503 | 0.3480919 | 0.2500980 | 0.2500980 | 0.2500980 | 0.2500980 | 0.2500980 | 0.2500980 | 0.2500980 | 0.2500980 | 0.2500980 | 0.2500980 | 0.2500980 | 0.2500980 |
| 420     | 3 | 1.1622173 | 0.9479757 | 0.4674719 | 0.2232241 | 0.2232241 | 0.2232241 | 0.2232241 | 0.2232241 | 0.2232241 | 0.2232241 | 0.2232241 | 0.2232241 | 0.2232241 | 0.2232241 | 0.2232241 |
| 49645   | 3 | 1.1161147 | 0.8640700 | 0.3620221 | 0.2380189 | 0.1470136 | 0.1470136 | 0.1470136 | 0.1470136 | 0.1470136 | 0.1470136 | 0.1470136 | 0.1470136 | 0.1470136 | 0.1470136 | 0.1470136 |
| 78_1    | 3 | 0.9780925 | 0.7193511 | 0.3128530 | 0.1921510 | 0.1207021 | 0.0936483 | 0.0803057 | 0.0795110 | 0.0795110 | 0.0795110 | 0.0795110 | 0.0795110 | 0.0795110 | 0.0795110 | 0.0795110 |
| 145_2   | 4 | 1.1012852 | 0.9055567 | 0.3549535 | 0.2277125 | 0.1413542 | 0.1413542 | 0.1413542 | 0.1413542 | 0.1413542 | 0.1413542 | 0.1413542 | 0.1413542 | 0.1413542 | 0.1413542 | 0.1413542 |
| 261_2   | 4 | 1.3315930 | 1.1074123 | 0.4415088 | 0.2645940 | 0.1790112 | 0.1256742 | 0.0966282 | 0.0966282 | 0.0966282 | 0.0966282 | 0.0966282 | 0.0966282 | 0.0966282 | 0.0966282 | 0.0966282 |
| 286     | 4 | 1.2844337 | 1.1756981 | 0.4980371 | 0.2679888 | 0.1706605 | 0.1335403 | 0.1054751 | 0.1054751 | 0.1054751 | 0.1054751 | 0.1054751 | 0.1054751 | 0.1054751 | 0.1054751 | 0.1054751 |
| 46099   | 4 | 1.0523464 | 0.9022932 | 0.3131294 | 0.2550706 | 0.1620494 | 0.0960469 | 0.0760066 | 0.0760066 | 0.0760066 | 0.0760066 | 0.0760066 | 0.0760066 | 0.0760066 | 0.0760066 | 0.0760066 |
| 46142   | 4 | 1.1940151 | 1.1260218 | 0.3930051 | 0.2920068 | 0.2010025 | 0.1360037 | 0.1040008 | 0.1040008 | 0.1040008 | 0.1040008 | 0.1040008 | 0.1040008 | 0.1040008 | 0.1040008 | 0.1040008 |
| 47009   | 4 | 1.2088379 | 1.0747823 | 0.4535559 | 0.2421673 | 0.1651091 | 0.1221024 | 0.0900500 | 0.0900500 | 0.0900500 | 0.0900500 | 0.0900500 | 0.0900500 | 0.0900500 | 0.0900500 | 0.0900500 |
| 52791   | 4 | 1.2516633 | 1.1318308 | 0.4410907 | 0.2736604 | 0.1844587 | 0.1363672 | 0.0962549 | 0.0962549 | 0.0962549 | 0.0962549 | 0.0962549 | 0.0962549 | 0.0962549 | 0.0962549 | 0.0962549 |
| 138     | 5 | 1.2023082 | 1.0081731 | 0.2693566 | 0.2804015 | 0.1688579 | 0.1085587 | 0.1014938 | 0.1014938 | 0.1014938 | 0.1014938 | 0.1014938 | 0.1014938 | 0.1014938 | 0.1014938 | 0.1014938 |
| 145_4   | 5 | 1.2490100 | 1.0850074 | 0.3500014 | 0.2780018 | 0.1570032 | 0.1190000 | 0.0910055 | 0.0910055 | 0.0910055 | 0.0910055 | 0.0910055 | 0.0910055 | 0.0910055 | 0.0910055 | 0.0910055 |
| 427     | 5 | 1.2472570 | 1.1991635 | 0.4067087 | 0.2504496 | 0.1873233 | 0.1382317 | 0.1202040 | 0.1202040 | 0.1202040 | 0.1202040 | 0.1202040 | 0.1202040 | 0.1202040 | 0.1202040 | 0.1202040 |
| 52_1    | 5 | 1.2710004 | 1.0860018 | 0.3390000 | 0.2970000 | 0.1760028 | 0.1150000 | 0.0890000 | 0.0890000 | 0.0890000 | 0.0890000 | 0.0890000 | 0.0890000 | 0.0890000 | 0.0890000 | 0.0890000 |
| 151     | 6 | 1.2474270 | 1.0668032 | 0.2659116 | 0.2720607 | 0.1334541 | 0.1133578 | 0.1033925 | 0.1033925 | 0.1033925 | 0.1033925 | 0.1033925 | 0.1033925 | 0.1033925 | 0.1033925 | 0.1033925 |
| 156     | 6 | 1.3590059 | 1.2980035 | 0.3350015 | 0.2930000 | 0.1850027 | 0.1450000 | 0.1360000 | 0.1360000 | 0.1360000 | 0.1360000 | 0.1360000 | 0.1360000 | 0.1360000 | 0.1360000 | 0.1360000 |
| 159     | 6 | 1.2823884 | 1.4850199 | 0.4485287 | 0.3130000 | 0.1997248 | 0.1524729 | 0.1354474 | 0.1354474 | 0.1354474 | 0.1354474 | 0.1354474 | 0.1354474 | 0.1354474 | 0.1354474 | 0.1354474 |
| 22      | 6 | 1.2474270 | 1.0668032 | 0.2659116 | 0.2720607 | 0.1334541 | 0.1133578 | 0.1033925 | 0.1033925 | 0.1033925 | 0.1033925 | 0.1033925 | 0.1033925 | 0.1033925 | 0.1033925 | 0.1033925 |
| 261_1   | 6 | 1.3627480 | 1.3728693 | 0.3830992 | 0.3208987 | 0.2136001 | 0.1474110 | 0.1132828 | 0.1132828 | 0.1132828 | 0.1132828 | 0.1132828 | 0.1132828 | 0.1132828 | 0.1132828 | 0.1132828 |
| 313_3   | 6 | 1.2435578 | 1.1222237 | 0.2837781 | 0.2868449 | 0.1594522 | 0.1234058 | 0.1102905 | 0.1102905 | 0.1102905 | 0.1102905 | 0.1102905 | 0.1102905 | 0.1102905 | 0.1102905 | 0.1102905 |
| 338     | 6 | 1.4781353 | 1.4821218 | 0.3920319 | 0.3180252 | 0.2020099 | 0.1590283 | 0.1450138 | 0.1450138 | 0.1450138 | 0.1450138 | 0.1450138 | 0.1450138 | 0.1450138 | 0.1450138 | 0.1450138 |
| 46120   | 6 | 1.4230594 | 1.4360682 | 0.4160192 | 0.2990150 | 0.2030099 | 0.1590031 | 0.1410142 | 0.1410142 | 0.1410142 | 0.1410142 | 0.1410142 | 0.1410142 | 0.1410142 | 0.1410142 | 0.1410142 |
| 134     | 7 | 1.3770058 | 1.4020057 | 0.3130016 | 0.3030000 | 0.1900026 | 0.1590000 | 0.1350037 | 0.1350037 | 0.1350037 | 0.1350037 | 0.1350037 | 0.1350037 | 0.1350037 | 0.1350037 | 0.1350037 |
| 136     | 7 | 1.3985721 | 1.3575603 | 0.3141592 | 0.3180252 | 0.2020099 | 0.1430559 | 0.1380580 | 0.1380580 | 0.1380580 | 0.1380580 | 0.1380580 | 0.1380580 | 0.1380580 | 0.1380580 | 0.1380580 |
| 149     | 7 | 1.4791095 | 1.4941208 | 0.3770332 | 0.2870279 | 0.2020099 | 0.1490134 | 0.1410142 | 0.1410142 | 0.1410142 | 0.1410142 | 0.1410142 | 0.1410142 | 0.1410142 | 0.1410142 | 0.1410142 |
| 160     | 7 | 1.4593618 | 1.7288959 | 0.4690256 | 0.3036593 | 0.2125300 | 0.1630031 | 0.1430035 | 0.1430035 | 0.1430035 | 0.1430035 | 0.1430035 | 0.1430035 | 0.1430035 | 0.1430035 | 0.1430035 |
| 168     | 7 | 1.4764721 | 1.4948769 | 0.3673962 | 0.3090955 | 0.2077811 | 0.1616075 | 0.1410319 | 0.1410319 | 0.1410319 | 0.1410319 | 0.1410319 | 0.1410319 | 0.1410319 | 0.1410319 | 0.1410319 |
| 171     | 7 | 1.4390136 | 1.5394691 | 0.3931272 | 0.3101032 | 0.2010622 | 0.1550516 | 0.1410319 | 0.1410319 | 0.1410319 | 0.1410319 | 0.1410319 | 0.1410319 | 0.1410319 | 0.1410319 | 0.1410319 |
| 191     | 7 | 1.4990564 | 1.5150558 | 0.3990200 | 0.3000067 | 0.1970102 | 0.1630031 | 0.1430035 | 0.1430035 | 0.1430035 | 0.1430035 | 0.1430035 | 0.1430035 | 0.1430035 | 0.1430035 | 0.1430035 |
| 25      | 7 | 1.4699660 | 1.5712495 | 0.3216224 | 0.3051819 | 0.2304886 | 0.1883826 | 0.1527318 | 0.1527318 | 0.1527318 | 0.1527318 | 0.1527318 | 0.1527318 | 0.1527318 | 0.1527318 | 0.1527318 |
| 290     | 7 | 1.4461594 | 1.5953739 | 0.4106446 | 0.3054194 | 0.2153346 | 0.1702381 | 0.1492146 | 0.1492146 | 0.1492146 | 0.1492146 | 0.1492146 | 0.1492146 | 0.1492146 | 0.1492146 | 0.1492146 |
| 357     | 7 | 1.4140354 | 1.4390347 | 0.3450058 | 0.2870070 | 0.2040025 | 0.1620031 | 0.1300038 | 0.1300038 | 0.1300038 | 0.1300038 | 0.1300038 | 0.1300038 | 0.1300038 | 0.1300038 | 0.1300038 |
| 44572   | 7 | 1.4392724 | 1.5512711 | 0.4000782 | 0.3080584 | 0.2150372 | 0.1590283 | 0.1440139 | 0.1440139 | 0.1440139 | 0.1440139 | 0.1440139 | 0.1440139 | 0.1440139 | 0.1440139 | 0.1440139 |
| 46020_2 | 7 | 1.4030000 | 1.4170000 | 0.3740000 | 0.2750000 | 0.1930000 | 0.1600000 | 0.1330000 | 0.1330000 | 0.1330000 | 0.1330000 | 0.1330000 | 0.1330000 | 0.1330000 | 0.1330000 | 0.1330000 |
| 46131   | 7 | 1.5272213 | 1.6802333 | 0.4320567 | 0.3290547 | 0.2220203 | 0.1640274 | 0.1600281 | 0.1600281 | 0.1600281 | 0.1600281 | 0.1600281 | 0.1600281 | 0.1600281 | 0.1600281 | 0.1600281 |
| 46219   | 7 | 1.5340698 | 1.6804101 | 0.4308468 | 0.3076508 | 0.2364762 | 0.1735154 | 0.1543243 | 0.1543243 | 0.1543243 | 0.1543243 | 0.1543243 | 0.1543243 | 0.1543243 | 0.1543243 | 0.1543243 |
| 68      | 7 | 1.4843450 | 1.4323142 | 0.3050803 | 0.2980604 | 0.2000400 | 0.1530294 | 0.1390575 | 0.1390575 | 0.1390575 |           |           |           |           |           |           |



| id      | d | PTS1      | PTS2      | PTS3      | PTS4      | PTS5      | PTS6      | PTS7      | PTS8 | PTS9 | PTS10 | PTS11 | PTS12 |
|---------|---|-----------|-----------|-----------|-----------|-----------|-----------|-----------|------|------|-------|-------|-------|
| 157_2   | 0 | NA        | NA        | NA        | NA        | NA        | NA        | NA        | NA   | NA   | NA    | NA    | NA    |
| 44564   | 0 | NA        | NA        | NA        | NA        | NA        | NA        | NA        | NA   | NA   | NA    | NA    | NA    |
| 141_1   | 1 | 0.2080024 | NA        | NA        | NA        | NA        | NA        | NA        | NA   | NA   | NA    | NA    | NA    |
| 144     | 1 | 0.2240089 | NA        | NA        | NA        | NA        | NA        | NA        | NA   | NA   | NA    | NA    | NA    |
| 147     | 1 | 0.2281074 | NA        | NA        | NA        | NA        | NA        | NA        | NA   | NA   | NA    | NA    | NA    |
| 15274   | 1 | 0.1971243 | NA        | NA        | NA        | NA        | NA        | NA        | NA   | NA   | NA    | NA    | NA    |
| 312     | 1 | 0.1909476 | NA        | NA        | NA        | NA        | NA        | NA        | NA   | NA   | NA    | NA    | NA    |
| 46020   | 1 | 0.146     | NA        | NA        | NA        | NA        | NA        | NA        | NA   | NA   | NA    | NA    | NA    |
| 84      | 1 | 0.1730029 | NA        | NA        | NA        | NA        | NA        | NA        | NA   | NA   | NA    | NA    | NA    |
| 14751   | 2 | 0.2195837 | 0.3569482 | NA        | NA        | NA        | NA        | NA        | NA   | NA   | NA    | NA    | NA    |
| 21_1    | 2 | 0.2010398 | 0.3370729 | NA        | NA        | NA        | NA        | NA        | NA   | NA   | NA    | NA    | NA    |
| 27      | 2 | 0.1980909 | 0.3031099 | NA        | NA        | NA        | NA        | NA        | NA   | NA   | NA    | NA    | NA    |
| 135_1   | 3 | 0.2300782 | 0.3490951 | 0.4211228 | NA        | NA        | NA        | NA        | NA   | NA   | NA    | NA    | NA    |
| 140     | 3 | 0.2556345 | 0.4140895 | 0.5404106 | NA        | NA        | NA        | NA        | NA   | NA   | NA    | NA    | NA    |
| 15      | 3 | 0.2175891 | 0.3699177 | 0.4892575 | NA        | NA        | NA        | NA        | NA   | NA   | NA    | NA    | NA    |
| 387     | 3 | 0.2247221 | 0.3521151 | 0.4514378 | NA        | NA        | NA        | NA        | NA   | NA   | NA    | NA    | NA    |
| 389     | 3 | 0.250098  | 0.3721349 | 0.4511602 | NA        | NA        | NA        | NA        | NA   | NA   | NA    | NA    | NA    |
| 420     | 3 | 0.2232241 | 0.3793811 | 0.4805048 | NA        | NA        | NA        | NA        | NA   | NA   | NA    | NA    | NA    |
| 49645   | 3 | 0.2380189 | 0.3850325 | 0.5020496 | NA        | NA        | NA        | NA        | NA   | NA   | NA    | NA    | NA    |
| 78_1    | 3 | 0.192151  | 0.3128531 | 0.4065014 | NA        | NA        | NA        | NA        | NA   | NA   | NA    | NA    | NA    |
| 145_2   | 4 | 0.2277125 | 0.3690667 | 0.470309  | 0.5506147 | NA        | NA        | NA        | NA   | NA   | NA    | NA    | NA    |
| 261_2   | 4 | 0.264594  | 0.4436052 | 0.5692794 | 0.6659075 | NA        | NA        | NA        | NA   | NA   | NA    | NA    | NA    |
| 286     | 4 | 0.2679888 | 0.4386493 | 0.5721895 | 0.6776647 | NA        | NA        | NA        | NA   | NA   | NA    | NA    | NA    |
| 46099   | 4 | 0.2550706 | 0.41712   | 0.5131668 | 0.5891734 | NA        | NA        | NA        | NA   | NA   | NA    | NA    | NA    |
| 46142   | 4 | 0.2920068 | 0.4930093 | 0.6290013 | 0.7330178 | NA        | NA        | NA        | NA   | NA   | NA    | NA    | NA    |
| 47009   | 4 | 0.2421673 | 0.4072764 | 0.5293788 | 0.6194288 | NA        | NA        | NA        | NA   | NA   | NA    | NA    | NA    |
| 52791   | 4 | 0.2736604 | 0.458119  | 0.5944862 | 0.6907411 | NA        | NA        | NA        | NA   | NA   | NA    | NA    | NA    |
| 138     | 5 | 0.2804015 | 0.4492594 | 0.5578182 | 0.659312  | 0.738823  | NA        | NA        | NA   | NA   | NA    | NA    | NA    |
| 145_4   | 5 | 0.2780018 | 0.435005  | 0.554005  | 0.6450105 | 0.7350105 | NA        | NA        | NA   | NA   | NA    | NA    | NA    |
| 427     | 5 | 0.2504496 | 0.4377728 | 0.5760045 | 0.6962085 | 0.7924634 | NA        | NA        | NA   | NA   | NA    | NA    | NA    |
| 52_1    | 5 | 0.297     | 0.4730028 | 0.5880028 | 0.6770028 | 0.74701   | NA        | NA        | NA   | NA   | NA    | NA    | NA    |
| 151     | 6 | 0.2704533 | 0.4776247 | 0.6355424 | 0.7661908 | 0.8697765 | 0.945202  | NA        | NA   | NA   | NA    | NA    | NA    |
| 156     | 6 | 0.293     | 0.4780027 | 0.6230027 | 0.7590027 | 0.8670073 | 0.9630073 | NA        | NA   | NA   | NA    | NA    | NA    |
| 159     | 6 | 0.313     | 0.5127248 | 0.6651978 | 0.8006452 | 0.9371736 | 1.0364963 | NA        | NA   | NA   | NA    | NA    | NA    |
| 22      | 6 | 0.2720607 | 0.4055148 | 0.5188726 | 0.6222651 | 0.7146122 | 0.8008966 | NA        | NA   | NA   | NA    | NA    | NA    |
| 261_1   | 6 | 0.3208987 | 0.5344988 | 0.6819098 | 0.7951927 | 0.8975059 | 0.9897718 | NA        | NA   | NA   | NA    | NA    | NA    |
| 313_3   | 6 | 0.2868449 | 0.4462971 | 0.5697029 | 0.6799935 | 0.7672746 | 0.8384504 | NA        | NA   | NA   | NA    | NA    | NA    |
| 338     | 6 | 0.3180252 | 0.5200351 | 0.6790634 | 0.8240771 | 0.9660807 | 1.0900968 | NA        | NA   | NA   | NA    | NA    | NA    |
| 46120   | 6 | 0.299015  | 0.5020249 | 0.6610228 | 0.8020422 | 0.9150467 | 1.0200514 | NA        | NA   | NA   | NA    | NA    | NA    |
| 134     | 7 | 0.303     | 0.4930026 | 0.6520026 | 0.7870063 | 0.9010063 | 1.0060111 | 1.0890111 | NA   | NA   | NA    | NA    | NA    |
| 136     | 7 | 0.250098  | 0.4471893 | 0.5902453 | 0.7283032 | 0.8393438 | 0.9393638 | 1.043407  | NA   | NA   | NA    | NA    | NA    |
| 149     | 7 | 0.2870279 | 0.4890378 | 0.6380512 | 0.7790654 | 0.9060693 | 1.0210867 | 1.1170919 | NA   | NA   | NA    | NA    | NA    |
| 160     | 7 | 0.3036593 | 0.5161893 | 0.7106244 | 0.8739309 | 1.0112954 | 1.1375491 | 1.2598806 | NA   | NA   | NA    | NA    | NA    |
| 168     | 7 | 0.3090955 | 0.5168766 | 0.6784841 | 0.8180012 | 0.9343498 | 1.0377422 | 1.1310857 | NA   | NA   | NA    | NA    | NA    |
| 171     | 7 | 0.3101032 | 0.5111654 | 0.666217  | 0.8072489 | 0.9322849 | 1.0413262 | 1.1463452 | NA   | NA   | NA    | NA    | NA    |
| 191     | 7 | 0.3000667 | 0.4970168 | 0.6600199 | 0.8030234 | 0.9350385 | 1.0340436 | 1.1160436 | NA   | NA   | NA    | NA    | NA    |
| 25      | 7 | 0.3518196 | 0.5823082 | 0.7706908 | 0.922957  | 1.0502755 | 1.1544484 | 1.2496377 | NA   | NA   | NA    | NA    | NA    |
| 290     | 7 | 0.3054194 | 0.520754  | 0.6909921 | 0.8402067 | 0.9784384 | 1.0996407 | 1.1847348 | NA   | NA   | NA    | NA    | NA    |
| 357     | 7 | 0.287007  | 0.4910094 | 0.6530125 | 0.7830164 | 0.9070204 | 1.0120251 | 1.0940312 | NA   | NA   | NA    | NA    | NA    |
| 44572   | 7 | 0.3080584 | 0.5230956 | 0.6821239 | 0.8261378 | 0.9461753 | 1.0561935 | 1.1421993 | NA   | NA   | NA    | NA    | NA    |
| 46020_2 | 7 | 0.275     | 0.468     | 0.628     | 0.761     | 0.874     | 0.97      | 1.043     | NA   | NA   | NA    | NA    | NA    |
| 46131   | 7 | 0.3290547 | 0.551075  | 0.7151024 | 0.8751444 | 1.0191444 | 1.1421607 | 1.2481795 | NA   | NA   | NA    | NA    | NA    |
| 46219   | 7 | 0.3076508 | 0.544127  | 0.7164784 | 0.8677463 | 1.0220707 | 1.1493224 | 1.2495671 | NA   | NA   | NA    | NA    | NA    |
| 68      | 7 | 0.2980604 | 0.4981004 | 0.6511298 | 0.7901873 | 0.9233024 | 1.0382415 | 1.1272471 | NA   | NA   | NA    | NA    | NA    |
| 76      | 7 | 0.3020811 | 0.5161652 | 0.6721941 | 0.8042546 | 0.9252712 | 1.0343125 | 1.1263342 | NA   | NA   | NA    | NA    | NA    |

|       |    |           |           |           |           |           |            |           |           |           |           |           |           |
|-------|----|-----------|-----------|-----------|-----------|-----------|------------|-----------|-----------|-----------|-----------|-----------|-----------|
| 126   | 8  | 0.3491733 | 0.6102672 | 0.806359  | 1.0014513 | 1.1835199 | 1.3405995  | 1.4796571 | 1.5956959 | NA        | NA        | NA        | NA        |
| 14    | 8  | 0.3054194 | 0.5157073 | 0.689944  | 0.8422048 | 0.9773861 | 1.0995868  | 1.2187925 | 1.3219671 | NA        | NA        | NA        | NA        |
| 142   | 8  | 0.3300242 | 0.5650434 | 0.7420547 | 0.9140663 | 1.0700791 | 1.2060938  | 1.3320978 | 1.4411162 | NA        | NA        | NA        | NA        |
| 15472 | 8  | 0.3040066 | 0.5340153 | 0.7080268 | 0.850301  | 0.9920338 | 1.1140379  | 1.2190427 | 1.3030486 | NA        | NA        | NA        | NA        |
| 165   | 8  | 0.3160142 | 0.556033  | 0.7320358 | 0.8990478 | 1.051061  | 1.1710651  | 1.2700702 | 1.3480766 | NA        | NA        | NA        | NA        |
| 178   | 8  | 0.3412477 | 0.5894492 | 0.7846133 | 0.9757415 | 1.1388917 | 1.2849773  | 1.4090781 | 1.5161528 | NA        | NA        | NA        | NA        |
| 337   | 8  | 0.3340733 | 0.5971038 | 0.791145  | 0.9731889 | 1.1372164 | 1.2872464  | 1.4042635 | 1.5042835 | NA        | NA        | NA        | NA        |
| 363   | 8  | 0.363435  | 0.6352088 | 0.8384033 | 1.0125555 | 1.1806329 | 1.3095088  | 1.4232541 | 1.5228634 | NA        | NA        | NA        | NA        |
| 44052 | 8  | 0.3540692 | 0.6191371 | 0.8231763 | 1.0052224 | 1.1692477 | 1.3332965  | 1.4833098 | 1.5993486 | NA        | NA        | NA        | NA        |
| 44424 | 8  | 0.3410718 | 0.6151375 | 0.8281962 | 1.0002224 | 1.1542743 | 1.2863084  | 1.4003479 | 1.4943532 | NA        | NA        | NA        | NA        |
| 46093 | 8  | 0.2610306 | 0.4830667 | 0.677077  | 0.8431041 | 0.9901177 | 1.1141338  | 1.2151388 | 1.3101598 | NA        | NA        | NA        | NA        |
| 155   | 9  | 0.3494639 | 0.6147826 | 0.8250205 | 1.0092921 | 1.1945108 | 1.3637503  | 1.504924  | 1.6210317 | 1.7291982 | NA        | NA        | NA        |
| 1544  | 9  | 0.4114863 | 0.7277963 | 1.0011057 | 1.2333663 | 1.4505966 | 1.648801   | 1.8229848 | 1.9651573 | 2.0903012 | NA        | NA        | NA        |
| 162   | 9  | 0.3301833 | 0.5963355 | 0.8124489 | 1.0015441 | 1.1906393 | 1.343721   | 1.4988016 | 1.6188683 | 1.7219119 | NA        | NA        | NA        |
| 174   | 9  | 0.3390236 | 0.6030406 | 0.8090504 | 1.0040734 | 1.1840762 | 1.3300899  | 1.4711041 | 1.5971081 | 1.7111124 | NA        | NA        | NA        |
| 177   | 9  | 0.3301227 | 0.5862184 | 0.8013021 | 0.9833708 | 1.147447  | 1.302476   | 1.4245416 | 1.5405803 | 1.6465992 | NA        | NA        | NA        |
| 185   | 9  | 0.3260552 | 0.563089  | 0.749132  | 0.9231578 | 1.0851856 | 1.2322162  | 1.3632315 | 1.4592523 | 1.5502578 | NA        | NA        | NA        |
| 50298 | 9  | 0.3391194 | 0.6232057 | 0.8322655 | 1.0193083 | 1.1863562 | 1.3314113  | 1.4644452 | 1.5814836 | 1.6895253 | NA        | NA        | NA        |
| 111   | 10 | 0.3180566 | 0.5880862 | 0.8071068 | 1.009129  | 1.1931535 | 1.336185   | 1.4701999 | 1.5882168 | 1.6902217 | 1.7602503 | NA        | NA        |
| 167   | 10 | 0.3270749 | 0.5811241 | 0.7861631 | 0.9802044 | 1.1522305 | 1.3162793  | 1.4713083 | 1.6033424 | 1.7133606 | 1.8103812 | NA        | NA        |
| 186   | 10 | 0.348023  | 0.6270517 | 0.8320614 | 1.0280716 | 1.2030973 | 1.3791087  | 1.5211228 | 1.6471267 | 1.7591446 | 1.8491446 | NA        | NA        |
| 356   | 10 | 0.308365  | 0.5416246 | 0.7258445 | 0.9030252 | 1.0531885 | 1.1923646  | 1.3205052 | 1.4396563 | 1.5457742 | 1.6308683 | NA        | NA        |
| 424   | 10 | 0.3420936 | 0.595143  | 0.8122006 | 1.0022427 | 1.1782682 | 1.3383182  | 1.4683528 | 1.5733719 | 1.6673931 | 1.7424198 | NA        | NA        |
| 425   | 10 | 0.3660123 | 0.6380141 | 0.8490165 | 1.0410191 | 1.2090221 | 1.3740251  | 1.5160286 | 1.6490286 | 1.7570333 | 1.8540384 | NA        | NA        |
| 44526 | 10 | 0.3404761 | 0.6107889 | 0.8571322 | 1.070416  | 1.2566846 | 1.44419034 | 1.5961111 | 1.7413316 | 1.8725185 | 1.9776375 | NA        | NA        |
| 141_2 | 11 | 0.3500914 | 0.6141388 | 0.8552134 | 1.0822685 | 1.2773095 | 1.4663518  | 1.6323789 | 1.77741   | 1.9124433 | 2.0264828 | 2.1215038 | NA        |
| 164   | 11 | 0.3523195 | 0.6235426 | 0.8366928 | 1.0428893 | 1.2460469 | 1.4181893  | 1.5663108 | 1.7024027 | 1.8285455 | 1.9396175 | 2.0236711 | NA        |
| 166   | 11 | 0.3580126 | 0.6470195 | 0.8400055 | 1.043008  | 1.2500008 | 1.4300108  | 1.5910139 | 1.7400139 | 1.8700139 | 1.9760186 | 2.0460578 | NA        |
| 176   | 11 | 0.3880206 | 0.7130268 | 0.9630348 | 1.1960434 | 1.4070528 | 1.5970555  | 1.7580679 | 1.8940716 | 2.038075  | 2.1510795 | 2.2530844 | NA        |
| 214   | 11 | 0.3631666 | 0.6483087 | 0.8924398 | 1.1165492 | 1.3106419 | 1.5257558  | 1.6978285 | 1.8459129 | 1.9899685 | 2.1150325 | 2.245094  | NA        |
| 423   | 11 | 0.4360183 | 0.7440248 | 0.9910329 | 1.2070422 | 1.4000526 | 1.5760554  | 1.7300586 | 1.8710622 | 1.9980661 | 2.1040708 | 2.1960763 | NA        |
| 43991 | 11 | 0.3980113 | 0.7100177 | 0.9590257 | 1.1930279 | 1.4170301 | 1.6030409  | 1.7670439 | 1.9140473 | 2.051051  | 2.1710551 | 2.2700551 | NA        |
| 44637 | 11 | 0.398664  | 0.7251606 | 0.9855929 | 1.2029245 | 1.4172606 | 1.6305984  | 1.8068823 | 1.9521613 | 2.0893947 | 2.2285708 | 2.3317454 | NA        |
| 45956 | 11 | 0.4080784 | 0.73218   | 0.9742298 | 1.218281  | 1.4423614 | 1.6224058  | 1.8094486 | 1.9634778 | 2.0824946 | 2.1865379 | 2.275434  | NA        |
| 46071 | 11 | 0.3880464 | 0.6860883 | 0.9321209 | 1.1531412 | 1.3661788 | 1.561189   | 1.7512127 | 1.9152401 | 2.0592714 | 2.1882869 | 2.2872919 | NA        |
| 46107 | 11 | 0.3530057 | 0.6210131 | 0.8420222 | 1.0470246 | 1.2440348 | 1.4170377  | 1.5790407 | 1.7210443 | 1.8380485 | 1.9580485 | 2.0510539 | NA        |
| 48253 | 11 | 0.3650342 | 0.6830594 | 0.9610882 | 1.2111062 | 1.4361262 | 1.6431479  | 1.8501576 | 2.0221837 | 2.1871959 | 2.3422088 | 2.4582131 | NA        |
| 49684 | 11 | 0.3530127 | 0.6110147 | 0.8150245 | 0.9980272 | 1.1630303 | 1.3140435  | 1.4450435 | 1.5650477 | 1.6560532 | 1.7380593 | 1.8130593 | NA        |
| 53    | 11 | 0.3700216 | 0.6460506 | 0.8720705 | 1.0770925 | 1.2641032 | 1.4491275  | 1.6161395 | 1.7531541 | 1.880158  | 1.9881765 | 2.0781821 | NA        |
| 335   | 11 | 0.3553168 | 0.6836596 | 0.9018453 | 1.0890163 | 1.2622012 | 1.446375   | 1.6075271 | 1.7336699 | 1.863766  | 1.9787756 | 2.0589311 | NA        |
| 402   | 12 | 0.3900462 | 0.6790758 | 0.9030939 | 1.091158  | 1.2961265 | 1.4681381  | 1.6311504 | 1.7631655 | 1.8721839 | 1.9801885 | 2.0752095 | 2.1682149 |
| 46063 | 12 | 0.4030447 | 0.7178859 | 0.9665383 | 1.198163  | 1.3966573 | 1.6061949  | 1.7796826 | 1.9400603 | 2.0924578 | 2.228825  | 2.3391155 | 2.4313814 |
| 46107 | 12 | 0.3600222 | 0.6540375 | 0.8740466 | 1.1010664 | 1.310076  | 1.4940869  | 1.659099  | 1.8261209 | 1.9621167 | 2.0821209 | 2.1851257 | 2.2531331 |
| 46063 | 12 | 0.3921543 | 0.7032845 | 0.9614085 | 1.2004838 | 1.442585  | 1.6487039  | 1.8457674 | 2.0158732 | 2.1659265 | 2.293989  | 2.4000079 | 2.5050841 |
| 49643 | 12 | 0.3790211 | 0.688047  | 0.9400649 | 1.1630738 | 1.3740951 | 1.5811048  | 1.7641157 | 1.9191286 | 2.069142  | 2.2021457 | 2.3161633 | 2.4071633 |
| 73    | 12 | 0.4001512 | 0.6852635 | 0.9263651 | 1.1354249 | 1.3485399 | 1.5386057  | 1.7126775 | 1.8677291 | 1.9867963 | 2.1158312 | 2.2138771 | 2.2959015 |
| 88    | 12 | 0.3670123 | 0.6570123 | 0.91502   | 1.1540221 | 1.3850243 | 1.5910243  | 1.7800243 | 1.9590243 | 2.1190243 | 2.2590243 | 2.3830283 | 2.5070323 |

## 10.4 Supplementary material for Chapter 7

### 10.4.1 Supplementary Tables / Figures

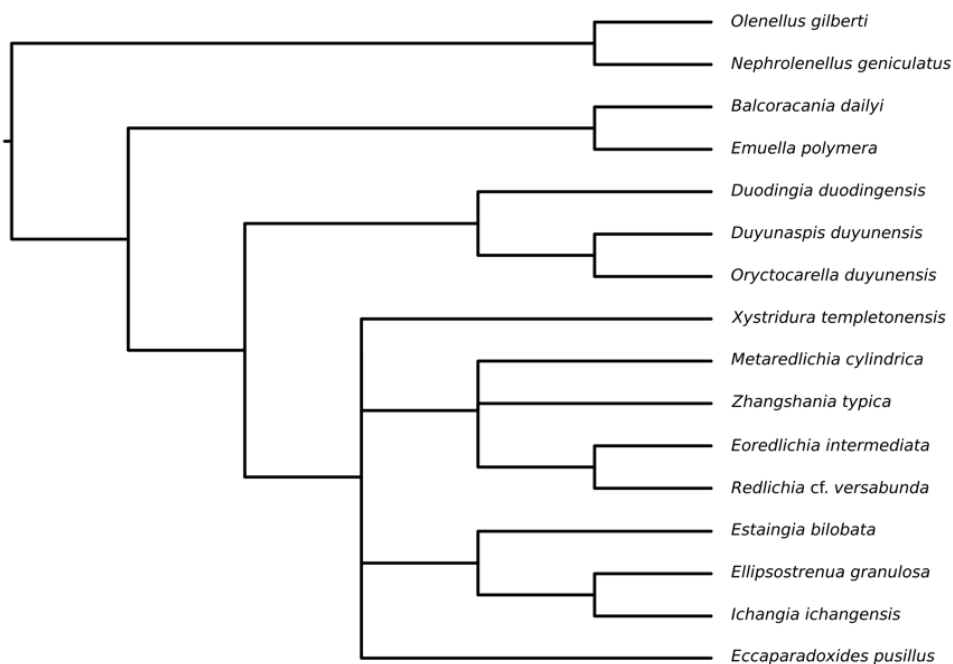


**Figure 10.3:** Strict consensus tree based on two most parsimonious trees obtained after removing ontogenetic characters from the analysis.

**Table 10.4:** Taxa included in the phylogenetic analysis and references used to obtain character information.

| Species                           | Family            | Reference(s)  |
|-----------------------------------|-------------------|---|
| <b>Order Redlichiida</b>          |                   |   |
| <i>Balcoracania dailyi</i>        | Emuellidae        | Paterson <i>et al.</i> (2019) and references therein                              |
| <i>Eccaparadoxides pusillus</i>   | Paradoxididae     | Paterson <i>et al.</i> (2019) and references therein                              |
| <i>Ellipsostrenua granulosa</i> * | Ellipsocephalidae | Ahlberg (1983); Laibl <i>et al.</i> (2018)  |
| <i>Emuella polymera</i>           | Emuellidae        | Paterson <i>et al.</i> (2019) and references therein                              |
| <i>Eoredlichia intermediata</i>   | Redlichiidae      | Paterson <i>et al.</i> (2019) and references therein                              |
| <i>Estaingia bilobata</i>         | Estaingiidae      | Holmes <i>et al.</i> (2020); Paterson <i>et al.</i> (2019) and references therein |
| <i>Ichangia ichangensis</i>       | Estaingiidae      | Paterson <i>et al.</i> (2019) and references therein                              |
| <i>Metaredlichia cylindrica</i> * | Redlichiidae      | Dai & Zhang (2012); Zhang <i>et al.</i> (1980)                                    |
| <i>Nephrolenellus geniculatus</i> | Biceratopsidae    | Paterson <i>et al.</i> (2019) and references therein                              |
| <i>Olenellus gilberti</i>         | Olenellidae       | Paterson <i>et al.</i> (2019) and references therein                              |
| <i>Redlichia cf. versabunda</i> * | Redlichiidae      | Holmes <i>et al.</i> in review  |
| <i>Xystridura templetonensis</i>  | Xystriduridae     | Paterson <i>et al.</i> (2019) and references therein                              |
| <i>Zhangshania typica</i>         | Gigantopygidae    | Paterson <i>et al.</i> (2019) and references therein                              |
| <b>Order Corynexochida</b>        |                   |   |
| <i>Duodingia duodingensis</i> *   | Oryctocephalidae  | Hou <i>et al.</i> (2015); Zhang <i>et al.</i> (1980)                              |
| <i>Duyunaspis duyunensis</i> *    | Oryctocephalidae  | Dai <i>et al.</i> (2017); Lei (2016); McNamara <i>et al.</i> (2006)               |
| <i>Oryctocarella duyunensis</i> * | Oryctocephalidae  | Du <i>et al.</i> (2020) <sup>^</sup> ; McNamara <i>et al.</i> (2003) <sup>^</sup> |

\*new taxa not included in the analyses of Paterson *et al.* (2019)

<sup>^</sup>these authors referred to this taxon as *Arthricocephalus chauveaui*



#### 10.4.2 List of characters used in the phylogenetic analysis

Numbers in brackets refer to the corresponding character of Paterson *et al.* (2019). An asterisk (\*) indicates that the character has been modified and/or character states removed/added. Characters 49–53 (in *italics*) are new characters.

##### **1. Dorsal ecdysial cephalic sutures (1):**

- 0. absent
- 1. present

##### **2. Dorsal ecdysial suture pattern (2\*):**

[Taxa coded as state 0 for character 1 are coded as inapplicable for this character]

- 0. opisthoparian
- 1. gonatoparian

##### **3. Opisthoparian suture pattern (3\*):**

[Taxa coded as state 1 (or inapplicable) for character 2 are coded as inapplicable for this character.]

- 0. gamma to alpha points long, straight or slightly curved, and divergent anteriorly; epsilon to omega points long and strongly divergent (defining narrow (exsag.) posterolateral projections)
- 1. gamma to beta points divergent anteriorly or subparallel, but with slight adaxial bend at beta points, with very short section between converging beta and alpha points; epsilon to omega points very short
- 2. gamma to alpha points straight, and subparallel or convergent anteriorly; epsilon to omega points very long and moderately to strongly divergent

##### **4. Preoccipital glabellar shape in holaspides (5\*):**

- 0. tapers anteriorly with narrow frontal lobe
- 1. subparallel/subquadrate, with gently rounded or truncated frontal lobe
- 2. subparallel, with strongly rounded frontal lobe
- 3. constricted at L1, L2 or L3 with enlarged frontal lobe

##### **5. SO (6\*):**

- 0. deepened laterally and shallow medially
- 1. subequal depth across glabella

**6. S1 (7\*):**

- 0. confined laterally and connected to axial furrow
- 1. transglabellar
- 2. isolated pits connected by medial furrow

**7. Shape of transglabellar S1 (8):**

[taxa coded as 0 or 2 for Character 6 are coded as inapplicable for this character]

- 0. straight or weakly convex
- 1. strongly convex posteriorly

**8. S2 (10\*):**

- 0. confined laterally
- 1. transglabellar
- 2. isolated pits connected by medial furrow

**9. Shape of laterally confined S2 (11\*):**

[taxa coded as 1 or 2 for Character 8 are coded as inapplicable for this character]

- 0. directed forwards abaxially
- 1. transverse

**10. S3 (14\*):**

- 0. confined laterally
- 1. transglabellar
- 2. isolated pits connected by medial furrow

**11. Shape of laterally confined S3 (15):**

[taxa coded as 1 or 2 for Character 10 are coded as inapplicable for this character]

- 0. straight or weakly convex
- 1. strongly convex anteriorly
- 2. isolated slots

**12. Orientation of laterally confined S3 (16):**

[taxa coded as 1 or 2 for Character 10 are coded as inapplicable for this character]

- 0. directed forwards abaxially
- 1. directed backwards abaxially
- 2. transverse

**13. Preglabellar field (30):**

- 0. absent
- 1. present

**14. Plectrum on dorsal surface (31):**

[taxa coded as 0 for Character 13 are coded as inapplicable for this character]

- 0. absent
- 1. present

**15. Shape of plectrum (32\*):**

[taxa coded as 0 for Character 13 are coded as inapplicable for this character]

- 0. very narrow (tr.), subparallel-sided ridge
- 1. broad (width >50% that of frontal glabellar lobe), subparallel-sided ridge

**16. Confluence of palpebro-ocular ridges (or palpebral lobe) and glabella (43):**

- 0. interrupted by axial furrow
- 1. strongly confluent

**17. Parafrontal band (44):**

- 0. absent
- 1. present

**18. Position of posterior tips of palpebral lobe or palpebro-ocular ridge (45\*):**

- 0. opposite LO or SO
- 1. opposite L1 or S1
- 2. opposite L2 or S2

**19. Fossulae (46):**

- 0. absent
- 1. present as small, discrete pits

**20. Width (tr.) of interocular area adjacent to posterior tip of palpebro-ocular ridge or palpebral lobe in holaspides (47):**

- 0. less than one-third the width (tr.) of the occipital ring
- 1. one-third to half the width (tr.) of the occipital ring
- 2. more than half to the entire width (tr.) of the occipital ring
- 3. more than the entire width (tr.) of the occipital ring

**21. Intergenal ridge (50):**

- 0. absent
- 1. present

**22. Genal spine (54):**

- 0. absent
- 1. present

**23. Hypostomal attachment (62):**

- 0. natant
- 1. conterminant

**24. Hypostome fused to cephalic doublure in holaspides (63):**

[taxa coded as 0 for Character 23 are coded as inapplicable for this character]

- 0. absent (= functional hypostomal suture)
- 1. present (= hypostome fused to rostral plate)

**25. Maculae (65):**

- 0. absent (or poorly developed)
- 1. present

**26. Tagmosis of thorax (69):**

- 0. pro- and opisthothorax undifferentiated
- 1. pro- and opisthothorax differentiated

**27. Prothoracic/opisthothoracic boundary marked by macropleural segment (70):**

[taxa coded as 0 for Character 26 are coded as inapplicable for this character]

- 0. absent (or decoupled when macropleural segment present)
- 1. present

**28. Macropleural thoracic spine(s) (71):**

- 0. absent
- 1. present

**29. Position of macropleural thoracic spine(s) developed on (72\*):**

[taxa coded as 0 for Character 28 are coded as inapplicable for this character]

- 0. third segment
- 1. sixth segment

**30. Inner portion of pleura on segment bearing macropleural thoracic spine(s) (73\*):**

[taxa coded as 0 for Character 28 are coded as inapplicable for this character]

- 0. strongly expands abaxially, distorting adjacent posterior segment(s) (= macropleural *sensu* Palmer 1998)
- 1. strongly expands abaxially, distorting adjacent anterior and posterior segments (= hyperpleural *sensu* Palmer 1998)

**31. Thoracic segments 5 and 6 fused (75):**

- 0. free
- 1. fused

**32. Hypertrophied thoracic axial spine(s), relative to other spines (76\*):**

[modified from Paterson et al.'s character 76]

- 0. absent
- 1. present on T9
- 2. present on T15

**33. Fulcrum on thoracic pleurae (77):**

- 0. absent
- 1. present

**34. Thoracic pleural tips (78\*):**

- 0. falcate/sentate spines (pleural margins continuous onto spines)
- 1. "thorn-like" spines (base of spine much narrower (exsag.) than pleural region)
- 2. spatulate (non-spinose)
- 3. bispinose

**35. Length of pleural spines along thorax (excluding macropleural spines) (79):**

- 0. of equal length or slightly increasing or decreasing posteriorly
- 1. strongly increasing posteriorly

**36. Differentiation of pygidial pleurae in late holaspides (80\*):**

0. anteriormost pleural segment resembles unreleased thoracic segment in similar orientation and expression of pleural and interpleural furrows and distal tips, such that the thoracic-pygidial boundary is indistinct
1. anteriormost pleura (or pleural region) differs from thoracic pleural morphology in the orientation and/or expression of pleural and interpleural furrows and distal tips

**37. Pygidial pleural furrows (81):**

0. well impressed from axial furrow to pygidial margin
1. well impressed near axial furrow, but become shallower or effaced near pygidial margin, including termination at border furrow
2. weakly developed or effaced

**38. Bilobate pygidial terminal piece (82):**

0. absent
1. present

**39. Posteromedial margin of pygidium immediately behind axis (in dorsal view) (86\*):**

0. smooth (non-spinose), continuously rounded
1. smooth (non-spinose) with shallow, rounded concavity
2. concave and bounded by pair of posterolateral marginal spines

**40. Paired marginal pygidial spines in late holaspides (87):**

0. absent
1. present

**41. Marginal pygidial spine morphology in late holaspides (88\*):**

[taxa coded as 0 for Character 40 are coded as inapplicable for this character]

0. single pair of short, anterolateral spines
1. single pair of short, posterolateral spines
2. two or more pairs of similar spines only
3. single pair of long spines that are decoupled from pleural segmentation, with outer edge of spine extending from anterolateral margin of pygidium

**42. Calcified protaspid stage (91):**

0. absent
1. present

**43. Anterior cranial/cephalic border in protaspides and/or early meraspides (92):**

- 0. absent
- 1. present

**44. Longitudinal medial glabellar furrow in protaspides (95):**

- 0. absent
- 1. present

**45. Transverse furrows on interocular cheeks in protaspides and/or early meraspides (97):**

- 0. absent
- 1. present

**46. Immature hypostome with inflated anterior lobe of middle body and spinose "frill" with five or six spine pairs on posterior margin (103\*):**

- 0. absent
- 1. present

**47. Thoracic macropleurality in meraspides (104):**

- 0. absent
- 1. present

**48. Development of thoracic macropleurality from meraspides to holaspides (105\*):**

[taxa coded as 0 for Character 47 are coded as inapplicable for this character]

- 0. macropleural segment/s retained in late holaspides
- 1. macropleural segment/s lost in late holaspides
- 2. macropleural segment/s occasionally retained in late holaspides

**49. *Macropleurae on first and second thoracic segments in early meraspides:***

[taxa coded as 0 for Character 47 are coded as inapplicable for this character]

- 0. absent
- 1. present

**50. *Number of pairs of fixigenal spines in protaspides:***

- 0. two
- 1. more than two
- 2. less than two

**51. Pattern of pygidial segmentation during meraspid period:**

0. pygidium retains a small, constant number of segments throughout meraspid period
1. pygidium progresses through accumulation and depletion phases
2. pygidium has initial accumulation phase and then similar number through to holaspid period

**52. High amount of intraspecific variation in pygidium segment number within meraspid degrees:**

0. absent
1. present

**53. Development of glabella across ontogeny:**

0. retracts and then extends across meraspid period
1. retracts in meraspides and remains retracted
2. retracts slightly in holaspides or does not retract

10.4.3 References

- Ahlberg, P.** 1983. A Lower Cambrian trilobite fauna from Jämtland, central Scandinavian Caledonides. *Gff*, **105**: 349–361.
- Dai, T. & Zhang, X.** 2012. Ontogeny of the redlichiid trilobite *Metaredlichia cylindrica* from the lower Cambrian (Stage 3) of South China. *Journal of Paleontology*, **86**: 646–651.
- Dai, T., Zhang, X.-L., Peng, S.-C. & Yao, X.-Y.** 2017. Intraspecific variation of trunk segmentation in the oryctocephalid trilobite *Duyunaspis duyunensis* from the Cambrian (Stage 4, Series 2) of South China. *Lethaia*, **50**: 527–539.
- Du, G.-Y., Peng, J., Wang, D.-Z., Wen, R.-Q. & Liu, S.** 2020. Morphology and trunk development of the trilobite *Arthrocephalus chauveaui* from the Cambrian Series 2 of Guizhou, South China. *Historical Biology*, **32**: 174–186.
- Holmes, J.D., Paterson, J.R. & García-Bellido, D.C.** 2020. The post-embryonic ontogeny of the early Cambrian trilobite *Estaingia bilobata* from South Australia: trunk development and phylogenetic implications. *Papers in Palaeontology*: doi:10.1002/spp2.1323.
- Holmes, J.D., Paterson, J.R., Jago, J.B. & García-Bellido, D.** *in review*. Ontogeny of the trilobite *Redlichia* from the lower Cambrian (Series 2, Stage 4) Ramsay Limestone of South Australia. *Geological Magazine*.



- Hou, J.-B., Hughes, N.C., Lan, T., Yang, J. & Zhang, X.-G.** 2015. Early postembryonic to mature ontogeny of the oryctocephalid trilobite *Duodingia duodingensis* from the lower Cambrian (Series 2) of southern China. *Papers in Palaeontology*, **1**: 497–513.
- Laibl, L., Cederström, P. & Ahlberg, P.** 2018. Early post-embryonic development in *Ellipsostrenua* (Trilobita, Cambrian, Sweden) and the developmental patterns in Ellipsocephaloidea. *Journal of Paleontology*, **92**: 1018–1027.
- Lei, Q.** 2016. New ontogenetic information on *Duyunaspis duyunensis* Zhang & Qian in Zhou et al., 1977 (Trilobita, Corynexochida) from the Cambrian and its possible sexual dimorphism. *Alcheringa*, **40**: 12–23.
- McNamara, K.J., Feng, Y. & Zhou, Z.** 2003. Ontogeny and heterochrony in the oryctocephalid trilobite *Arthricocephalus* from the early Cambrian of China. *Special Papers in Palaeontology*, **70**: 103–126.
- McNamara, K.J., Feng, Y. & Zhou, Z.** 2006. Ontogeny and heterochrony in the early Cambrian oryctocephalid trilobites *Changaspis*, *Duyunaspis* and *Balangia* from China. *Palaeontology*, **49**: 1–19.
- Palmer, A.R.** 1998. Terminal early Cambrian extinction of the Olenellina: documentation from the Pioche Formation, Nevada. *Journal of Paleontology*, **72**: 650–672.
- Paterson, J.R., Edgecombe, G.D. & Lee, M.S.Y.** 2019. Trilobite evolutionary rates constrain the duration of the Cambrian explosion. *Proceedings of the National Academy of Sciences of the USA*, **116**: 4394–4399.
- Zhang, W.-T., Lu, Y.-H., Zhu, Z.-L., Qian, Y.-Y., Lin, H.-L., Zhao, Z.-Y., Zhang, S.-G. & Yuan, J.-L.** 1980. Cambrian trilobite faunas of southwestern China. *Palaeontologia Sinica, new series B (no.16)*, **159**: 1–497 (in Chinese with English summary).

#### 10.4.4 Phylogenetic character matrix

|                            | 1 | 2 | 3 | 4 | 5   | 6   | 7 | 8 | 9 | 10 | 11 | 12 | 13 | 14 | 15 | 16 | 17 | 18 | 19 | 20  | 21 | 22 | 23 | 24 |
|----------------------------|---|---|---|---|-----|-----|---|---|---|----|----|----|----|----|----|----|----|----|----|-----|----|----|----|----|
| Balcoracania_dailyi        | 1 | 0 | 1 | 3 | 1   | 1   | 0 | 1 | - | 1  | -  | -  | 1  | 1  | 1  | 1  | 1  | 1  | 1  | 2   | 0  | 1  | 1  | 0  |
| Eccaparadoxides_pusillus   | 1 | 0 | 1 | 3 | 0/1 | 1   | 1 | 1 | - | 0  | 0  | 2  | 0  | -  | -  | 0  | 0  | 0  | 0  | 2   | 0  | 1  | 1  | 0  |
| Emuella_polymera           | 1 | 0 | 1 | 3 | 1   | 1   | 0 | 1 | - | 1  | -  | -  | 0  | -  | -  | 1  | 1  | 1  | 1  | 2   | 0  | 1  | 1  | 0  |
| Eoredlichia_intermediata   | 1 | 0 | 0 | 0 | 0/1 | 0/1 | 1 | 0 | 0 | 0  | 0  | 2  | 1  | 1  | 1  | 0  | 0  | 1  | 0  | 0   | 0  | 1  | 1  | 0  |
| Estaingia_bilobata         | 1 | 0 | 1 | 2 | 1   | 0   | - | 0 | 0 | 0  | 0  | 2  | 1  | 1  | 0  | 0  | 0  | 0  | 0  | 2   | 0  | 1  | 0  | -  |
| Ichangia_ichangensis       | 1 | 0 | 1 | 2 | 1   | 0   | - | 0 | 0 | 0  | 0  | 2  | 1  | 1  | 0  | 0  | 0  | 1  | 0  | 2   | 0  | 1  | ?  | ?  |
| Nephrolenellus_geniculatus | 0 | - | - | 3 | 0   | 0   | - | 0 | 1 | 0  | 2  | 1  | 0  | -  | -  | 1  | 0  | 1  | 0  | 1/2 | 1  | 1  | 1  | 0  |
| Olenellus_gilberti         | 0 | - | - | 3 | 0   | 0   | - | 0 | 1 | 0  | 2  | 0  | 1  | 1  | 0  | 1  | 0  | 0  | 0  | 0   | 0  | 1  | 1  | 0  |
| Redlichia_cf_versabunda    | 1 | 0 | 0 | 0 | 0   | 0/1 | 1 | 0 | 0 | 0  | 0  | 2  | 1  | 1  | 1  | 0  | 0  | 0  | 0  | 0   | 0  | 1  | 1  | 0  |
| Xystridura_templetonensis  | 1 | 0 | 1 | 3 | 0/1 | 0/1 | 1 | 0 | 1 | 0  | 1  | 2  | 0  | -  | -  | 0  | 0  | 0  | 0  | 2   | 0  | 1  | 1  | 0  |
| Zhangshania_typica         | 1 | 0 | 0 | 0 | 1   | 1   | 1 | 1 | - | 1  | -  | -  | 0  | -  | -  | 0  | 1  | 1  | 0  | 0   | 0  | 1  | 1  | 0  |
| Ellipsostrenua_granulosa   | 1 | 0 | 1 | 2 | 1   | 0   | - | 0 | 0 | 0  | 0  | 2  | 1  | 0  | -  | 0  | 0  | 1  | 0  | 2   | 0  | 1  | ?  | ?  |
| Metaredlichia_cylindrica   | 1 | 0 | 0 | 3 | 0   | 1   | 1 | 1 | - | 1  | -  | -  | 1  | ?  | ?  | 1  | 0  | 0  | 0  | 1   | 0  | 1  | 1  | ?  |
| Duodingia_duodingensis     | 1 | 0 | 2 | 3 | 1   | 1   | 1 | 1 | - | 0  | 0  | 0  | 0  | -  | -  | 0  | 0  | 2  | 0  | 2   | 0  | 1  | 1  | ?  |
| Duyunaspis_duyunensis      | 1 | 1 | - | 1 | 1   | 2   | - | 2 | - | 2  | -  | 0  | -  | -  | 0  | 0  | 1  | 0  | 2  | 0   | 0  | 1  | 1  | 1  |
| Oryctocarella_duyunensis   | 1 | 1 | - | 1 | 0   | 2   | - | 2 | - | 2  | -  | -  | 0  | -  | -  | 0  | 0  | 1  | 0  | 3   | 0  | 0  | 1  | ?  |

| 25 | 26 | 27 | 28 | 29 | 30 | 31 | 32 | 33 | 34 | 35 | 36 | 37 | 38 | 39  | 40 | 41 | 42 | 43 | 44 | 45 | 46 | 47 | 48 | 49 | 50 | 51 | 52 | 53 |
|----|----|----|----|----|----|----|----|----|----|----|----|----|----|-----|----|----|----|----|----|----|----|----|----|----|----|----|----|----|
| ?  | 1  | 1  | 1  | 1  | 0  | 1  | 0  | 1  | 1  | 0  | ?  | 2  | 0  | 0   | 0  | -  | 1  | 0  | 0  | 1  | 0  | 1  | 0  | 0  | ?  | ?  | ?  | 2  |
| 1  | 0  | -  | 0  | -  | -  | 0  | 0  | 0  | 0  | 0  | 1  | 2  | 0  | 2   | 1  | 1  | 1  | 1  | 1  | 0  | ?  | 1  | ?  | 1  | ?  | ?  | ?  | 0  |
| ?  | 1  | 1  | 1  | 1  | 0  | 1  | 0  | 1  | 1  | 0  | ?  | 2  | 0  | 0   | 0  | -  | 1  | 0  | 0  | 1  | ?  | 1  | 0  | 0  | ?  | ?  | ?  | 2  |
| 0  | 0  | -  | 0  | -  | -  | 0  | 1  | 0  | 1  | 0  | 0  | 0  | 1  | 0   | 1  | 0  | 1  | 1  | ?  | 1  | ?  | 1  | 2  | 1  | ?  | 0  | 0  | ?  |
| 0  | 0  | -  | 0  | -  | -  | 0  | 0  | 1  | 3  | 0  | 0  | 0  | 1  | 2   | 1  | 2  | 1  | 1  | 0  | 0  | ?  | 1  | 1  | 1  | 0  | 1  | 0  | 1  |
| 0  | ?  | ?  | ?  | ?  | ?  | ?  | ?  | ?  | ?  | ?  | ?  | 0  | 0  | 2   | 1  | 2  | 1  | 1  | 0  | 0  | 1  | ?  | ?  | ?  | ?  | 0  | ?  | ?  |
| ?  | 1  | 0  | 1  | 0  | 1  | 0  | 0  | 0  | 0  | 0  | ?  | ?  | ?  | ?   | ?  | 0  | 1  | ?  | 1  | 1  | 1  | 0  | 0  | ?  | ?  | ?  | ?  | 0  |
| 1  | 1  | 0  | 1  | 0  | 0  | 0  | 2  | 0  | 0  | 1  | 1  | 2  | 0  | 0   | 0  | -  | 0  | 1  | ?  | 0  | 1  | 1  | 0  | 0  | ?  | ?  | ?  | 0  |
| 0  | 0  | -  | 0  | -  | -  | 0  | ?  | 0  | 1  | 0  | 0  | 0  | 1  | 1   | 1  | 0  | 1  | 1  | 1  | 1  | ?  | ?  | ?  | ?  | 1  | 0  | ?  | 0  |
| 1  | 0  | -  | 0  | -  | -  | 0  | 0  | 0  | 0  | 0  | 0  | 1  | 0  | 2   | 1  | 2  | 1  | 1  | ?  | 0  | ?  | 1  | 1  | 1  | ?  | ?  | ?  | 0  |
| 0  | 0  | -  | 0  | -  | -  | 0  | 0  | 0  | 0  | 0  | 1  | 1  | 0  | 0/1 | 1  | 3  | 1  | 1  | ?  | 1  | ?  | 0  | -  | -  | ?  | 0  | 0  | 2  |
| ?  | ?  | ?  | ?  | ?  | ?  | ?  | ?  | 1  | 0  | ?  | 0  | 0  | ?  | 1   | ?  | 1  | 1  | 0  | 0  | 1  | ?  | ?  | ?  | ?  | 0  | 1  | ?  | 1  |
| ?  | ?  | ?  | ?  | ?  | ?  | ?  | ?  | ?  | ?  | ?  | ?  | 0  | 0  | 1   | 0  | 1  | 1  | 1  | 1  | 1  | ?  | ?  | ?  | ?  | 1  | ?  | 0  | 2  |
| ?  | 0  | -  | 0  | -  | -  | 0  | 0  | 0  | 2  | 0  | 0  | 0  | 0  | 0   | 0  | -  | 1  | 0  | ?  | ?  | ?  | 0  | -  | -  | 2  | 2  | 1  | 2  |
| ?  | 0  | -  | 0  | -  | -  | 0  | 0  | 0  | 2  | 0  | 0  | 0  | 0  | 1   | 0  | -  | 1  | 1  | 1  | 1  | ?  | 0  | -  | -  | 2  | 1  | 1  | 2  |
| ?  | 0  | -  | 0  | -  | -  | 0  | 0  | 0  | 2  | 0  | 0  | 0  | 0  | 1   | 0  | -  | 1  | ?  | ?  | 1  | ?  | 0  | -  | -  | ?  | 2  | 1  | 2  |

